DESIGN AND APPLICATION OF NERVE GROWTH FACTOR-β BINDING PEPTIDE NANOFIBERS FOR NEURAL REGENERATION

A THESIS SUBMITTED TO

THE GRADUATE SCHOOL OF ENGINEERING AND SCIENCE

OF BILKENT UNIVERSITY

IN PARTIAL FULFILLMENT OF THE REQUIREMENTS FOR

THE DEGREE OF

MASTER OF SCIENCE

IN

NEUROSCIENCE

By

Zeynep Orhan

November, 2016

DESIGN AND APPLICATION OF NERVE GROWTH FACTOR-β BINDING PEPTIDE NANOFIBERS FOR NEURAL REGENERATION

By Zeynep Orhan

November, 2016

We certify that we have read this thesis and that in our opinion it is fully adequate, in scope and in quality, as a thesis for the degree of Master of Science.

Ayşe Begüm Tekinay(Advisor)

Michelle Marie Adams

Yusuf Şükrü Çağlar

Approved for the Graduate School of Engineering and Science:

Ezhan Karaşan
Director of the Graduate School

ABSTRACT

DESIGN AND APPLICATION OF NERVE GROWTH FACTOR-β BINDING PEPTIDE NANOFIBERS FOR NEURAL REGENERATION

Zeynep Orhan
M.S. in Neuroscience
Advisor: Ayşe Begüm Tekinay
November, 2016

Promotion of neurite outgrowth is an important limiting step for the regeneration of nerve injury and depends strongly on the local expression of nerve growth factor (NGF). Rational design of bioactive materials is a promising approach for the development of novel therapeutic methods for nerve regeneration, and biomaterials capable of presenting NGF to nerve cells are especially suitable for this purpose. This thesis describes development of nanofibrous peptide amphiphile (PA) nanofibers capable of promoting neurite outgrowth by displaying high density binding epitopes for NGF. The high-affinity NGF-binding sequence was identified by phage display and combined with a beta-sheet forming motif to produce a self-assembling PA molecule. Our results revealed that the bioactive nanofiber had higher affinity for NGF compared to control nanofiber and *in vitro* studies showed that the NGF binding peptide amphiphile nanofibers (NGFB-PA nanofiber) significantly promote the neurite outgrowth of PC-12 cells. In addition, the nanofibers induced differentiation of PC-12 cells into neuron-like cells by enhancing NGF/high-activity NGF receptor (TrkA) interactions and activating MAPK pathway elements. The first time with this study a seven amino acid phage display peptide library was utilized for high affinity epitope screening for NGF, the NGF binding sequence was incorporated into peptide amphiphile structure, and the effect of NGF binding material on differentiation pathway of NGF was analyzed. This material will pave the way for development of new therapeutic agents for nervous system injuries.

Keywords: Nerve growth factor, epitope screening, phage display, neural differentiation, PC-12 cells, peptide amphiphiles.

ÖZET

NGF'E BAĞLANAN PEPTİT NANOFİBERLERİN DİZAYNI VE NÖRAL REJENERASYON ÇALIŞMALARINDA UYGULANMASI

Zeynep Orhan
Nörobilimler, Yüksek Lisans
Tez Danışmanı: Ayşe Begüm Tekinay
Kasım, 2016

Nörit uzatımı hasar sonrası sinir hücrelerinin rejenerasyonunda önemli bir aşamadır ve sinir büyüme faktörünün (NGF) lokal üretimine de oldukça bağlıdır. Biyoaktif malzemelerin rasyonel dizaynı sinir yenilenmesi için özgün ve iyileştirici yöntemlerin geliştirilmesi için umut vericidir ve özellikle NGF'in hücrelere uygun bir şekilde sunulmasını sağlayabilecek biyomalzemeler bu tür yöntemlerin geliştirilmesine çok uygundur. Bu tezde, NGF'e yüksek afinite göstererek nörit uzatımını arttıran nanofiber yapılı peptit amfifil nanofiberlerin geliştirilmesi tanımlanmıştır. NGF'e yüksek afinite ile bağlanan peptit sekansı faj gösterim kütüphanesi kullanılarak bulunup, bulunan peptit sekansı beta-yaprağı oluşturma özelliği olan öz-toplanan peptit amfifil nanofiber yapısıyla kombine edilmiştir. Yapılan deneyler sonucunda dizayn edilen biyoaktif peptit nanofiberin (NGFB-PA) kontrol nanofibere (scrNGFB-PA) kıyasla NGF'e daha çok bağlandığı ve yapılan hücre çalışmaları sonucunda PC-12 hücrelerinde daha iyi nörit uzatımı sağladığı gösterilmiştir. Bu sonuçlara ek olarak, NGF'e bağlanan peptit nanofiberin PC-12 hücreleri üzerinde bulunan NGF reseptörü olan TrkA reseptörü ile NGF'in etkileşimini MAPK yolağı üzerinden artırarak, PC-12 hücrelerinin nöron-benzeri hücrelere dönüştürdğü gösterilmiştir. İlk defa bu çalışma ile 7 aminoasitlik faj gösterim kütüphanesi NGF'e yüksek afinite ile bağlanan epitop sekansı bulmak için kullanılmış ve bulunan epitope sekansı peptit amfifil yapısı içerisine eklenerek NGF'e bağlanan peptit nanofiber dizayn edilmiştir. Ve ilk defa bu çalışma ile NGF'e bağlanan biyomalzemenin PC-12 hücrelerinde NGF kaynaklı farklılaşma yolağı üzerindeki etkisi incelenmiştir. Bu çalışmada kullanılan biyomalzeme sinir sistemi yaralanmaları için yeni terapötik ajanların geliştirilmesine yol açacaktır.

Anahtar sözcükler: sinir büyüme faktörü, epitop tarama, faj gösterim kütüphanesi, nöral farklılaşma, PC-12, peptit amfifil.

Acknowledgement

Firstly I would like to thank my academic advisor, Prof. Ayşe Begüm Tekinay, for her support and guidance throughout my dissertation. She has provided me a broad view of the scientific community and independence during my master studies. I believe her open-minded and enthusiastic approach to research had invaluable contribution to my perspective on science. I would like to thank Prof. Mustafa Özgür Güler for his valuable supervision and for support. I would like to thank my jurors Prof. Yusuf Şükrü Çağlar and Prof. Michelle Marie Adams for their valuable contributions of this dissertation.

I would like to acknowledge the M.Sc. scholarship from TÜBİTAK (The Scientific and Research Council of Turkey) BIDEB 2210-C and from the 1001 project with project number 215S770.

I would like to express my special thanks to Dr. Büşra Mammadov for her scientific contributions and guidance at major steps of this dissertation. It was a great pleasure to work with Dr. Mammadov. I would like to thank Dr. Gülcihan Gülseren and Oya İlke Şentürk for their collaboration in synthesis and characterization parts. We could produce good data for publication of this project in high impact journal. I would like to thank Alper Devrim Özkan for his vauable comments and for proofreading both for this dissertation and the publication. I would like to thank Melike Sever, İdil Uyan, Canelif Yılmaz, Nuray Gündüz, Çağla Eren and Gökhan Günay for their scientific contributions for this project. I would like to thank Zeynep Erdoğan for her immense technical help in chemical characterization methods and Mustafa Güler for TEM imaging of peptide nanofibers. I also would like to thank New England Biolabs Technical Support Service for answering all of my questions about phage display library screening method.

I have enjoyed working and exchanging ideas with the many interesting and talented characters of the nanobiotechnology research group. I would like to thank Melike Sever for her helps whenever I needed and for her friendship during my master studies. I enjoyed to work with her in our collaborative projects as well as being one of my friends rather than a colleague. I would like to especially thank Çağla Eren for being a great colleague and great friend and I enjoyed every moment I had with her both in the lab and outside the lab-life. While I was complaining about being in Ankara, she was trying to convince me that Ankara is the best place to build good friendships and now her friendship is one of the most important benefits of Ankara for me. I would like to express my special thanks to Şehmus Tohumeken, Mustafa Beter, Canelif Yılmaz, Ahmet Emin Topal, Yasin Tümtaş, Gülistan Tansık, Özge Uysal, Burak Demircan, İslam Oğuz Tuncay and Elif Arslan for our discussions about everything and meeting with them was a great contribution for my future life. Also, I would like to thank all previous and current nanobiotechnology and biomimetics laboratory members for being great colleagues.

I would like to express my special thanks to Mustafa and Nazan Fadlelmula, Hatice Kübra Kara, Ömer Ulaş Kudu, Sağnak Sağkal and Abubakar Adamu for their great friendship and being in my life.

This dissertation could not be completed without the endless and exceptional support of my family. First of all, I would like to express my special thanks to my father, my mother, my grandmothers and my uncle and all of my relatives who always supported me throughout my entire life. I work for day and night to elevate their name and honor. I especially thank my mother Esma Orhan for her endless love and support to become who I am now. Therefore, I would like to dedicate this thesis to her.

I would like to express my most sincere thanks to my best friends Merve Şen, Nurcan Haştar, İdil Uyan, Fatih Yergöz; my IYTE family and Şeyma Köksal, Pınar Baş, Hatice Sivri and Raziye Kuru; my ADMAL family for their companionship in this long marathon.They were like siblings for me and their endless support and tremendous friendship which enabled me to stand for every hardness

throughout my journey. Their friendship deserves all compliments.

My last but the most special thanks is to my fiance, Faruk Okur, for his unique love and endless support and being not only a partner but also one of my best friends. He is the most valuable benefit of Ankara for my future life and his encouraging liveliness kept me motivated all the time. Therefore, I dedicate this thesis also to him.

All the best,

Zeynep

Contents

List of Figures

List of Tables

Chapter 1

Introduction

This study is partially described in the following publication (manuscript is submitted):

"Promotion of neurite outgrowth by rationally designed NGF-β binding peptide nanofibers"

Zeynep Orhan[a,b], Oya I. Senturk[a,c], Gulcihan Gulseren[a,c], Busra Mammadov[a,c], Mustafa O. Guler[a,c*] and Ayse B. Tekinay[a,b,c,*]

[a]National Nanotechnology Research Center (UNAM), Bilkent University, Ankara, 06800, Turkey

[b]Neuroscience Graduate Program, Bilkent University, Ankara, 06800, Turkey

[c]Institute of Materials Science and Nanotechnology, Bilkent University, Ankara, 06800, Turkey

*Corresponding author

1.1 The nervous system and its diseases

1.1.1 The nervous system

The nervous system (NS) consists of the central nervous system (CNS) and peripheral nervous system (PNS) (Figure 1.1). There are two major parts of the CNS: The brain, the brain stem and the cerebellum form the encephalon, which is responsible for the interpretation of information coming from the environment and the regulation of homeostasis, perception, emotions and cognition (Figure 1.1. The second region is the spinal cord, which is responsible for the delivery of information from the peripheral parts of body to the encephalon, as well as the transmission of the motor and autonomic information from the encephalon to peripheral targets. [1] The PNS is also subdivided into two distinct regions, called autonomic and somatic PNS. Cranial nerves and spinal nerves compose the somatic PNS, while autonomic nerves and their respective ganglia function as the autonomic PNS (Figure 1.1). [1] The PNS is responsible for the interaction of CNS with other organs, as well as with the environment.

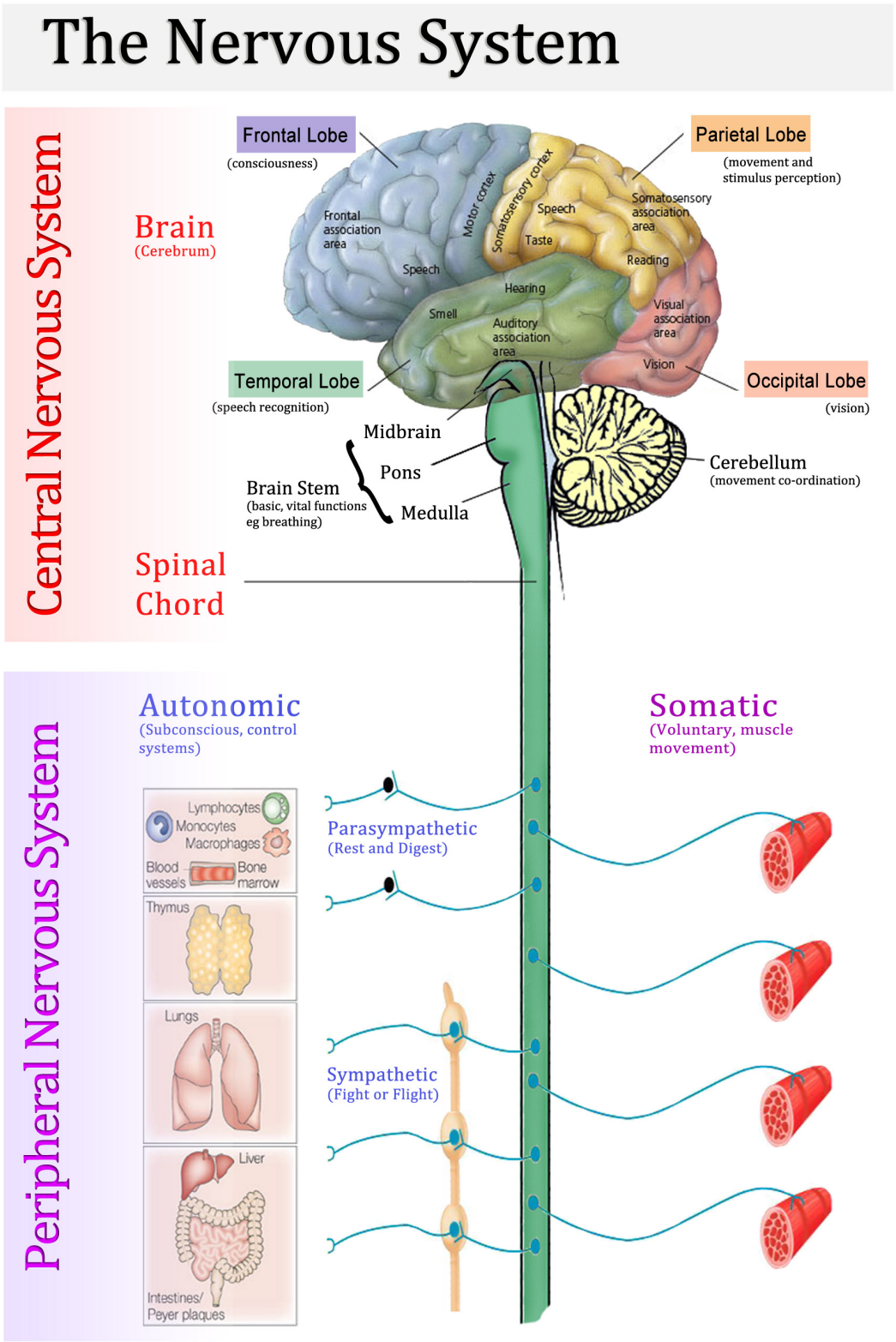

Figure 1.1: Anatomy of the nervous system. [2]

Nerves consist of bundles of nerve fibers and their role is to form communicating paths between the CNS, PNS, and the various organs of the body. Nerves are named according to their anatomical distribution. Afferent neurons are sensory neurons which carry impulses from sense organs to the CNS. Efferent neurons are motor neurons which connect to muscles and other effector organs. Cranial nerves arise from brain in vertebrates and they connect to spinal cord through spinal nerves. [1]

Neurons and glia are the two main cell types found in NS. Neurons are specialized cells of the NS and serve to transmit electrical signals, while glia protect, support, myelinate, and regulate the homeostasis of neurons and other NS elements. [1] All neurons share three major structural features: the cell body (or soma), the dendrites and the axon. [1] The cell body contains the nucleus of the neuron and maintains the life of the cell. Dendrites are short extensions that form a tree-like branched structure from their points of origin. Their number varies from neuron to neuron, and they are generally considered to be responsible for maintaining the information-receiving channels of the neuron. Axons are filament-like structures and connects the cell body and dendrites to other cells (Figure 1.2). Axons are considered to be the information-transmitter fibers of the neurons. The axonal transport system has great importance for neuron maintenance, because the replacement of old cells is a slow process following the initial development of the CNS. Therefore, the original cells should be maintained and protected throughout life.

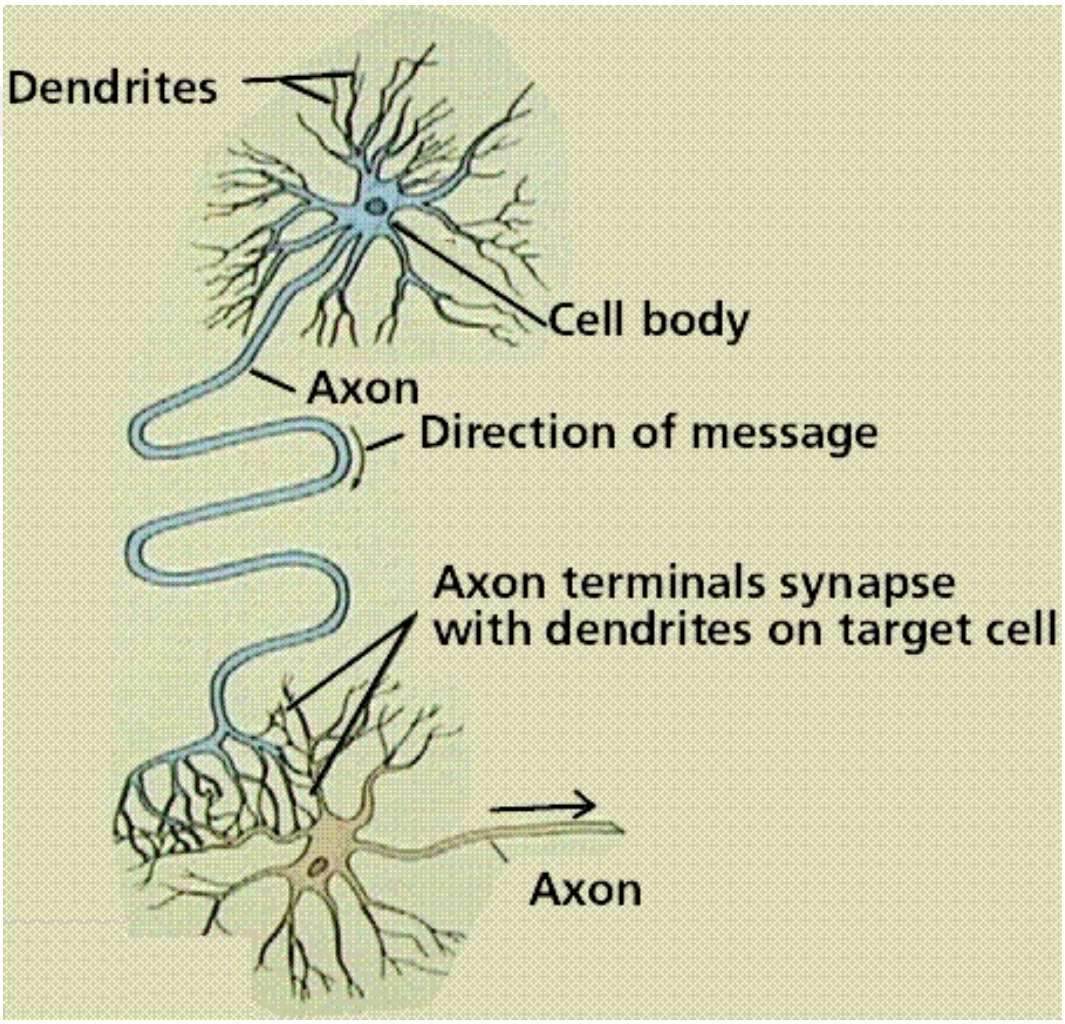

Figure 1.2: Structure of a neuron and direction of message transmission. [3]

There are three types of glia found in the CNS, which are astrocytes, oligodendrocytes and microglia. Astrocytes are the most abundant glial cells in the CNS and form links between neurons and the blood-brain barrier through their numerous cellular projections. They play several roles in the maintenance of the CNS, such as the recycling of neurotransmitters during synaptic transmission or clearance of excess potassium ions. [4] Oligodendrocytes are the building elements of myelin sheaths over neurons in the CNS and they are responsible for the insulation of the axon, which allows the propagation of electrical signals more efficiently. [5] Microglia are specialized types of macrophages which are found in all regions of the brain and spinal cord. Microglia are responsible for the protection of neurons in the CNS and multiply rapidly following injury to the CNS, which serves to raise an effective immune response and generate the necessary neuroinflammatory markers for neural regeneration. CNS diseases such as Alzheimer's disease (AD), Parkinson's disease (PD) and Amyotrophic Lateral Sclerosis (ALS) have been linked to deficiencies in microglia. [4, 6]

Schwann cells (SCs) and satellite cells are the glia cells found in the PNS. SCs are similar to the oligodendrocytes of the CNS and provide myelination to axons in the PNS. In most of the axons, the myelin sheath is interrupted at intervals which are called *nodes of Ranvier* and enable axons to conduct the nerve impulses faster than unmyelinated fibers. They also partially take over the role of the microglia of the CNS and clear cellular debris following injury, which enables PNS neurons to regrow. [7] Satellite cells are similar to the astrocytes of the CNS and they regulate the external chemical environment of PNS neurons. Satellite cells are also interconnected by gap junctions and contribute to pathological outcomes such as chronic pain because they are highly sensitive to injury and inflammation. [8]

Although the CNS is highly protected by rigid cranial bones, a flexible backbone and an insulating, oligodendrocyte-secreted myelin sheath, any injuries that may occur are difficult to repair because the adult mammalian CNS is deficient in growth factors and does not support the regrowth of damaged axons. In addition, the wound environment is typically flooded with growth-inhibitory molecules, which stimulate the formation of a non-functional glial scar. [9–11] As a result of a break in communication between healthy neurons, neuronal degeneration and

cell death occurs. According to the breakthrough studies of Ramõn y Cajal in 1928, it was shown that the CNS has very limited regeneration capacity after injury, while the PNS has a remarkable ability to recover from injuries. [12] This difference comes from the characteristic feature of the damaged environment, which either does not support or outright prevents regeneration. As such, a range of outcomes varying from successful recovery to complete lack of regrowth may occur at the site of injury. The modulation of environmental factors can therefore greatly affect the prognosis of nerve injuries, and the molecular and cellular mechanisms of both PNS and CNS regenerative and non-regenerative mechanisms have been studied in detail.

In the CNS, myelin-associated inhibitors, astrocytes, oligodendrocytes, oligodendrocyte precursors and microglia migrate to the injury site and form an inflammatory response that generates a non-permissive growth environment. Macrophage recruitment is limited in the CNS and occurs later than in injured PNS. [13,14] Growth factor expression or re-expression does not occur, the expression of growth associated elements such as growth associated protein (GAP-43) is inhibited and glial scars rapidly form through the activity of glial cells that produce inhibitory factors against remyelination and axon repair. [15] In addition, oligodendrocytes undergo apoptosis due to the axonal loss [16], oligodendrocyte precursors that migrate to the injury site do not secrete the necessary factors for the clearance of myelin debris, and astrocytes build a dense scar that prevents young neurons to penetrate through the injury site. [16] All together, the clearance of myelin in the CNS is slower than the PNS, which results in the prolonged regeneration process and the potential formation of a growth-inhibitory glial scar (Figure 1.3). [17]

After nerve injury occurs in the adult PNS, several factors supporting axonal regeneration are upregulated by the surrounding SCs to elicit three main responses: neuronal survival and neurite growth, phagocytosis of axonal and myelin debris, and axonal guidance. At the beginning of this process, both myelinating and nonmyelinating SCs dedifferentiate and start to proliferate, which leads the secretion of neurotrophic factors, cytokines and growth-associated proteins responsible for axon regeneration and nerve repair (Figure 1.4). [19] Nerve growth

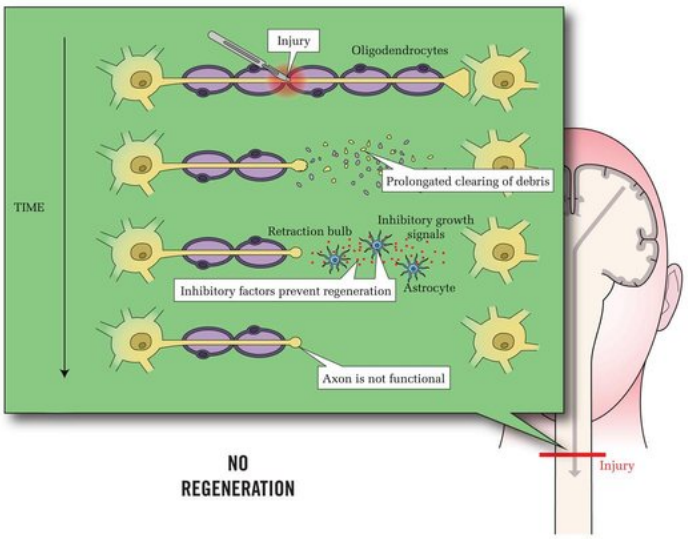

Figure 1.3: Regeneration process in the CNS after injury. [18]

factor (NGF) and p75^{NTR} upregulation occurs after changes in gene expression by SCs, which then leads to substantial infiltration by inflammatory cells such as macrophages, mast cells and T cell types which are able to express NGF. [20] NGF is retrogradely transported towards the neuronal cell body, which enables neurons to express anti-apoptotic and regeneration-associated genes. [21]

Besides the upregulation of NGF and p75^{NTR}, SCs initiate the phenomenon of Wallerian degeneration (WD) which is the overriding step of axonal regeneration in the PNS. WD leads to the rapid clearance of myelin debris produced by degenerated nerve fibers. Although both CNS and PNS myelin sheaths contain non-permissive proteins such as MAG [22] and myelin oligodendrocyte glycoprotein (MOG) [23], SCs can rapidly clear myelin debris via two mechanisms. At first, SCs break their own myelin sheath into small ovoids and then the resulting debris is phagocytosed. As a second process, blood-derived monocytes are recruited at the injury site by the chemo- and cyto-kines secreted by SCs (Figure 1.5).

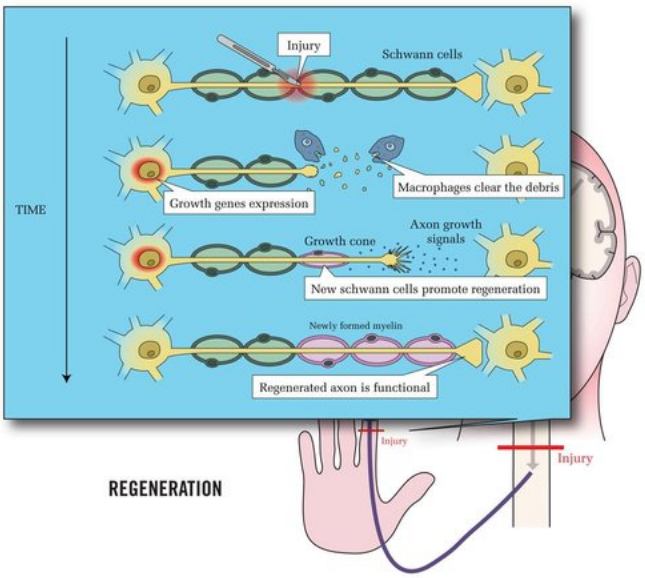

Figure 1.4: Regeneration process in the PNS after injury. [18]

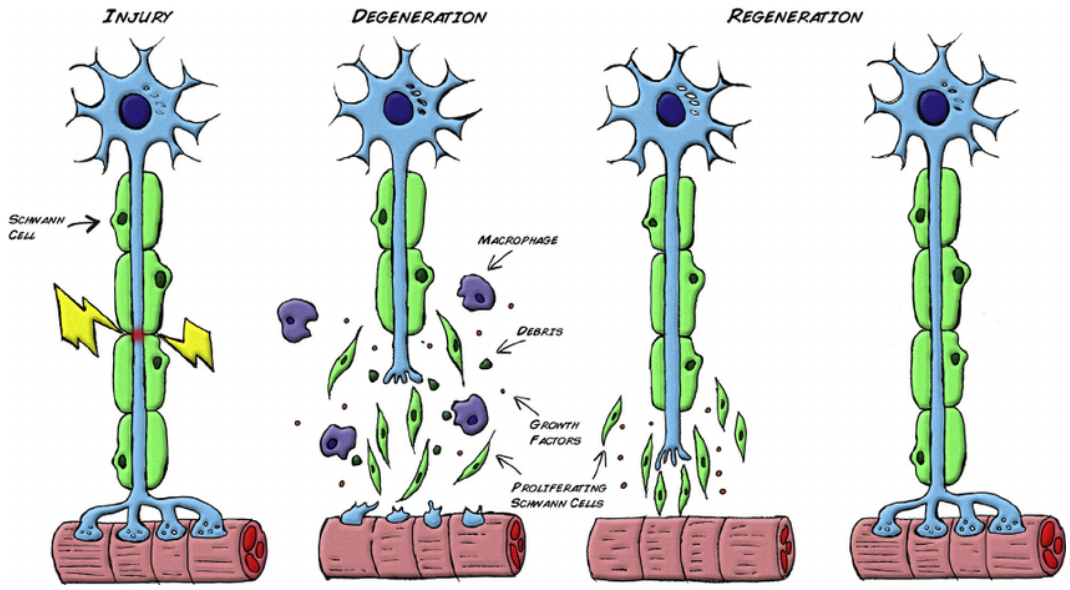

Figure 1.5: Wallerian degeneration in the PNS regulated by SCs. Reused from the reference [24] with the permission from Elsevier.

After the initial steps are completed, SCs provide structural guidance for axonal regrowth and remyelination after their migration and alignment by forming tube-like structures called 'bands of Büngner'. [25] They also produce basal lamina elements which interact with integrins of axon fibers. [26]

1.1.2 Nervous system diseases

Injuries of CNS and PNS or damage to neurons can cause severe diseases in the NS. Because of the differences in CNS and PNS regeneration mechanisms and their prospective environments, the outcomes of diseases occurring in the CNS and PNS are also different.

Neurodegenerative disorders are the outcome of progressive loss of structural and functional features of nerve cells. The main reasons of neurodegenerative disorders are the accumulation of insoluble filamentous aggregates in some parts of the brain, which results in cell death and inflammatory damage at the accumulation regions. The accumulated aggregates which are expressed systematically but accumulate only in CNS, form patterns that are characteristic of each individual disorder. [27] Alzheimer's and Parkinson's disease (AD and PD, respectively) are the most common neurodegenerative diseases in the world. Because of the increased life expectancy and changing population demographics, neurodegenerative dementias and movement disorders are becoming more common. [27] Neurodegenerative diseases are on the rise because of the increase in the aged population and an improved understanding of these diseases has become vital to develop more efficient therapies and combat the personal, social and economic costs of these diseases. [28] Although the reason behind almost all neurodegenerative diseases is the accumulation of insoluble aggregates; the temporal and regional patterns of aggregate deposition, cellular mechanisms of aggregation, and different protein constitutes formed by the aggregates create a staggering variety of phenotypic differences. Together with the innate responses of the patients to the aggregates, several cellular cascades cause different patterns of neuronal dysfunction such as dementia in AD or movement abnormalities in

PD. Therefore, the type and pattern of amyloid deposition in CNS determine the disease and its prognosis (Figure 1.6). [27]

The incidence of the AD and PD are being investigated by health organizations and according to the reports published in 2012, there are 5.2 million patients of AD in the U.S. [29] and 35.6 million patients of AD in the world (as of 2010). [30] This number is expected to double every 20 years because of the increase in life expectancy. Each year, approximately 50,000 people are diagnosed with PD. [30]

Besides the neurodegenerative diseases, traumatic brain injuries (TBI) and spinal cord injuries (SCI) are other causes of neuronal loss in the CNS. More than 2 million people in the U.S. suffer from TBIs annually, over 500,000 people per year suffer from stroke and at least 10,000 people per year suffer from SCIs. [31] These injuries cause irreversible disabilities such as permanent loss of of sensation and motor function in SCI. According to the 2014 report of National Spinal Cord Injury Statistical Center, less than 1% of SCI patients could completely recover after injury.

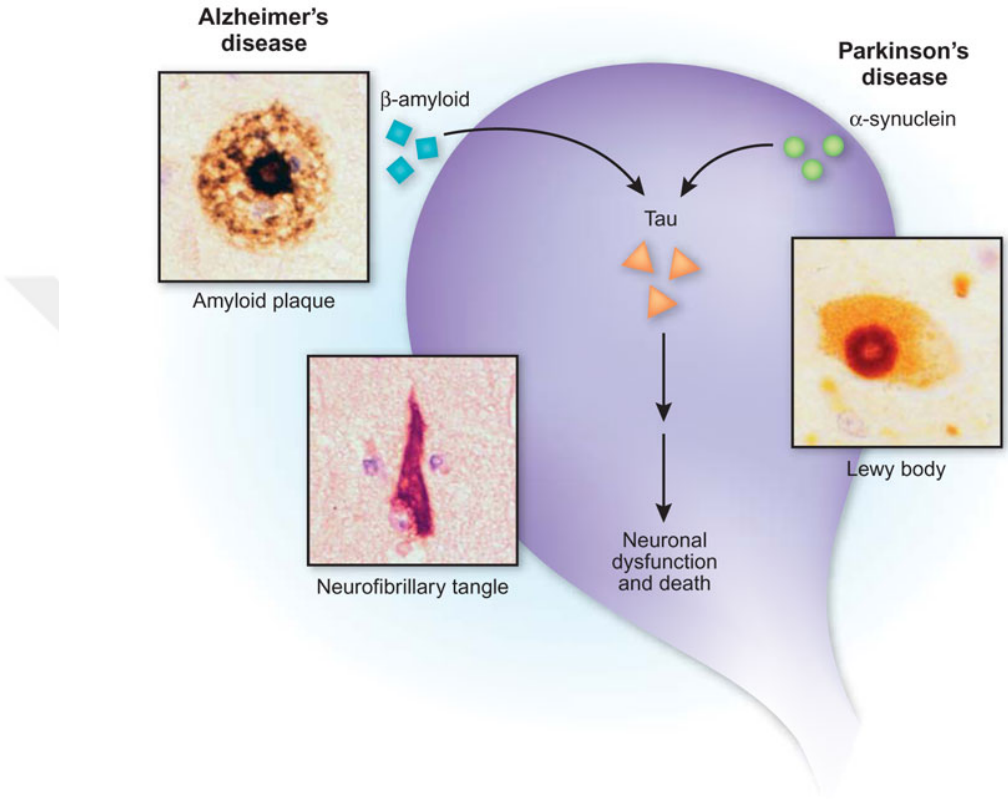

Figure 1.6: Most common neurodegenerative diseases and causes. The formation of AD is mostly caused by amyloid plaques, while PD is caused by Lewy body formation. Reused from the reference [32] with the permission from Nature Publishing Group.

PNS diseases are most commonly caused by injuries, because the PNS is more prone to external damages due to the absence of protective layers found in CNS (such as the cranium and spine). Systemic disorders such as diabetes are another reason for peripheral neuropathies. [33] PNS injuries were first investigated in detail during American Civil War by neurologist S. Weir Mitchell and many of the advances in knowledge about the PNS injuries have occurred during that time. [34] Seddon and Sunderland classifications are commonly used for the classification of PNS injuries. Seddon classification was described in 1942 and divides

the injuries into three categories: neurapraxia, axonotmesis and neurotmesis (Figure 1.7). [35] In neurapraxia, the nerve is intact but cannot transmit impulses; in axonotmesis, the axon is damaged but most of the connective tissue is maintained and, in neurotmesis, the nerve trunk (collection of neurons) is disrupted and most of the connective tissue is lost. [34]

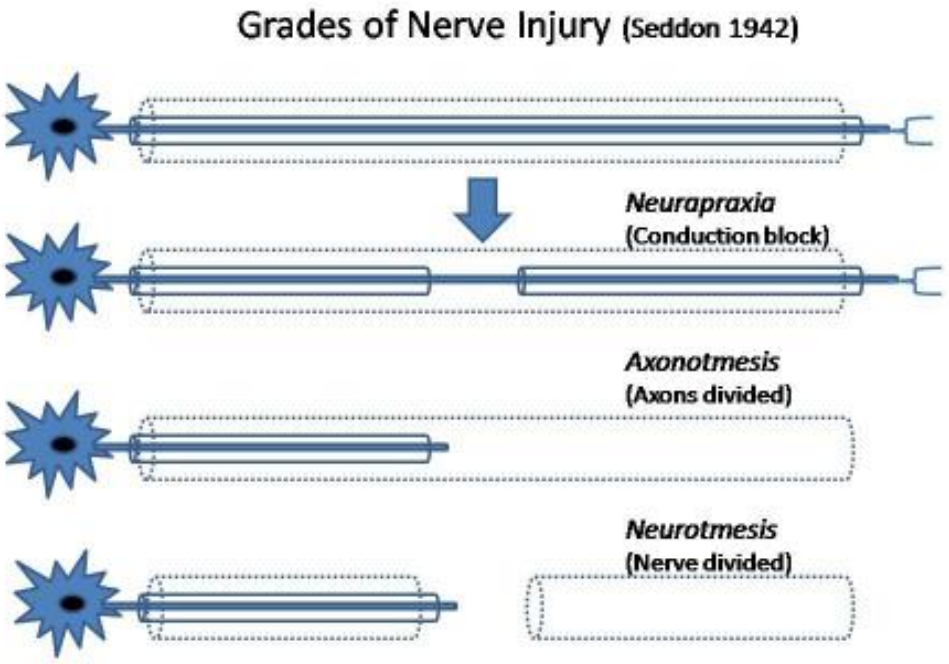

Figure 1.7: Seddon classification of the PNS injuries which are divided as neurapraxia, axonotmesis and neurotmesis. [36]

There are 20 million people suffering from peripheral neuropathy in the U.S. and approximately $150 billion is spent annually for health care to PNS injury patients, which shows that health care costs associated with these disorders constitute a major economic burden. [37]

Since a high number of patients are suffering from neurodegenerative diseases and traumatic injuries, regenerative therapies for the restoration of the lost neurological function are urgently required in the modern world. Although these diseases, which are caused by aging and injuries, affect a great number of people across the world, efficient therapies are not yet present for their treatment. As extracellular factors are the most decisive factors in NS regeneration, the role of environmental factors (such as extracellular matrix components of nerve cells or neurotrophic factors) on neural regeneration should be well understood, and therapeutic materials that target these elements for the enhancement of their activity at the injury site should be designed to effectively induce neural regeneration.

1.2 NGF and nervous system regeneration

Nerve growth factor (NGF) belongs to the neurotrophic factor family, which are soluble peptide growth factors and play important roles for the development, survival, proliferation and differentiation of neurons. These molecules bind to surface membrane receptors and then interact with diverse types of intracellular messengers. Many of the growth factors can act on various cell types at different stages of development and in adults.

NGF was first discovered over 50 years ago, and it was first isolated by Rita Levi-Montalcini and Stanley Cohen, who also discovered epidermal growth factor and were the co-winners of the Nobel Prize in 1986. [38] The discovery of NGF began with the curiosity of Rita Levi-Montalcini, who was a student in Brazil, about the hypothesis that transplanted tumor tissues released a diffusible agent which stimulated the growth and differentiation of the developing nerve cells. After her further investigations, she observed that the tumor could release a diffusible factor which directly promoted neurite outgrowth and stimulated nerve cell differentiation in a dose-dependent manner. [38]

Then, after collaboration with Stanley Cohen from Washington University in St Louis, USA, they performed a series of experiments for the biochemical characterization of this diffusible factor. In order to determine whether this biologically active molecule was a protein or nucleic acid, they used snake venom to destroy any nucleic acids. Surprisingly, they observed that snake venom enabled the nerve cells to extend more neurites than non-envenomed cell cultures. The finding of this molecule in snake venom led Cohen to think that it might be valuable to analyze the mammalian analog of snake venom gland and continued with mouse salivary gland. After this analysis, it was understood that mouse salivary gland is also rich in this diffusible factor. Through this discovery, Levi-Montalcini and Cohen were able to isolate this molecule and demonstrated that it was a protein. [39, 40] Since the diffusible factor, which was then named Nerve Growth Factor, could be isolated in high amounts from mouse salivary glands, they could

produce antibodies against NGF and could demonstrate the functional significance of NGF in the development of sympathetic and sensory ganglia with *in vivo* studies. [41]

In 1970, it was shown that NGF is part of a precursor and that a processor enzyme remains associated with NGF to form a multimolecular complex called 7S NGF (Figure 1.8A). The 7S NGF complex contains three different types of molecules: the α subunit, of which function is still not completely known, the γ subunit, which exhibits protease activity, and the β subunit, which is the biologically active form of NGF (Figure 1.8B). [42] The recombinant forms of NGF from human and rodents were then produced using only the β subunit for basic and clinical studies, and this form was called NGF-β. [43] Through subsequent studies, it was understood that NGF is highly conserved among species and shares high structural homology with other neurotrophic factors. Follow-up studies conducted by Levi-Montalcini and other scientists have further determined the roles of NGF in the nervous system, other systems (such as the immune system) and homeostatic responses. [43] NGF is being used as a therapeutic agent for human corneal neurotrophic ulcers and pressure ulcers, [44, 45] and is currently under intense investigation because of its potential effects on promoting the survival of damaged neurons and on neuroinflammation and neuroimmunopathologies. [46]

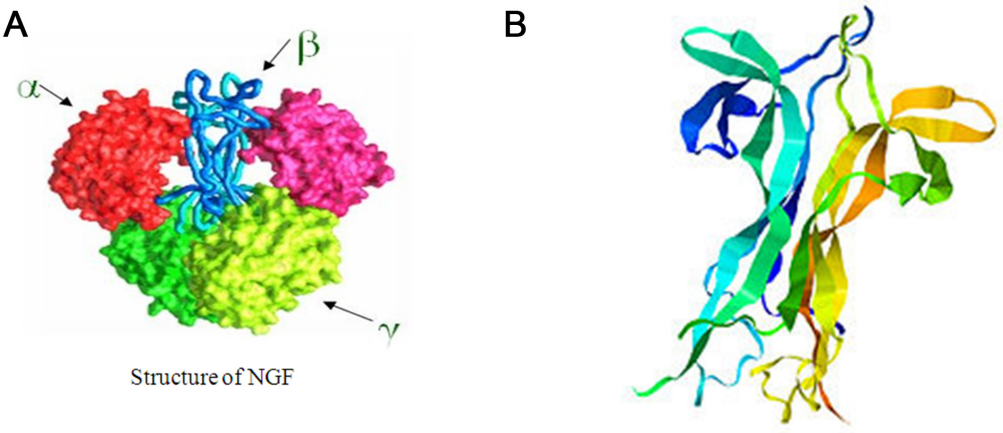

Figure 1.8: Structure of NGF. The 7S NGF complex with subunits are shown in (A) and the structure of β subunit of NGF is shown in (B). [47, 48]

The biological activity of NGF is regulated by two distinct receptors: the high

affinity tyrosine kinase A receptor (TrkA) from the trk family and low affinity p75 non-Tyrosine Kinase Receptor ($p75^{NTR}$). [49] The signaling of NGF through TrkA elicits many of the neurotrophic actions of NGF, such as neuronal survival and differentiation. [50] $p75^{NTR}$ regulates signaling through the TrkA receptor and binding of NGF to ($p75^{NTR}$) receptor activates several signaling pathways mainly related with the apoptosis of nerve cells. The three-dimensional structure of NGF bound to its TrkA receptor has been investigated, and it was shown that the amino terminus of NGF is responsible for NGF-TrkA binding interactions. [51] The three dimensional structure of NGF bound to ($p75^{NTR}$) receptor is also known [52] , and recent findings revealed that NGF could bind to both TrkA and $p75^{NTR}$ simultaneously. [51]

NGF can activate several cell signaling pathways through both TrkA (Ras (or MAPK), Akt (or PI3K) and PLC pathways) and $p75^{NTR}$ receptors (NFκB and JNK pathways) and most of the signaling pathways carried out by NGF were studied in PC-12 cells, which are NGF responsive neural progenitor cells derived from rat pheocromocytoma of the rat adrenal medulla and express NGF receptors on their cell membrane. One of the most widely known pathways of the TrkA receptor is MAPK pathway. After the binding of NGF to TrkA receptor, TrkA is autophosphorylated and Shc adaptor protein is recruited for the activation of the Ras signaling cascade. [53] After the recruitment of Shc, it is also phosphorylated and Grb2-Sos complex binds to phospho-Shc via an SH2 domain. [54] This event enables Sos to be in close proximity to membrane-associated Ras and facilitates the activation of MAPK signaling cascade by promoting the transition of inactive Ras-GDP to active Ras-GTP, which then results in the recruitment of serine-threonine kinase C-Raf to the plasma membrane. [55] In PC-12 cells, MAP kinase kinase MEK1/2 is phosphorylated by Raf family proteins, which then leads to the phosphorylation of two members of the MAPK family, extracellular signal-related kinases 1 and 2 (ERK1/2). [56] Phosphorylated ERK1/2 then can translocate into the nucleus and activate the genes responsible for the generation of survival, differentiation and migration signals in nerve cells (Figure 1.9) [57, 58]

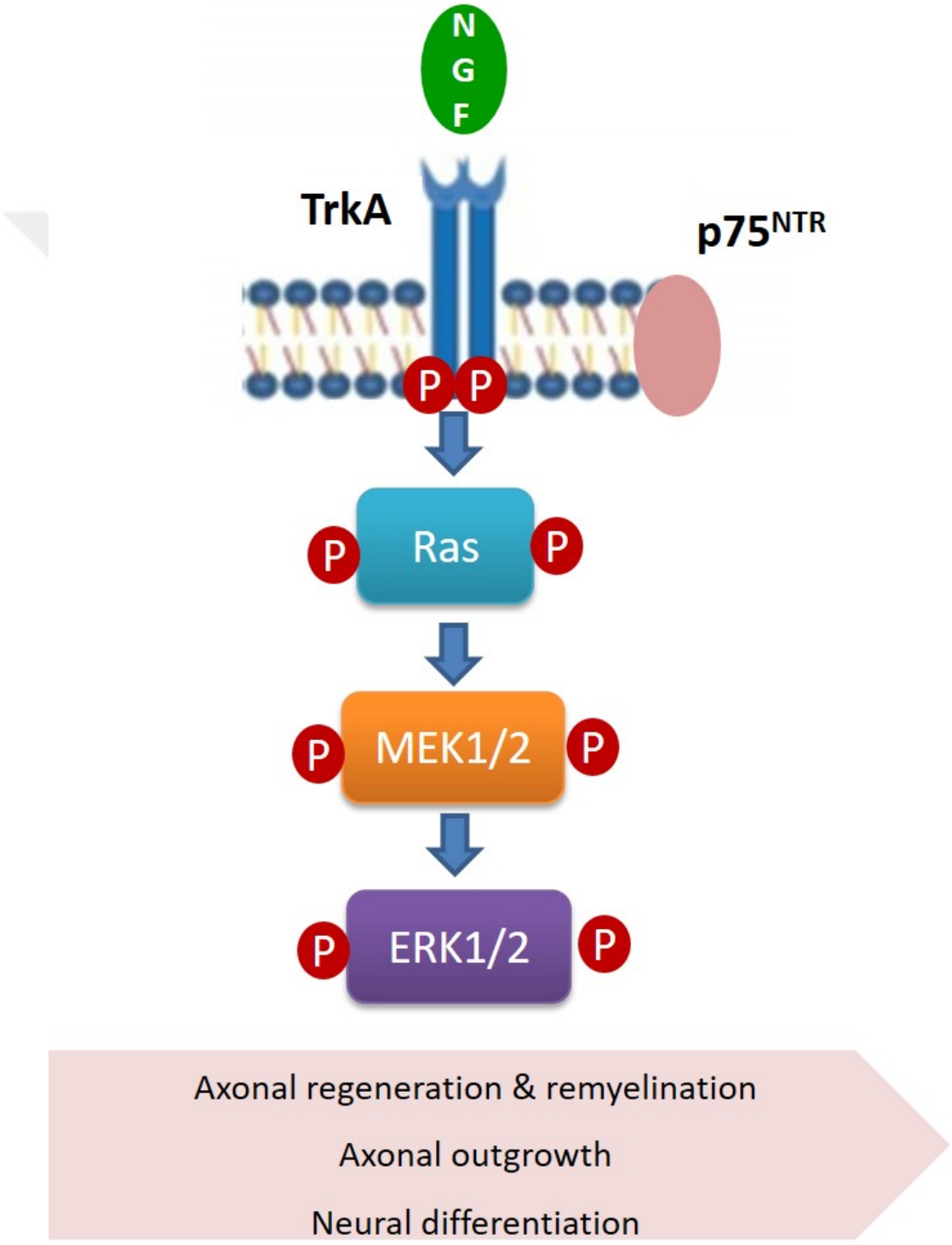

Figure 1.9: MAPK pathway is activated after binding of NGF to TrkA receptor on NGF responsive neurons. This figure is edited from the reference [59].

As with many other growth factors, NGF is also expressed during development, adult life and aging by several cell types in the CNS and PNS, immune system and some other tissues. During development, NGF is critical for the survival and maturation of afferent neurons and, in adult life, NGF expression is upregulated by both neuronal and non-neuronal cells after injury occurs in nervous system.

1.2.1 Role of NGF in PNS

Sympathetic neurons and peripheral sensory neurons express both TrkA and $p75^{NTR}$ receptors during development and in adulthood. [60] Most of the α-motor neurons transiently express $p75^{NTR}$ during the axon elongation step in development, while the expression of this factor is downregulated in adults but returns after peripheral nerve injury. [61] Schwann cells in the PNS also express $p75^{NTR}$ during development, but expression levels in adults are reduced to 1% of those seen during development. [62] Similar to α-motor neurons, the expression of $p75^{NTR}$ expression is significantly upregulated in SCs after the loss of contact with axons after PNS injury occurs or after the stimulatory effect of cytokines. [62]

During development, NGF is produced by non-neuronal target cells, which serve as the destinations of neural projections of sympathetic and sensory neurons. NGF is then transported retrogradely through the cell bodies of these neurons and its production continues during adult life in response to stimuli. Immature SCs and satellite cells also markedly upregulate their NGF production during development, but NGF production is downregulated in mature myelinating SCs. [63] When injury occurs, NGF expression from SCs is upregulated by cytokines and other inflammatory elements. [63] It can be understood that the expression patterns of NGF and its receptors in the PNS change in response to the distinct functions performed by the growth factor during development, in adulthood and after PNS injury.

Injury in the PNS causes axotomy, which leads to dedifferentiation of both myelinating and non-myelinating SCs distal to the injury. These SCs then reenter the cell cycle and start to proliferate, which enables them to secrete GFs,

cytokines and growth associated proteins that have significant roles in the regeneration of injured nerves. These changes in SCs lead to the upregulation of both NGF and $p75^{NTR}$ expression, together with infiltration of macrophages, mast cells and T cells, which also have the capacity to express NGF. [63, 64] Although the exact role of NGF secretion from different cells in PNS repair is not known, the overall function of secreted NGF is to increase both the number and myelination of regenerating axons in the PNS, due to the stimulatory effect of NGF on regenerating nerve fibers, SCs and inflammatory cells. [65, 66] SC migration is also the major process responsible for the promotion of axon elongation through the injury site. The secretion of NGF triggers SCs to express NGF receptors and NGF, and then migrate through the injury site in response to denervation. [67] The proximity of regenerating axons to SCs then suppresses the expression of both NGF and $p75^{NTR}$ receptor expressions after the contact with axons is established by SCs. At the end of this process, SC accumulation around the regenerating axons promotes remyelination at the injury site and allows it to recover from degeneration. [68] During axotomy, sensory neurons downregulate the expression of TrkA and $p75^{NTR}$ while motor neurons that are allowed to regenerate start to reexpress $p75^{NTR}$ and require retrograde transportation from axons growing through the injury site. [69] Although TrkA expression is downregulated after injury, sensory neurons regenerate robustly and reexpress TrkA at preinjury levels following their regrowth.

1.2.2 Role of NGF in CNS

The expression profile of NGF in the CNS is similar to the PNS: trauma, ischemia or degenerative diseases can trigger the rapid upregulation of NGF and NGF receptors by local astrocytes and microglia, invading inflammatory cells, and certain types of neurons. In the CNS, forebrain cholinergic neurons express both TrkA and $p75^{NTR}$ receptors, which exhibit neurite outgrowth in response to NGF after injury. [70] In spite of the uncertain role of NGF in CNS repair, it can be assumed that NGF may take role in the stimulation of regrowth and the reorganization of connectivity in receptor expressing neurons after injury. Cerebellar

Purkinje cells, hippocampal pyramidal neurons and retinal neurons also express $p75^{NTR}$ in a similar manner to motor neurons of the PNS, which express $p75^{NTR}$ during development and downregulate its expression in adult life. When injury occurs, $p75^{NTR}$ expression is also upregulated in the above-mentioned CNS cells in a manner similar to the motor neurons of the PNS.

According to recent findings, the structure of myelin oligodendrocyte glycoprotein (MOG), which is a myelin specific molecule expressed on the outer lamellae of myelin in CNS, is very similar to the structure of TrkA receptor and was shown to directly bind to NGF and modulate axon growth and survival in the CNS. [71] It has also been suggested that the binding of NGF to MOG may be related to the pain pathways of the CNS.

Consequently, NGF is vital for cell survival and axonal outgrowth following injury, and several studies and clinical trials are currently underway for its use in the treatment of nervous system injuries.

1.2.3 Treatment strategies of nervous system injuries with NGF

As described above, NGF is vital for the development and regeneration of the nervous system and its expression is upregulated in the distal stump following injury in the PNS, and in both distal and proximal stumps following spinal cord transection in the CNS. [72] Therefore, a great volume of research has been performed for the delivery of NGF to neuronal injuries. Studies focusing on filling nerve guidance channels with NGF solutions yielded conflicting results, which can be caused by the leakage of NGF from the channel or by NGF inactivation. [65,66,73] The use of exogenous NGF for PNS and CNS injuries (and especially for SCI regeneration) has also been proposed, and sensory neuron regeneration could be enhanced in dorsal root ganglia, spinal cord and even in the PNS-CNS transition zone. [74, 75] However, NGF-mediated sprouting of uninjured sensory axons has been linked to serious side effects such as chronic pain and inappropriate

neuronal reflexes in these studies. [76, 77] Because of the drawbacks associated with direct exposure to NGF, novel systems have been developed to ensure the controlled delivery of a limited concentration of NGF at the site of injury. Nerve guidance conduits (NGCs) are the most commonly used synthetic and polymeric materials for PNS regeneration, and functionalization of NGCs for NGF release has become a popular approach in recent years. The effect of slowly released NGF from synthetic guidance channels was analyzed in a rat sciatic nerve injury model and both sensory and motor neuron regeneration could be obtained over long gaps. [78] In a similar study, the slow and continuous release of NGF from guidance channels was shown to promote the regeneration of the transected rat dorsal roots derived from chick embryos. [79] Although these studies provided promising results, the application of exogenous NGF to the injury site is controversial because of the possible adverse effects of delivered NGF. For instance, even if the NGF is derived from the same species, cross-contamination can occur or excess amount of NGF at injury site can cause surrounding cells to become tumorigenic. Therefore, therapeutic materials that enhance the presentation of NGF secreted by surrounding glia and inflammatory cells after injury can facilitate a more effective recovery process and also prevent adverse effects of NGF on surrounding neurons.

Consequently, several studies were performed for the development of NGF-binding therapeutic materials for nervous system injuries. Extracellular matrix (ECM) components of nerve cells such as laminin, collagen or glycosaminoglycan molecules play important roles during the development and regeneration of nervous system. Therefore, therapeutic materials targeting the enhancement of NGF-ECM affinity is one approach for NS regeneration. In the study published by W. Sun et al. in 2009, a collagen-binding epitope was discovered and then incorporated into the structure of NGF-β, and the recombinant growth factor was shown to improve peripheral nerve regeneration by promoting NGF-collagen interactions in a rat sciatic nerve injury model. [80, 81] Another approach for the development of GF-binding therapeutic materials for regenerative purposes is the screening of short epitope sequences against GFs in order to discover high affinity binding moieties. This kind of screening method was made possible by

the development of phage display peptide libraries, which enabled scientists to discover epitope sequences for specific proteins, DNA or RNA. The phage display library method was first described by George P. Smith in 1985 and he showed the display of peptides on a filamentous phage by fusing the peptide of interest onto gene III (gIII) of the M13 bacteriophage. [82] A commercially available phage display peptide library structure, derived from the M13 bacteriophage, is shown in Figure 1.10.

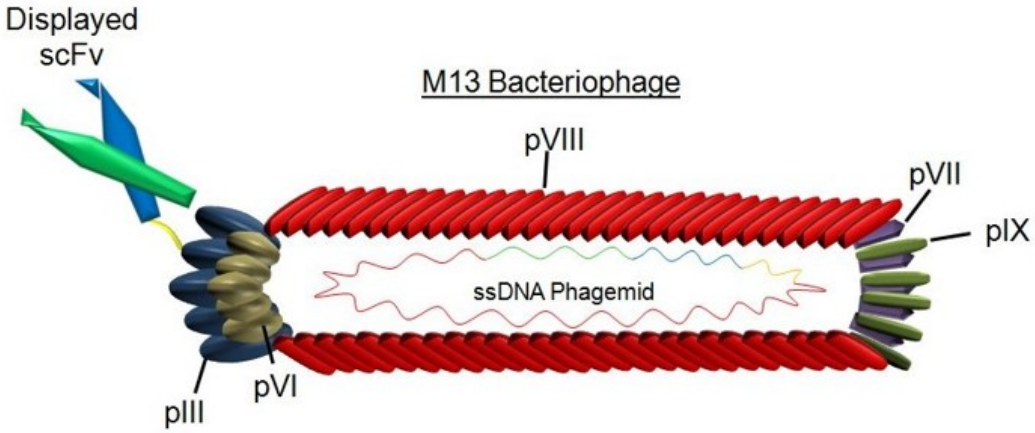

Figure 1.10: M13 bacteriophage structure is given. Displayed peptide sequences are incorporated into the genome of coat protein pIII (gIII) and displayed at the N terminus of phage structure. [83]

Each phage display library consists of a series of epitopes that are displayed by genetically engineered bacteriophages and can be tested against a target molecule (which can be a protein, cell surface receptor or another bioactive material) to determine the sequences that exhibit maximum affinity against it. [82] Phage display library method can be performed against a coated molecule, for the identification of cell surface receptor binding epitopes by *in vitro* biopanning, or for the discovery of immunobodies by *in vivo* biopanning. Phage libraries typically contain 7-amino acid linear, 12-amino acid linear or 7-amino acid cyclic epitopes (Figure 1.11), which can be mass-produced at relatively low costs for the functionalization of biomaterial surfaces following the identification of high-affinity

epitopes. [83] Following its discovery, phage display became one of the most effective biomedical tools in human medicine as well as in the fields of materials science, biotechnology, and nanotechnology. [84]

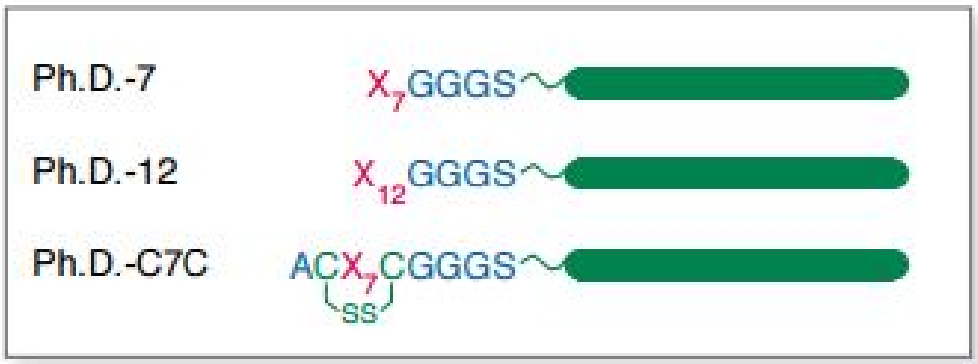

Figure 1.11: Commercially available phage display peptide libraries. Ph.D.-7 represents seven aminoacid peptide library, Ph.D.-12 represents twelve aminoacid peptide library and Ph.D.-C7C represents seven aminoacid cyclic peptide library. [83]

The phage display-peptide library screening method is advantageous for a broad variety of applications due to the low cost and non-demanding execution of the technique, which utilizes the recombinant genomic features of a filamentous phage. The biopanning method of phage display library only requires the coating of the target molecule to the surface and application of the library on the target molecule. After several washing steps, high affinity phages can be eluted by changing the pH of the solution (Figure 1.12). The screening of eluted phage clones can also be easily performed by the blue-white screening method. This technique depends on the conversion of colorless X-gal molecule into blue-colored 5,5'-dibromo-4,4'-dicholoro-indigo molecule by β-galactosidase enzyme, which is expressed by the LacZ gene from the lac-operon of the bacterial genome. [85] In this screening method, a short region from the LacZ gene is deleted and this genomic sequence is inserted into the M13 bacteriophage genome. When bacteria are transfected by eluted M13 bacteriophage clones, β-galactosidase enzyme can be successfully synthesized, which then enables the production of blue-colored product and the eluted phage clones are observed as blue plaques on LB-agar plates. [86] After at least three successful biopanning steps, phage clones with

the highest affinity for the target molecule can be obtained and the epitope sequence displayed by phage clone can be easily inferred by sequencing M13 phage DNA.

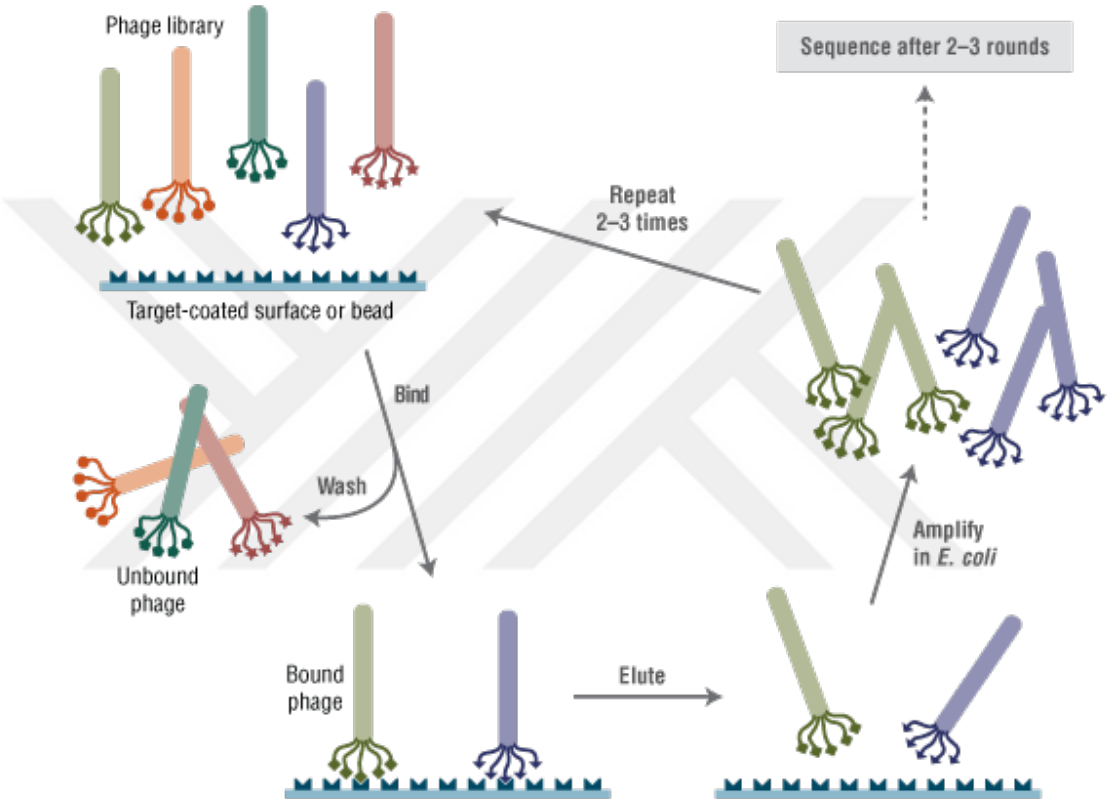

Figure 1.12: Epitope screening from phage display peptide library against target molecule. [83]

In one of the previous studies, a 12-amino acid phage display peptide library was utilized for the identification of an NGF-binding epitope sequence, and this epitope sequence was utilized in the design of NGF-binding fibrin matrices. The effect of the developed material on neural regeneration was then analyzed with chick embryo-derived dorsal root ganglion cells and the material was shown to enhance the axonal outgrowth in this culture model. [87]

Although prior studies concerning the development of NGF-binding therapeutic materials have yielded promising results, the effect of the these NGF-binding materials on the molecular mechanism of NGF still remains unclear. In addition, the effect of the amino acid sequence on the affinity for NGF was not investigated.

Therefore, there still exists a need to develop biomaterials that selectively bind to NGF and enhance its effect for neural differentiation and recovery from injuries.

1.3 Peptide nanofibers as scaffolds for nervous system regeneration

Epitopes can also be incorporated into synthetic biomaterials in order to be displayed efficiently to neuronal cells at the site of injury. These biomaterials can be programmed to interact with growth factors through the decoration of bioactive epitope sites for stability, increased local concentration and prolonged release of growth factors at the site of action. [88] The design of bioactive synthetic materials that are able to present the maximum number of epitopes and provide precise control over their number would be advantageous in the development of regenerative medicine strategies. Peptide amphiphile (PA) nanofibers are synthetic biomaterials that are widely used for regenerative purposes and can be modified easily through a straightforward and well-characterized set of chemical reactions. [89] PA nanofiber formation occurs through electrostatic interactions between positively and negatively charged groups and results in a structure where hydrophobic alkyl tails are internalized while bioactive epitopes are displayed on the surface. These assemblies are effective for promoting a range of biological responses: A laminin-derived PA (LN-PA; Figure 1.13), for example, was previously shown to promote the differentiation of neural progenitor cells into neurons [90], while a heparin-mimetic PA (HSM-PA) molecule was able to enhance the axonal outgrowth of PC-12 cells. [91] In addition, the combination of LN-PA and HSM-PA was found to enhance axonal outgrowth to a greater extent than the individual PA nanofibers, and could reverse the inhibitory effect of chondroitin sulfate proteoglycan on neurite outgrowth. [92]

PA nanofibers have also been tested *in vivo* for regeneration of nervous system injuries and degenerative diseases; for example, we have recently observed that the cooperative effect of LN-PA and HSM-PA is able to facilitate recovery from

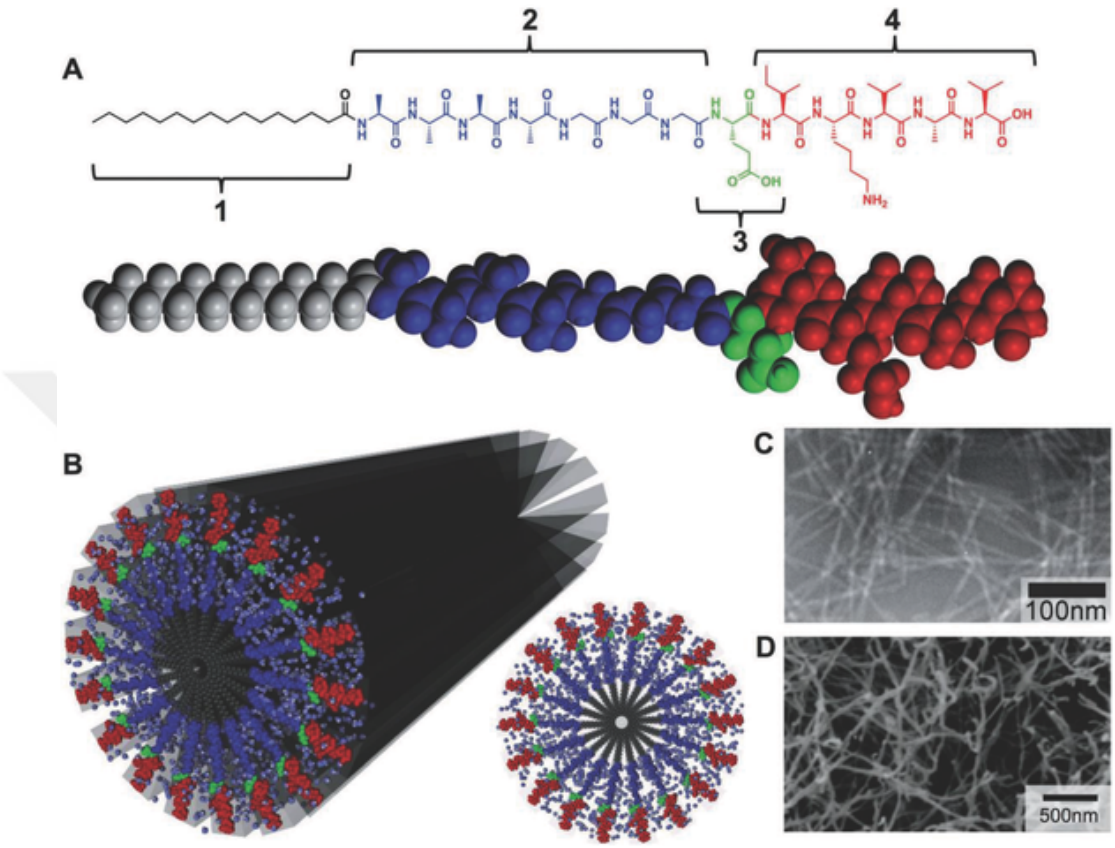

Figure 1.13: Molecular structure of LN-PA nanofiber. A-1) hydrophobic alkyl tail, A-2) β-sheet forming segment, A-3) charged amino acids providing solubility and further gelation, A-4) bioactive epitope. B) Self-assembly of PA molecules into nanofibers. C) Transmission electron microscope (TEM) image of PA nanofibers. D) SEM image of PA gel. Reproduced from the reference [93] with permission from John Wiley and Sons.

neuronal loss in an experimental Parkinsons disease model in rats [94], as well as enhancing neuronal formation (βIII-tubulin staining for neurons) and remyelination by SCs around regenerating neurons (S100 staning for SCs) in rat sciatic nerve injury model (Figure 1.14). [95]

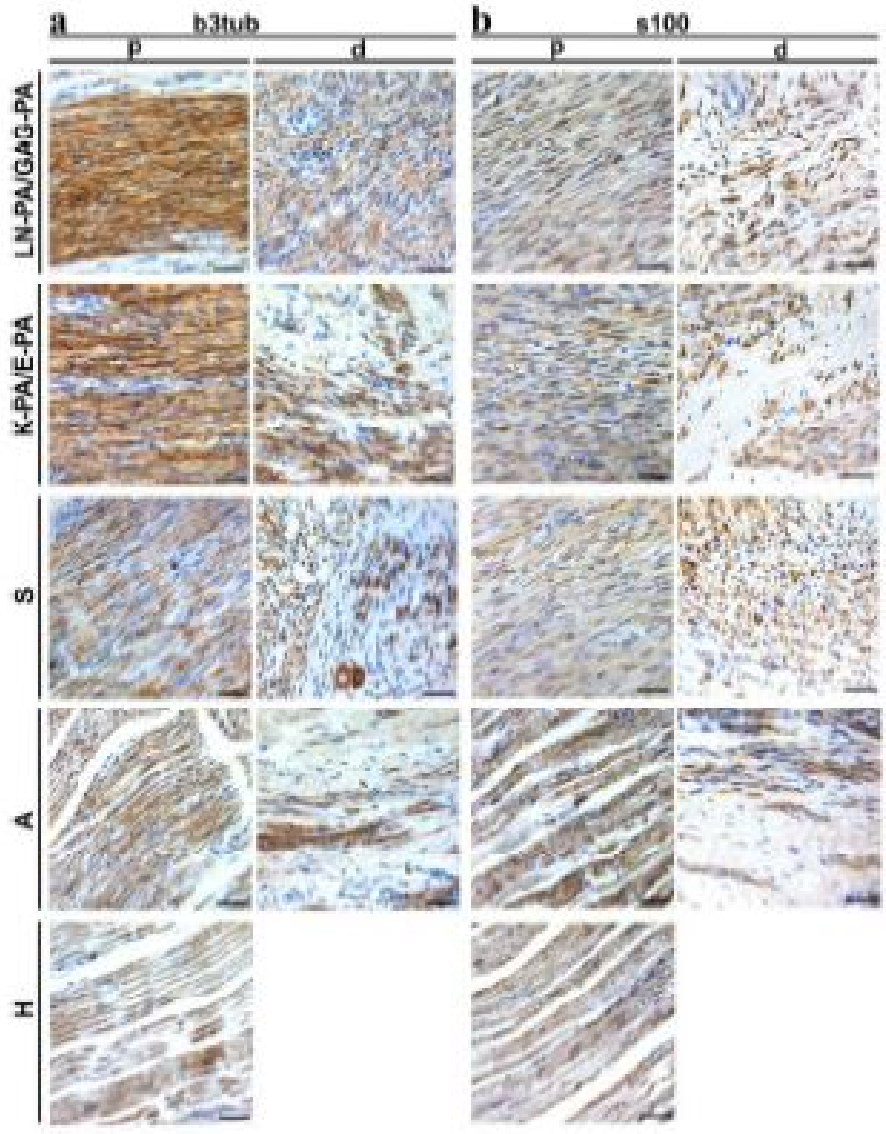

Figure 1.14: Sciatic nerve regeneration induced by glycosaminoglycan and laminin mimetic peptide nanofiber gels. βIII-tubulin staining (a) indicates a densely packed nerve tissue formation with good linear ordered structure at proximal region in LN-PA/GAG-PA treated nerves.Renervation at distal region is observed in all tissues except LN-PA/GAG-PA functionalized conduit treatment. Higher magnification (400X) images of Schwann cell staining against S100 (b) show higher number of Schwann cells exerting linear alignment in LN-PA/GAG-PA treated nerves at distal region. p indicates the proximal tissue and d indicates the distal tissue. A: Autograft, H: Healthy tissue, S: Sucrose filled conduit treated group. Reproduced from Ref. 95 with permission from The Royal Society of Chemistry.

1.4 Objective

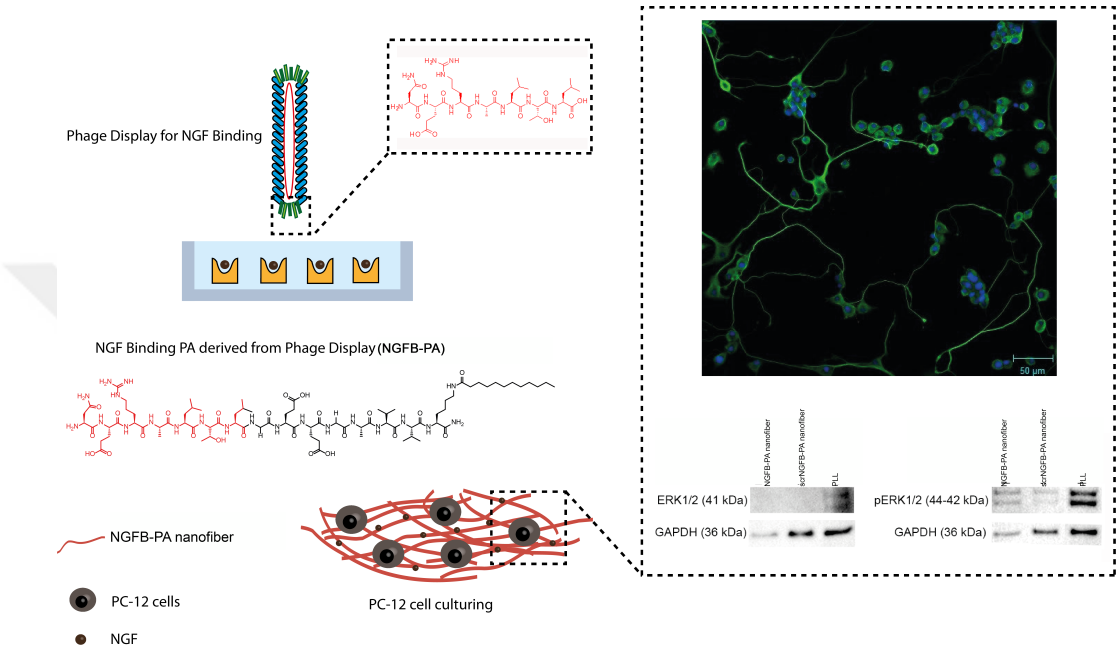

Figure 1.15: Overall representation of described study.

In the present study, a 7-amino acid phage library was used in order to identify a high-affinity epitope for NGF-β, which was then incorporated into a PA nanofiber structure for the promotion of neurite growth. The affinity of the designed NGF binding PA molecule (NGFB-PA) for NGF-β was compared with a scrambled version (scrNGFB-PA) of the sequence in order to determine the role of the order of sequence on the strength of binding. The effect of the PA scaffold on neurite outgrowth was evaluated using an *in vitro* model using PC-12 cells. PC-12 cells cultured on PA scaffolds were shown to differentiate into neuron-like cells by analysis of βIII-tubulin expression. Furthermore, the effect of the designed NGFB-PA scaffold on MAPK pathway was investigated and NGFB-PA nanofiber was shown to enhance the MAPK pathway. The biocompatibility of developed NGFB-PA nanofiber for primary rat SCs was also analyzed. Overall, our results suggest that NGFB-PA nanofiber is able to bind to NGF-β with selective affinity and is biocompatible for both PC-12 cells and primary rat SCs. The developed NGF-binding peptide nanofiber enabled differentiation of PC-12 cells into neuron-like cells by altering the essential differentiation pathway of NGF which makes

NGFB-PA nanofiber a novel promising scaffold for neural regeneration studies.

Chapter 2

Results and Discussion

2.1 Results

2.1.1 Phage library screening against NGF-β

In this study, a 7-amino acid phage display library was screened against NGF-β in order to identify epitopes of varying affinity for NGF-β. In order to enhance the specificity of peptide binding, the screening process was repeated three times. At the end of third round of biopanning, 24 randomly selected phage plaques were isolated for DNA sequencing. The images of the plates taken after each round are shown in Figure 2.1. The peptide sequences obtained from DNA sequences are given in Figure 2.2.

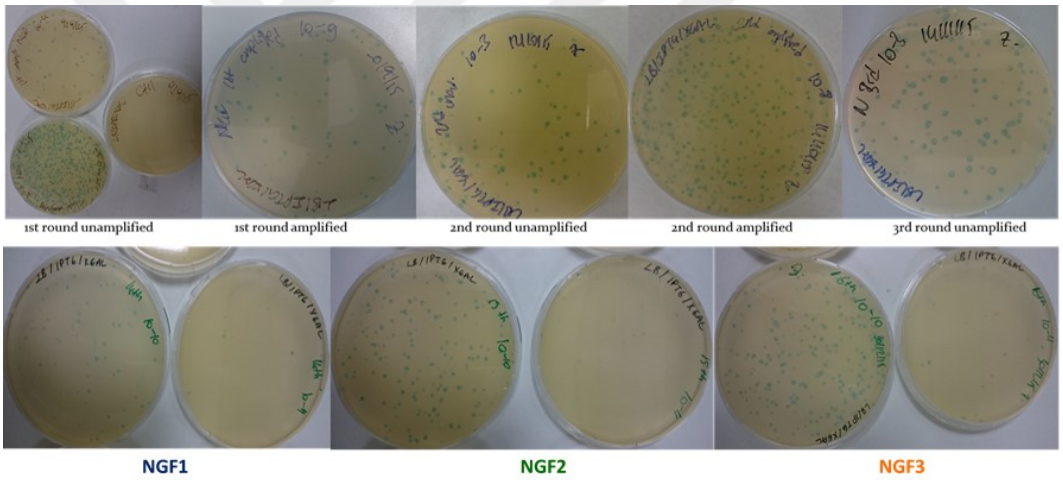

Figure 2.1: Titering results after each selection round against NGF-β. The images of plates obtained after titering were taken for each step. Plaques in blue represent the M13 phage from the library and were counted to calculate the plaque forming unit (pfu) for the following rounds.

Number	Sequence	Frequency
1	WHYVRPP	4/24
2	LGSPMSN	4/24
3	NERALTL	4/24
4	FSRPAFL	2/24
5	NHSTQMY	2/24
6	WHWRYAP	1/24
7	VHKTDYL	1/24
8	IGNTPAI	1/24
9	ANHQSAN	1/24
10	EHTRSMN	1/24
11	TFASHDQ	1/24
12	ITSTFTT	1/24
13	HWSTTIS	1/24

Figure 2.2: Identification of phage-displayed peptide sequences binding to NGF-β by using Ph.D.^{TM}-7 Phage Display Peptide Library. Summary of consensus Nerve Growth Factor binding peptides obtained after three rounds of biopanning.

Among 24 phage plaques, three of the peptide sequences were observed to be displayed in four distinct plaques. These sequences were selected for further analysis, and the affinity of these individual phage plaques for NGF-β was analyzed with phage ELISA. As shown in Figure 2.3, phage clone number 3 (NGF3) has higher affinity for NGF-β than blocking buffer (BSA 3) when compared to other clone numbers NGF1 and NGF2. In addition, the affinity of NGF3 to NGF-β is maintained even at lower concentrations of phage clones, and the solubility of this peptide sequence is higher than the others because of its increased number of hydrophilic amino acid residues, which is important for the design of peptide amphiphile molecules. Therefore, peptide sequence displayed by N3 was chosen

for the synthesis of the NGF-β binding peptide amphiphile (NGFB-PA).

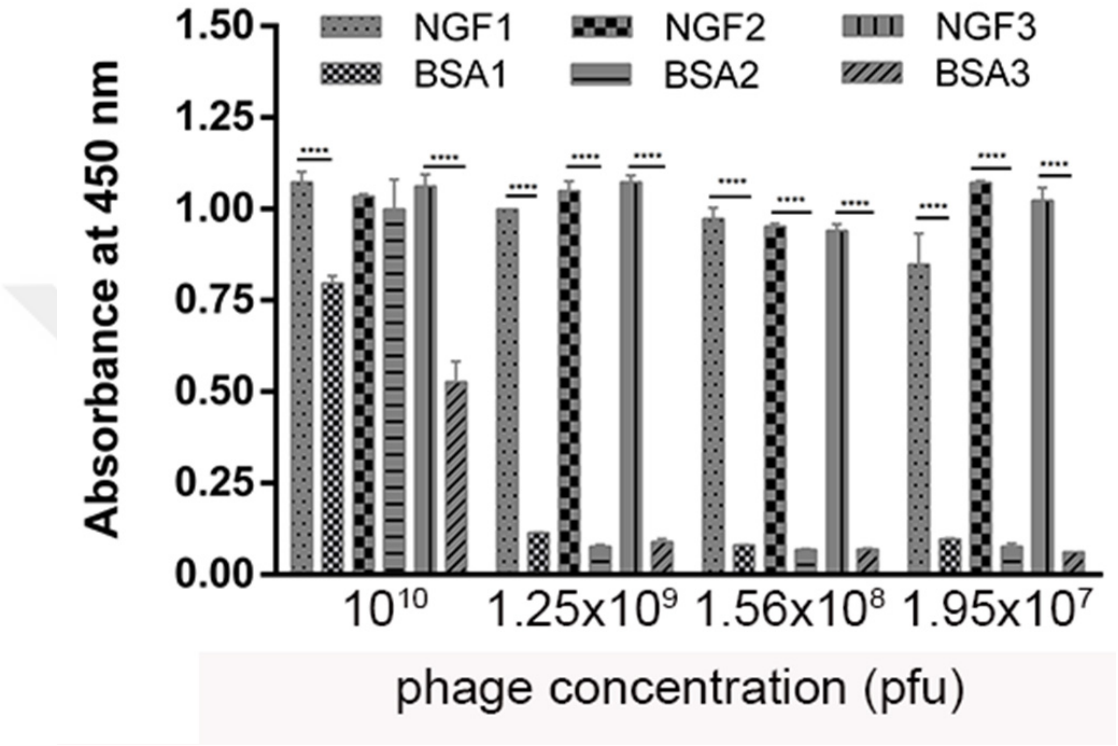

Figure 2.3: Affinity analysis of selected phage colonies for NGF-β. ELISA of binding ability of selected serially diluted (with 1:8 ratio) phage clones (number 1, number 2 and number 3 are represented as NGF 1, NGF 2 and NGF 3, respectively) to NGF ****P$<$ 0.0001 versus blocking buffer sample (BSA). Data presented are the mean OD values ($\pm$SEM) of triplicate samples.

2.1.2 PA synthesis and characterizations

Two different peptide amphiphile molecules were designed and synthesized to study the NGF- binding and neurite-outgrowth-supporting ability of peptide amphiphile scaffolds containing the NGF-β binding epitope NGF3. All PA molecules had a hydrophobic alkyl tail, which consists of lauric acid and a β-sheet forming peptide sequence, VVAG. In order to increase the solubility, two glutamic acid residues are added to the peptide amphiphile backbone and glycine was used as a spacer amino acid between the hydrophilic part of the sequence and the epitope region. [96, 97] Since the incorporated epitope region was obtained from phage structure and the epitope is displayed at the N terminus of M13 phage, the peptide amphiphile synthesis was performed from C to N terminus by leaving the N terminus of the peptide as a free amine. NERALTL-GEEGAVVK(Lauryl)-Am (NGFB-PA) was designed as the NGF binding PA molecule (Figure 2.4A) and RNTLLAE-GEEGAVVK(Lauryl)-Am (scrNGFB-PA; Figure 2.4B) was designed as the scrambled version of NGF binding epitope sequence in order to analyze whether the sequence order is important for the activity of PA molecule. Lauryl-VVAGKK-Am (KK-PA; Figure 2.4C) was synthesized with solid phase peptide synthesis as a filler PA in order to form nanofiber structures through charge neutralization.

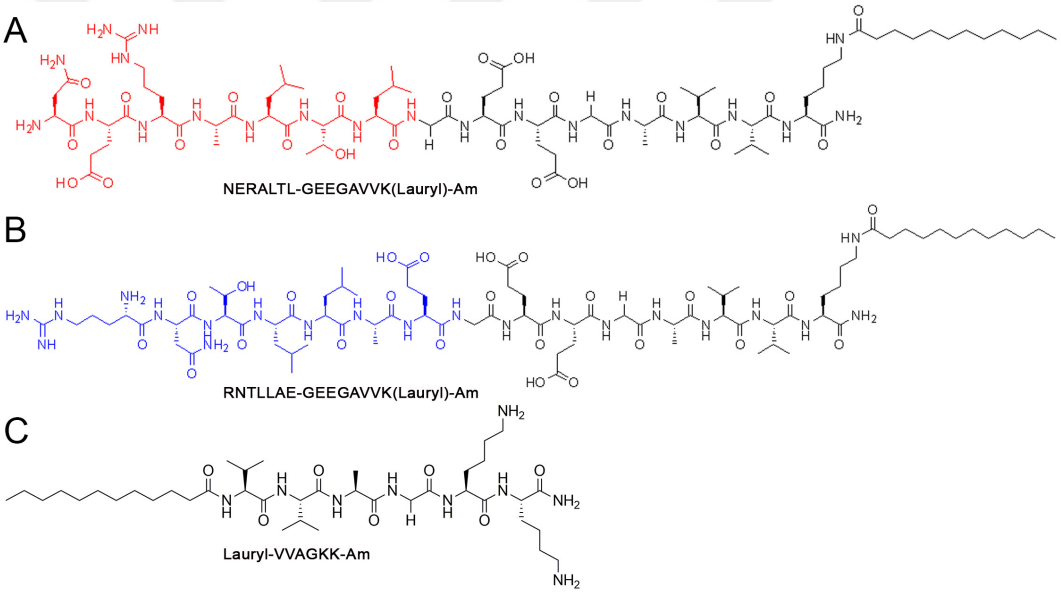

Figure 2.4: Chemical structures and sequences of self-assembling peptide amphiphile molecules. Chemical structures of NGFB-PA, scrNGFB-PA and KK-PA are given in (A), (B) and (C) respectively.

Peptide molecules were characterized by LC-MS and purified with preparative HPLC (Figure 2.5). TEM images were taken for each PA combination and these images showed that the combinations formed nanofibers with lengths ranging from a few hundred nanometers to several microns and diameters ranging between 10-20 nm (Figure 2.6A and 2.6B). The SEM imaging of nanofiber networks in PA gels (Figure 2.6C and 2.6D) showed the morphological similarity of nanofibrous PA scaffolds to the natural ECM structure which surrounds nerve cells in tissues. [98] ECM plays an important role for the differentiation of neural stem cells into mature neurons during development and the guidance of nerve ends for appropriate formation of neural networks during regeneration process, and the nanofibrous scaffold presented herein is observed to closely resemble the physical structure of ECM networks.

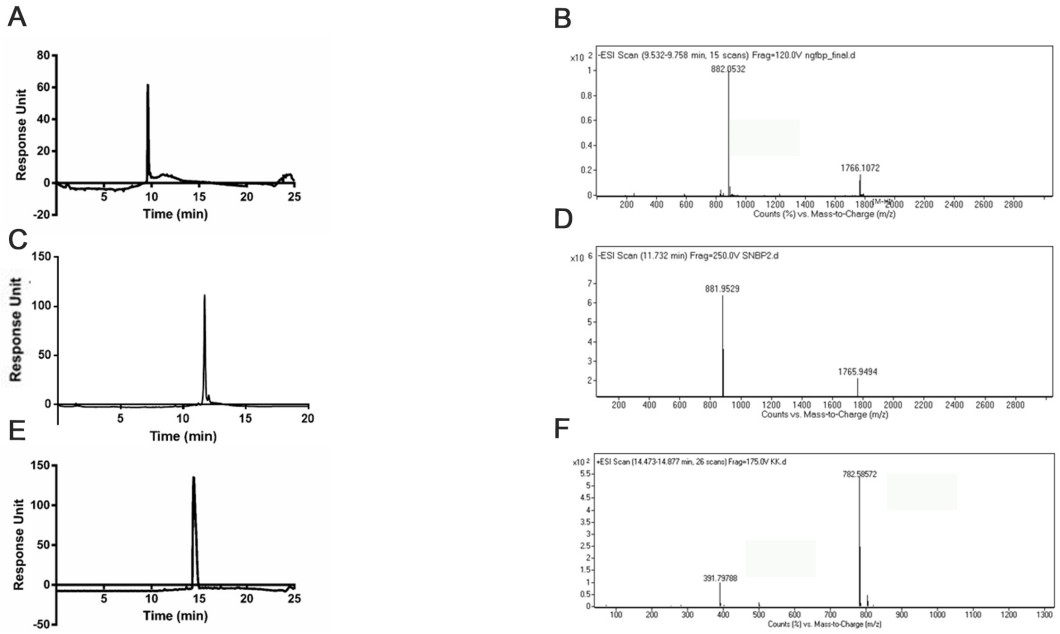

Figure 2.5: Liquid chromatography and mass spectrometry analysis of peptide amphiphile (PA) molecules. HPLC chromatogram of purified NGFB-PA (A), scrNGFB-PA (C) and KK-PA (E) molecules at 220 nm. Mass spectra of peptides; for NGFB-PA $[M\text{-}H]^-$ (calculated) = 1766.03, $[M\text{-}H]^-$ (observed) = 1766.10 (A), $[M/2\text{-}H]^-$(calculated) = 883.01, $[M/2\text{-}H]^-$ (observed) = 882.05 (B), for scrNGFB-PA $[M\text{-}H]^-$ (calculated) = 1766.03, $[M\text{-}H]^-$ (observed) =1765.94, $[M/2\text{-}H]^-$ (calculated) = 883.01, $[M/2\text{-}H]^-$ (observed) = 881.95 (D), for KK-PA $[M+H]^+$ (calculated) = 781.58, $[M+H]^+$ (observed) = 782.58, $[M/2+H]^+$ (calculated) = 390.79, $[M/2+H]^+$ (observed) = 391.79 (F).

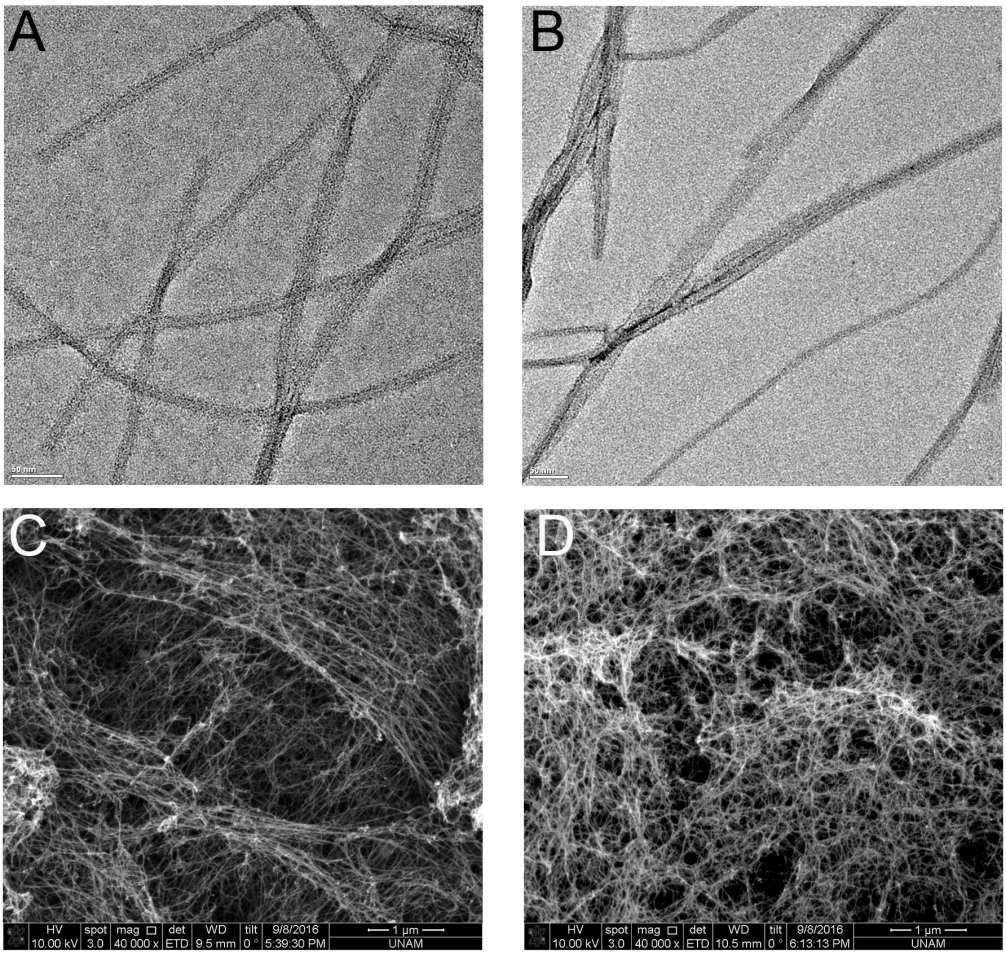

Figure 2.6: Imaging of self-assembling peptide amphiphile molecules at pH 7.4. TEM images of NGFB-PA nanofiber (A) and scrNGFB-PA nanofiber (B) gels show the individual nanofiber structures which were stained with uranyl acetate (scale bars are 50 nm). SEM images of NGFB-PA nanofiber (C) and scrNGFB-PA nanofiber (D) gels reveal the ECM-like structure formed by PA scaffolds. Scale bars are 1 μm. Peptides were dissolved in ddH_2O and their pH was adjusted with NaOH for all experiments.

Circular dichroism (CD) spectroscopy was employed to analyze the secondary structures of PA nanofibers, and the β-sheet motif was found to predominate in nanofibers formed by all PA combinations tested (Figure 2.7A). Secondary structure formation by individual PA molecules was also analyzed with CD (Figure 2.8B), and individual NGFB-PA and scrNGFB-PA molecules also formed β-sheet structures because of the presence of both negatively and positively charged amino acid residues.

Zeta potential measurements were also performed for both individual PA molecules and nanofiber structures to determine whether the experimental surface charges of PA scaffolds were in agreement with theoretical predictions (2.8A). The NGFB-PA nanofiber scaffold was formed by mixing bioactive NGFB-PA with the nonbioactive KK-PA at 1:1 molar ratio, and the scrNGFB-PA nanofiber scaffold was similarly formed by mixing scrNGFB-PA with the nonbioactive KK-PA at 1:1 molar ratio, resulting in neutral net charges for both nanofiber types (Figure 2.8A). Neutral or near-neutral surface charges were also observed for all nanofibers under zeta potential analysis (Figure 2.7B).

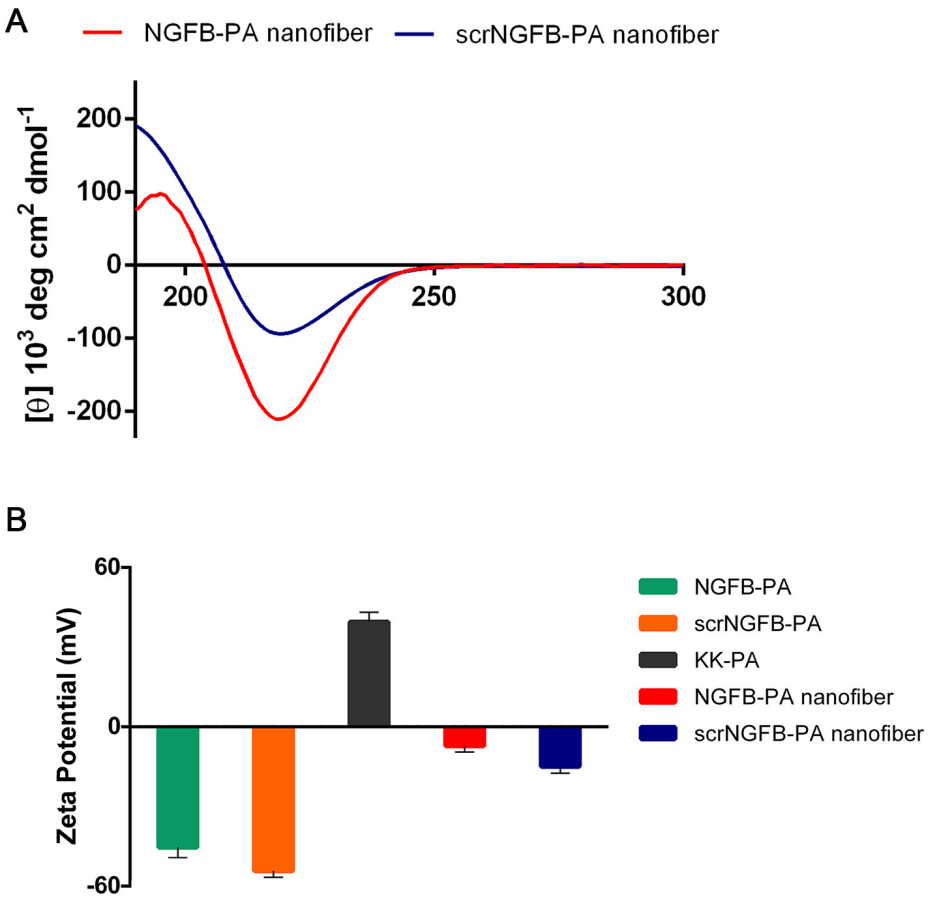

Figure 2.7: Characterization of secondary structure formation by peptide scaffolds and analysis of charge properties of PA molecules. NGFB-PA nanofiber and scrNGFB-PA nanofiber formed β sheet secondary structures as analyzed by CD measurements (A). Charge properties of individual PA molecules and nanofiber scaffolds (NGFB-PA nanofiber and scrNGFB-PA nanofiber) are analyzed with zeta potential measurements (B).

A

Peptide sequence	Nomenclature	Net charge (*)
NERALTL-GEEGAVVK(Lauryl)-Am	NGFB-PA	-2
RNTLLAE-GEEGAVVK(Lauryl)-Am	scrNGFB-PA	-2
Lauryl-VVAGKK-Am	KK-PA	+2
Peptide Mixtures		
NGFB-PA/KK-PA	NGFB-PA nanofiber	0
scrNGFB-PA/KK-PA	scrNGFB-PA nanofiber	0

(*) Theoretical net charge at pH 7.4

B

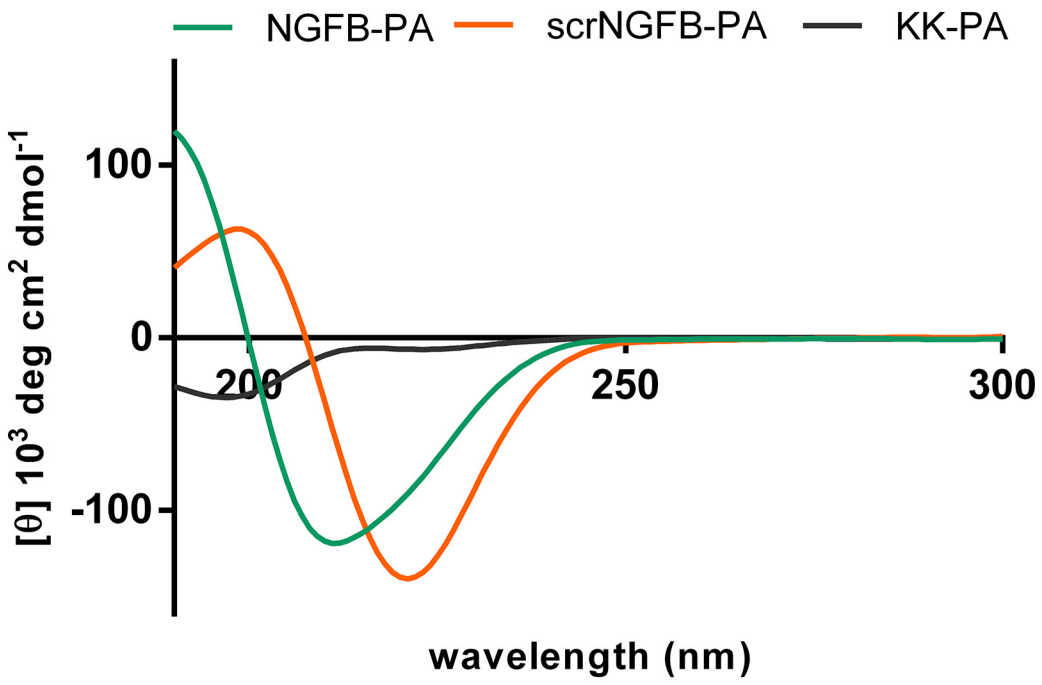

Figure 2.8: Abbreviations and charges of peptide sequence and peptide mixtures (A). The secondary structure analysis of peptide amphiphiles were analyzed by circular dichroism at pH 7.4(B).

2.1.3 Affinity analysis of PA nanofibers for NGF-β

The affinity of NGFB-PA nanofiber and scrNGFB-PA nanofibers to NGF-β was tested with ELISA method. Two different NGF-β concentrations (10 ng/mL; and 50 ng/mL) and three different nanofiber concentrations (0.1 mM, 0.25 mM and 0.5 mM) were used to determine whether the affinity of NGFB-PA nanofiber to NGF-β is concentration dependent Figure 2.9. The interaction between NGFB-PA nanofiber and NGF-β was found to depend on the concentration of both the nanofiber and the growth factor, with higher concentrations of either resulting in higher absorbance at 450 nm. In addition, for both NGF-β concentrations, it was shown that NGFB-PA nanofiber binds to NGF-β with significantly higher affinity than scrNGFB-PA nanofiber. As a control, NGF standard graph was provided in Figure 2.10 and it was shown that human NGF-β antibody gives absorbance only in the presence of NGF-β.

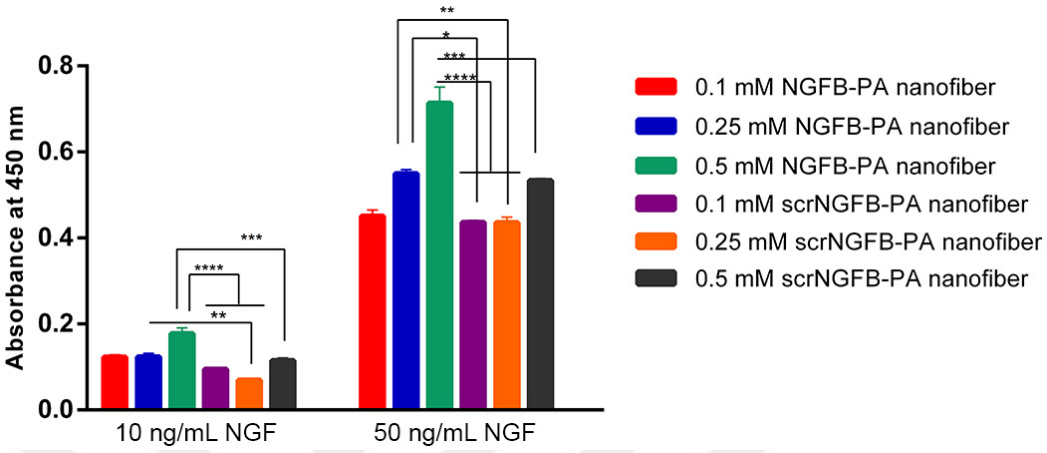

Figure 2.9: ELISA-based binding assay of PA combinations for NGF-β. Binding levels of 10 ng/mL NGF to increasing concentrations of NGFB-PA nanofiber and scrNGFB-PA nanofibers are compared in (A). Binding levels of 50 ng/mL NGF to increasing concentrations of NGFB-PA nanofiber and scrNGFB-PA nanofibers are compared in (B). The difference between NGFB-PA nanofiber and scrNGFB-PA nanofiber was significant for both concentrations of NGF. *P$<$ 0.05, **P$<$0.01, ***P$<$0.001 and ****P$<$ 0.0001. Data presented are the mean OD values ($\pm$ SEM) of triplicate samples and statistical analyses were performed with one-way ANOVA with Bonferroni posthoc analysis.

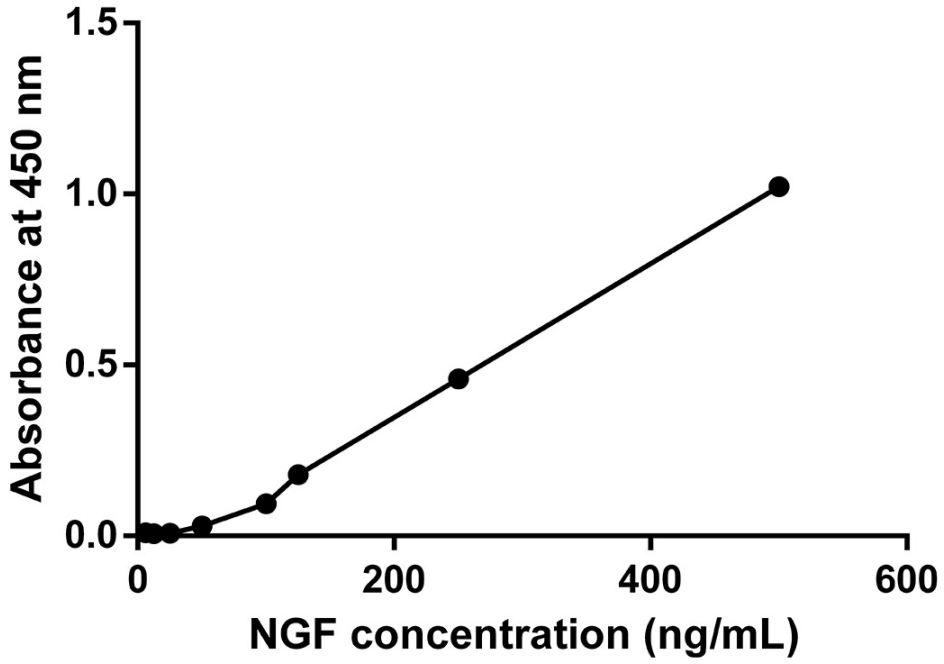

Figure 2.10: ELISA standard graph of human NGF-β antibody (R&D systems) against NGF-β shows that the affinity of the antibody for NGF-β is concentration dependent.

2.1.4 Toxicity analysis of PA nanofibers on PC-12 cells

The effect of peptide scaffolds on the cellular viability of neural progenitor PC-12 cells was analyzed with Alamar Blue assay and representative images were taken after the staining of live cells with calcein-AM and dead cells with ethidium homodimer. It was observed that PA nanofibers are not toxic for PC-12 cells after 24 h and 72 h of incubation Figure 2.11. PC-12 cells cultured on all treatment groups including PLL (positive control group) behaved similarly, which indicates that all PA combinations were biocompatible.

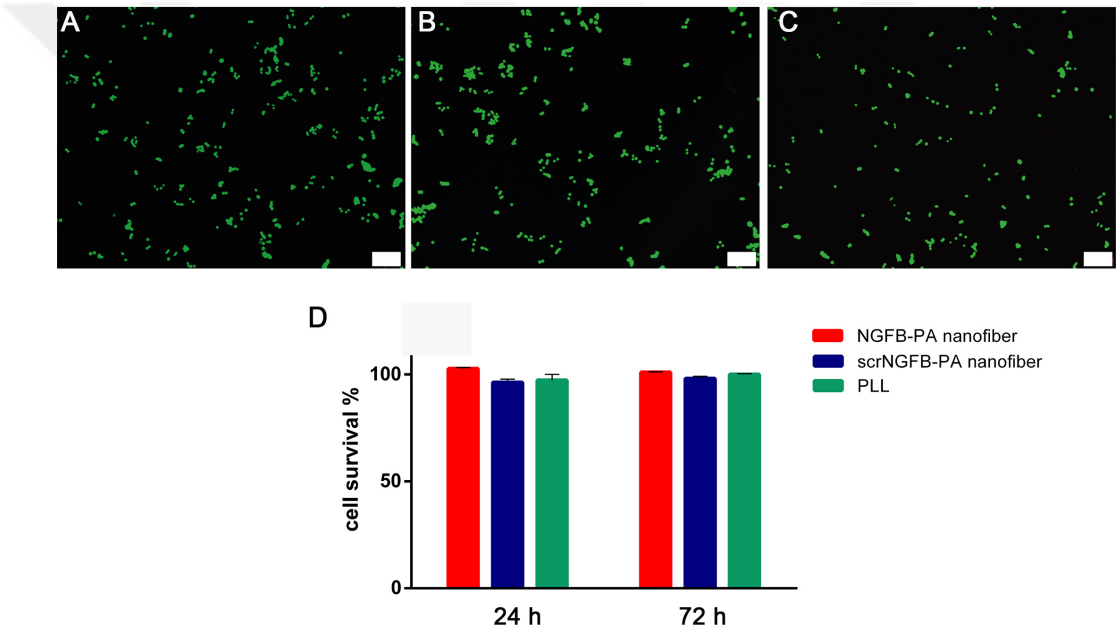

Figure 2.11: Viability of PC-12 cells cultured on NGFB-PA nanofiber (A), scrNGFB-PA nanofiber (B) and PLL (C) was analyzed by Alamar Blue Assay for 24 h (D) and 72 h (E) and representative images were taken after cells were co-stained with 2 μM calcein-AM (green) and 4 μM ethidium homodimer (red) in 1X PBS. Qualitative and quantitative results showed that peptide nanofibers were not toxic for PC-12 cells compared to PLL. No significant differences exist between cell survival percentages of cells cultured. Scale bar is 50 μm.

2.1.5 Analysis of neural differentiation of PC-12 cells cultured on PA nanofibers

PC-12 cells, a cell line derived from rat adrenal gland pheochromocytoma, are a commonly used model system to analyze the activity of different molecules on neural differentiation and axonal growth. [99] These cells express TrkA receptor, which is the high-affinity receptor of NGF. As such, these cells can be induced to terminally differentiate into neuron like cells in presence of NGF. [100, 101] Materials developed for peripheral nervous system regeneration should ideally promote neurite outgrowth, because this is one of the crucial steps of synapse formation during regeneration. In addition, improving the presentation efficiency of neurotrophic factors such as nerve growth factor to regenerating nerve cells is another crucial step of peripheral nervous system regeneration. Here, we aimed to enhance the interaction of NGF with PC-12 cells by using an NGF binding epitope in a PA scaffold for enhanced axonal outgrowth. In order to analyze the effect of the NGF-binding PA scaffold on neural differentiation, the lengths of neurites produced by PC-12 cells were measured. PC-12 cells cultured on NGFB-PA nanofibers were shown to have longer neurites than the scrNGFB-PA nanofiber group, and there were no significant differences between the cells cultured on NGFB-PA nanofiber and PLL (Figure 2.12D). In addition to the neurite length, significantly higher number of cells could extend neurites on the NGFB-PA nanofiber scaffold when compared to the scrNGFB-PA nanofiber scaffold (Figure 2.12E).

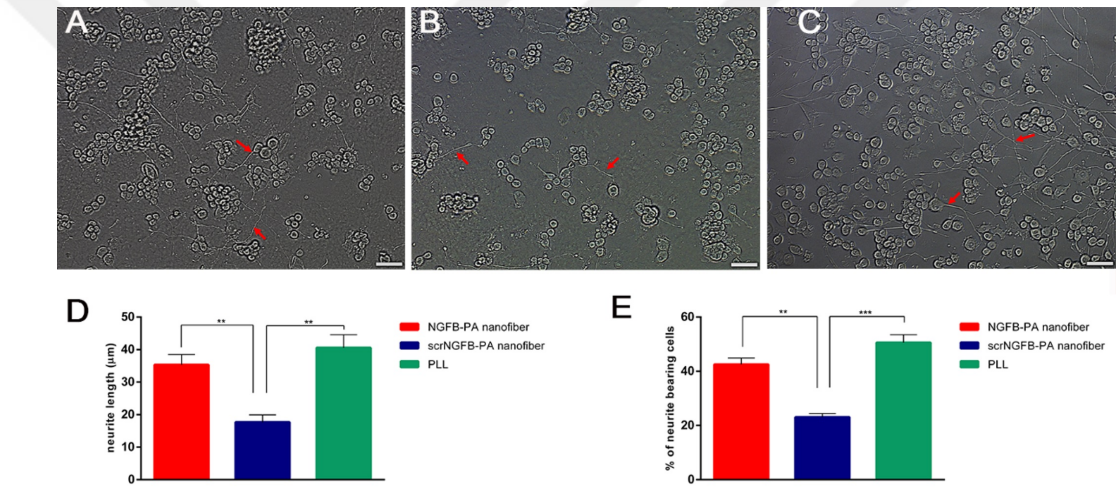

Figure 2.12: NGFB-PA nanofiber enables the extension of much longer neurites than the scrNGFB-PA nanofiber. Light microscope imaging of PC-12 cells cultured and differentiated on NGFB-PA nanofiber, scrNGFB-PA nanofiber and PLL in presence of 20 ng/mL NGF at six days after induction are shown in (A), (B) and (C) respectively (scale bar = 50 μm). Images were taken at 200x magnification. Neurite length (D) and percentage of neurite-bearing PC-12 cells (E) quantified by ImageJ on day 6 after induction shows that the incorporation of NGF-binding epitope into the PA scaffold was able to induce neurite outgrowth. **P<0.01 and ***P<0.001. Statistical analyses were performed with one-way ANOVA with Bonferroni posthoc analysis, n=3).

In order to further analyze the differentiation of PC-12 cells into neuron-like cells on PA scaffolds, the expression of βIII-tubulin, a general neuronal marker was analyzed with immunostaining (Figure 2.13). The βIII-tubulin is expressed almost exclusively in neurons and is used to separate neurons from glial cells, which do not express βIII-tubulin. [102] As shown in Figure 2.13, PC-12 cells cultured on NGFB-PA nanofiber scaffold are observed to extend more neurites and the number of PC-12 cells with neurites were higher than the cells cultured on scrNGFB-PA nanofiber scaffolds. These results also support the neurite length and percentage of neurite bearing cells quantification results described above.

For quantification of the expression levels of βIII-tubulin by PC-12 cells cultured on PA scaffolds, quantitative real time PCR (qRT-PCR) analysis for gene expression level and Western blot analysis of βIII-tubulin for protein expression level was performed. As shown in Figure 2.14, there was a significant increase in βIII-tubulin protein expression in PC-12 cells cultured on NGFB-PA nanofiber, compared the cells cultured on scrNGFB-PA nanofiber. As such, it is likely that βIII-tubulin expression is stimulated in cells differentiated on NGFB-PA nanofiber scaffold. As shown in Figure 2.15, there was no significant difference between NGFB-PA nanofiber and scrNGFB-PA nanofibers in terms of gene expression analysis of βIII-tubulin. Therefore, it could be concluded that βIII-tubulin is regulated at protein level rather than gene expression level and its expression was increased in PC-12 cells cultured on NGFB-PA nanofiber scaffolds.

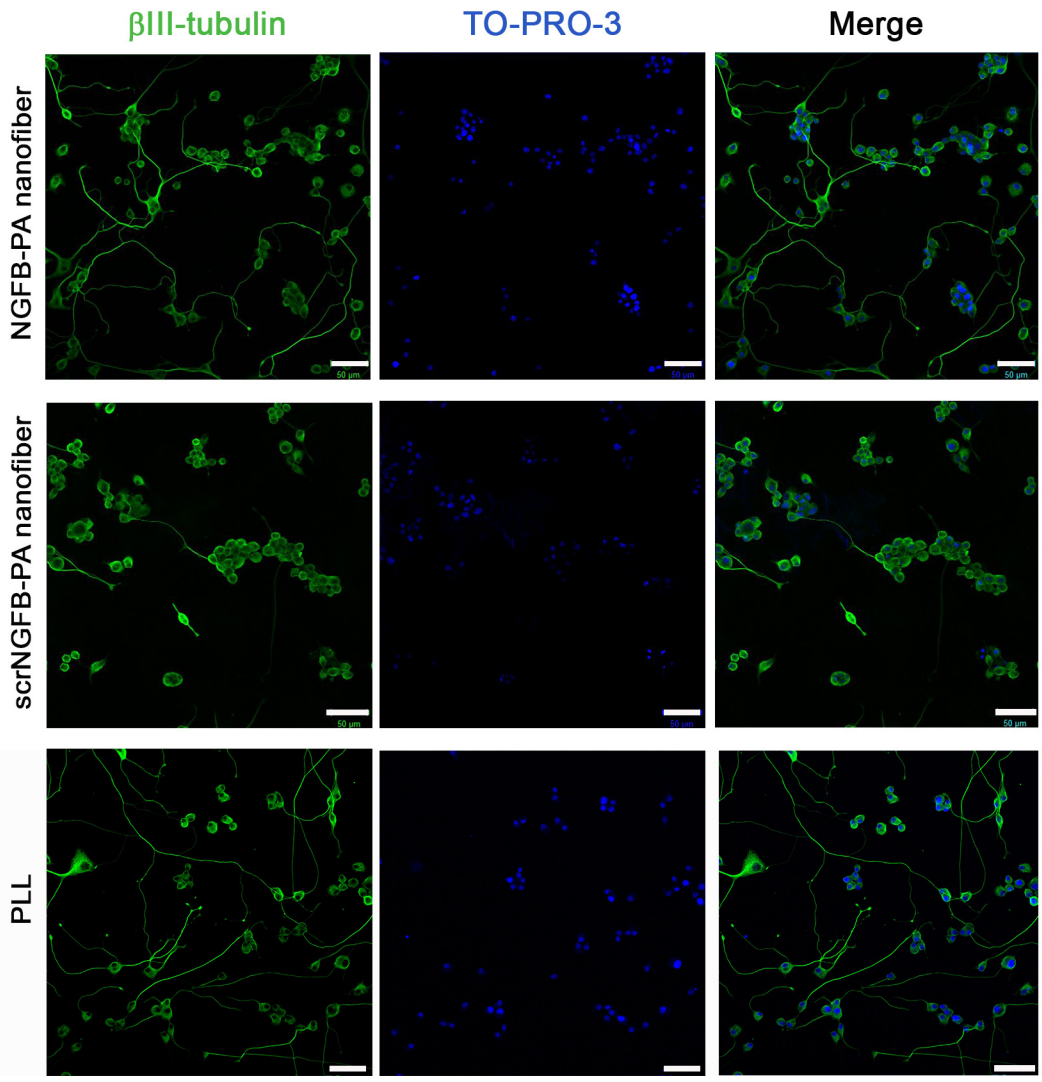

Figure 2.13: Immunostaining of PC-12 cells against βIII-tubulin on NGFB-PA nanofiber, scrNGFB-PA nanofiber and PLL after six days of culture and induction for neural differentiation in the presence of 20 ng/mL NGF. Higher expression of neural marker βIII-tubulin was clear in PC-12 cells cultured on NGFB-PA nanofiber and positive control group (PLL). Nuclei were stained with TO-PRO-3 and images were taken with confocal microscopy at 200x magnification.

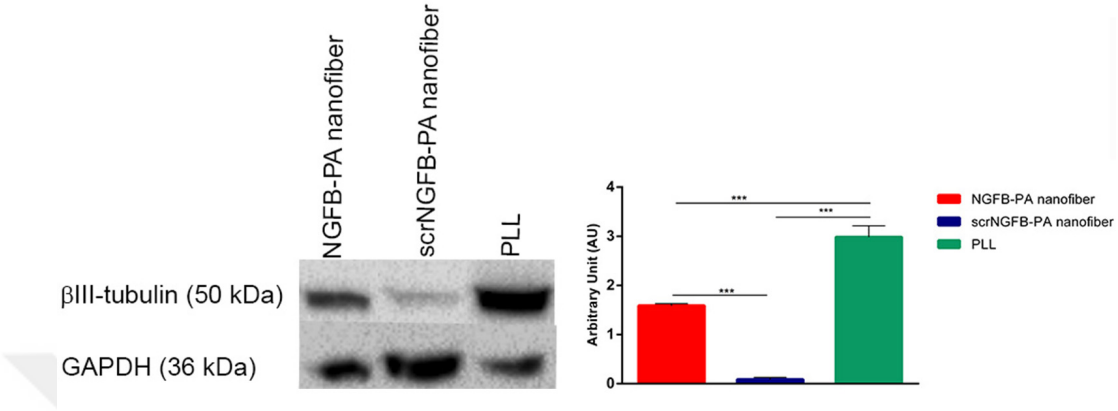

Figure 2.14: βIII-tubulin expression was enhanced in PC-12 cells after 6 days of culture and induction for neural differentiation on NGFB-PA nanofiber in the presence of 20 ng/mL NGF, whereas lower expression was observed in cells cultured on scrNGFB-PA nanofiber scaffold. The density of the bands was evaluated by Image J and normalized to GAPDH signal. Western blot analysis revealed that βIII-tubulin expression in NGFB-PA nanofiber was almost 2 folds higher than scrNGFB-PA nanofiber. Data are presented as means $\pm$ SEM and ***P<0.001.

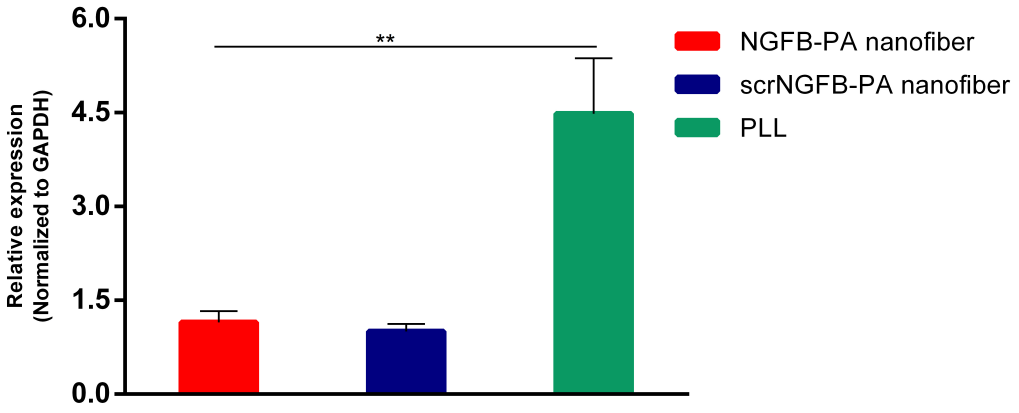

Figure 2.15: There is no significant difference in βIII-tubulin gene expression levels in PC-12 cells differentiated on NGFB-PA nanofiber and scrNGFB-PA nanofiber scaffolds. Data are presented as means ± SEM and **P<0.01

MAPK pathway is one of the major pathways implicated in the NGF-induced neural differentiation process. During the differentiation of PC-12 cells into neuron like cells, NGF binds to TrkA receptor and induces the phosphorylation of MEK1/2 protein complex (pMEK1/2), which also induces the phosphorylation of ERK1/2. [58, 103] Phosphorylated ERK1/2 protein complex (pERK1/2) is then activated and translocate into the nucleus and enable the transcription of genes responsible for the differentiation of PC-12 cells. [57] In order to determine whether the NGFB-PA nanofiber scaffold enhances the MAPK pathway, PC-12 cells were cultured on PA scaffolds and induced for neural differentiation for 24 h in presence of 20 ng/mL NGF. pMEK1/2 and pERK1/2 levels were subsequently examined via Western blotting. As shown in Figure 2.16A, PC-12 cells cultured on NGFB-PA nanofiber were observed to express lower levels of MEK1/2 than cells cultured on PLL, but the expression of pMEK1/2 was increased eight-fold in the cells cultured on NGFB-PA nanofiber compared to the cells cultured on scrNGFB-PA nanofiber and PLL (Figure 2.16B). In addition, it was shown that the expression of pERK1/2 was fivefold higher in PC-12 cells cultured on NGFB-PA nanofiber than the cells cultured on scrNGFB-PA nanofiber, and two-fold higher than the cells cultured on PLL (Figure 2.17B). The ERK1/2 protein expression could not be detected in both NGFB-PA nanofiber and scrNGFB-PA nanofiber groups (Figure 2.17A). Taken together, these results suggest that NGF

binding PA scaffold synergistically enhances the NGF-induced MAPK pathway to induce differentiation of PC-12 cells.

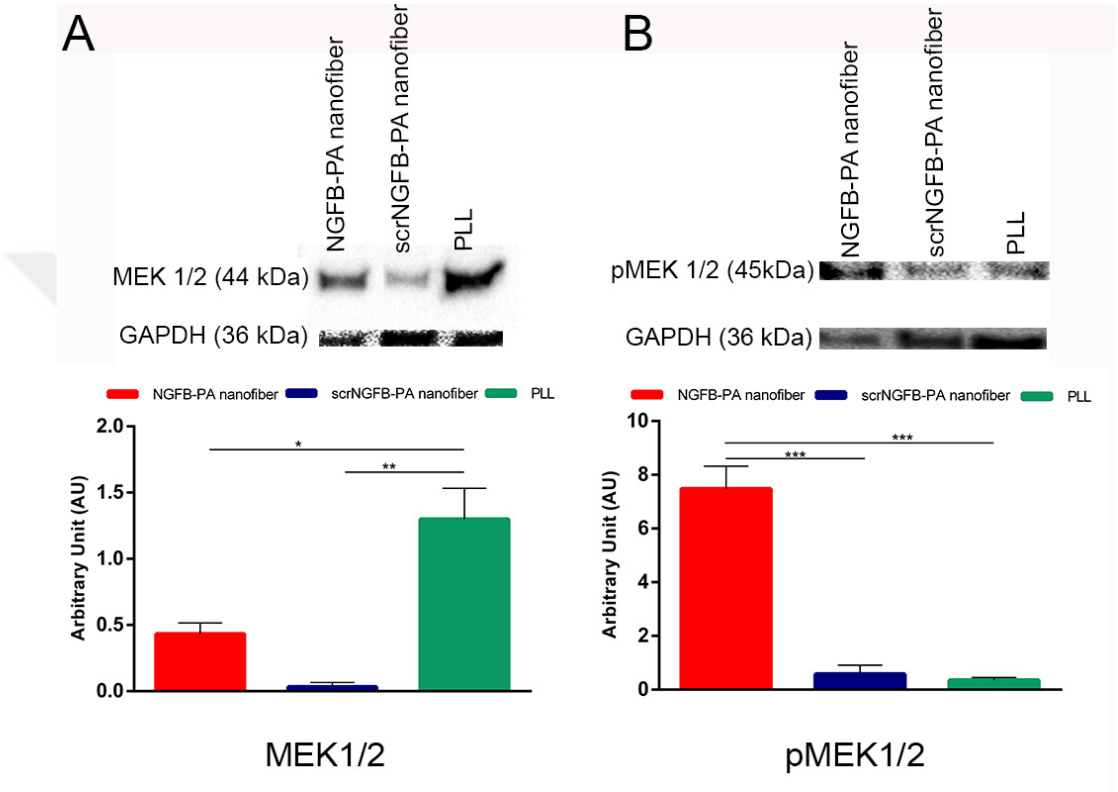

Figure 2.16: PC-12 cells were cultured on NGFB-PA nanofiber, scrNGFB-PA nanofiber and PLL, and induced for neural differentiation with 20 ng/mL of NGF. 1 day after induction, the expression levels of downstream proteins of the NGF pathway (MEK1/2 (A) and pMEK1/2 (B)) were analyzed with Western blot. Density of bands was evaluated by Image J and normalized to GAPDH signal. Western blot analysis revealed that pMEK 1/2 expression in NGFB-PA nanofiber was almost 8 folds higher than scrNGFB-PA nanofiber and positive control group (PLL). Data are presented as means ± SEM and *P<0.05, **P<0.01 and ***P<0.001.

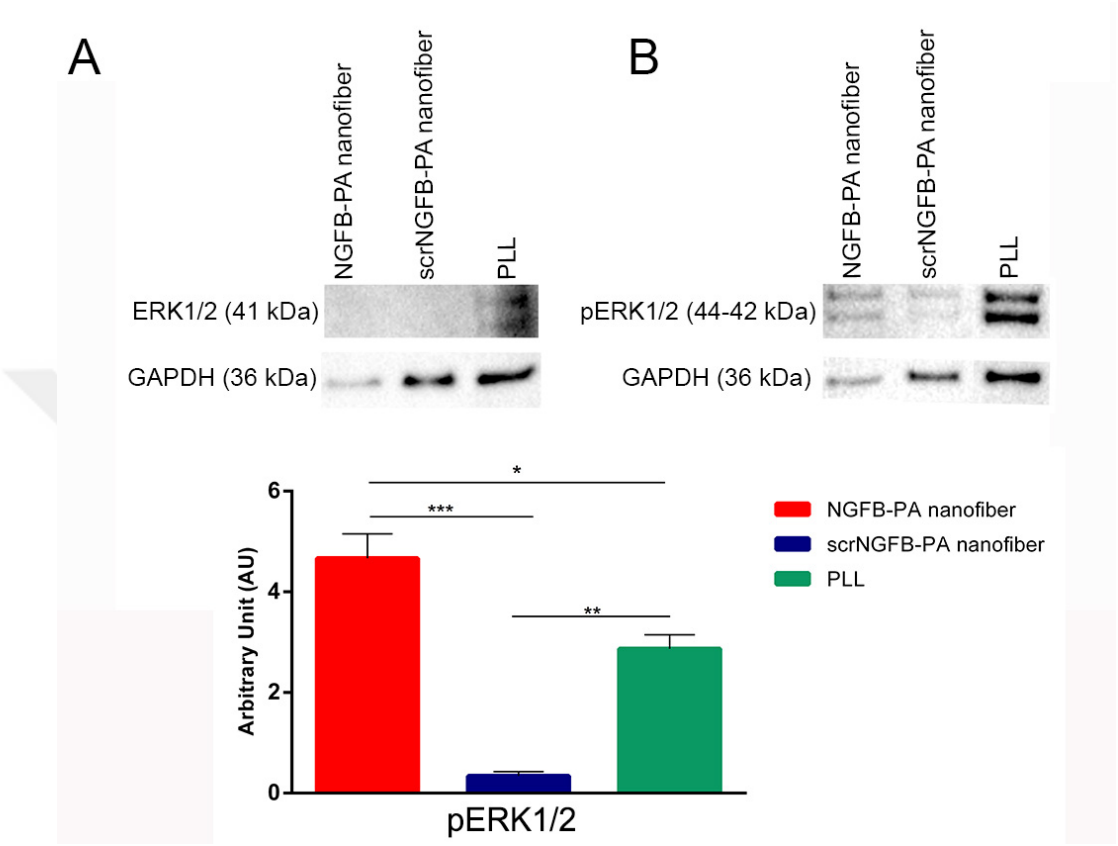

Figure 2.17: PC-12 cells were cultured on NGFB-PA nanofiber, scrNGFB-PA nanofiber and PLL, and were induced for neural differentiation with 20 ng/mL of NGF. 1 day after induction, the expression levels of downstream proteins of the NGF pathway (MEK1/2 (A) and pMEK1/2 (B)) were analyzed with Western blot. Density of bands was evaluated by Image J and normalized to GAPDH signal. Western blot analysis revealed that pERK 1/2 expression on NGFB-PA nanofiber was almost 5 folds higher than scrNGFB-PA nanofiber and 2 folds higher than positive control group (PLL). Data are presented as means ± SEM and *P<0.05, **P<0.01 and ***P<0.001.

2.1.6 Toxicity analysis of PA nanofibers on rat Schwann cells

Since the aim of designing the NGFB-PA nanofiber was to enhance peripheral nervous system regeneration and obtain functional recovery from injury, the biocompatibility of PA scaffolds for rat Schwann cells was analyzed with live/dead assay for 72 h. According to the results shown in Figure 2.18, it was shown that NGFB-PA nanofiber scafffold is biocompatible for Schwann cells and no significant differences were observed among the groups.

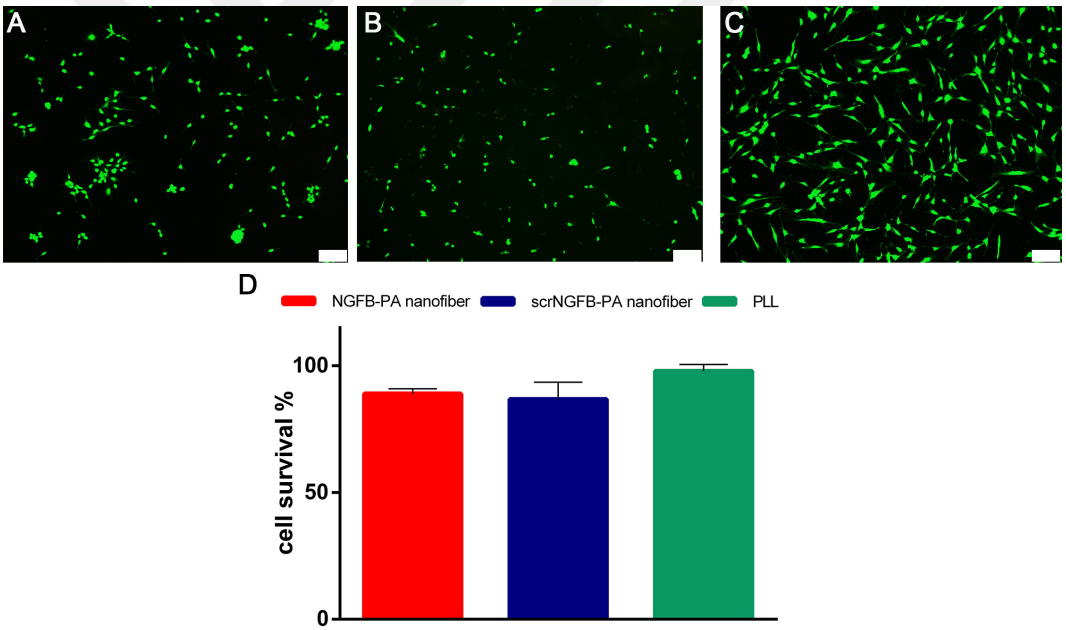

Figure 2.18: Viability of Schwann cells cultured on NGFB-PA nanofiber (A), scrNGFB-PA nanofiber (B) and PLL (C) was analyzed by Live/Dead Assay for 72 h (D). Qualitative and quantitative results showed that peptide nanofibers were biocompatible for Schwann cells compared to PLL. No significant results exist between cell survival percentages of cells cultured. Scale bar is 50 μm.

2.2 Discussion

NGF is one of the most widely studied neurotrophic factors because of its importance in survival and differentiation of sensory neurons. The role of NGF in peripheral nervous system has been widely studied. It is well-known that SCs produce NGF after injury, and that the gradient of NGF enables broken nerve ends to extend their axons through the injury site to overcome degeneration. NGF binds to a high affinity receptor (TrkA) expressed by nerve cells and activates signaling pathways such as MAPK pathway, Akt pathway and PKC pathway for the survival and differentiation of nerve cells. Besides the PNS, the role of NGF in central nervous system is also being investigated and NGF binding domain was discovered in myelin oligodendrocyte protein, which was shown to directly bind to NGF and modulate central axon circuitry. [71] Because of these crucial roles of NGF in the nervous system, it is important to develop therapeutic strategies for the efficient presentation of NGF to nerve cells. Several controlled delivery studies were performed for NGF, but there are concerns about the safety of these methods. [104–106] Furthermore, development of a material that is able to mediate the interactions between injured neural cells and NGF that is naturally secreted by surrounding cells would be safer and more effective than materials that release exogenous NGF to the wound environment. [104, 107] In this study, we developed a synthetic peptide nanofiber scaffold material, which binds to NGF-β with high affinity and promotes axonal outgrowth *in vitro*. A phage display library containing randomly displayed seven-amino acid peptide sequences was used in order to find peptide sequences exhibiting strong affinity for NGF-β. Then, the DNA of selected phage clones was sequenced to obtain the epitope sequences. Among these sequences, three of them were expressed by four different clones since they were selected as candidate clones for further affinity analysis. Their affinity for NGF-β was analyzed with phage ELISA, and clone number 3 (NGF3) was observed to have higher affinity for NGF-β and was therefore chosen as an effective candidate for further analysis.

The epitope sequence expressed by NGF3 was incorporated into a peptide amphiphile structure that is capable of self-assembling into stable, gel-like nanofiber

scaffolds. [108] Reverse solid phase peptide synthesis method was utilized for the synthesis of the bioactive PA molecule, as this method was previously reported to resemble the manner in which peptide sequences are displayed on the M13 phage surface. [109] The NGFB-PA contains both hydrophobic and hydrophilic residues, which enable its self-assembly through electrostatic interactions and hydrophobic collapse in order to generate ordered structures. The availability of the bioactive sequence and the biocompatibility of the material for cells are critical for design of nanofiber scaffolds, and can be controlled by adjusting the concentration, hydrogen bonding and charge properties of the material. [110, 111] In our previous study, the optimal charge condition for PC-12 cells was determined as neutral at pH 7.4. [92] Therefore, the net charge of the nanofibrous scaffolds used in this study was also adjusted as neutral at pH 7.4. The biocompatibility of the PA nanofiber scaffolds was analyzed with Alamar Blue assay and both NGFB-PA nanofiber and scrNGFB-PA nanofiber combinations were found to be biocompatible for PC-12 cells at a concentration of 1.5 mM when compared to PLL. The availability of the epitope for the binding pocket of the affine molecule is also critical for the development of protein-binding molecules, and can be controlled by the concentration and charge properties of the scaffold. In this study, the affinity of NGF-β for the developed NGFB-PA nanofiber was analyzed with ELISA. For antibody development strategies, the affinity of the developed antibody for the target molecule is concentration-dependent and the affinity reaches to a plateau after binding pocket is filled with the epitope. Three different PA scaffold concentrations and two different NGF-β concentrations were used to determine whether the interaction between NGF-β and scaffold is concentration-dependent. The bioactive NGFB-PA nanofiber group was observed to exhibit a similar, concentration-dependent binding profile with the NGF antibody-NGF-β binding interaction. A significant difference was also observed between the affinities of NGFB-PA nanofiber and scrNGFB-PA nanofiber groups at both 10 ng/mL and 50 ng/mL NGF-β concentrations, suggesting that the strong affinity between NGF-β and NGFB-PA nanofiber is sequence-specific.

The effect of the affinity of NGFB-PA nanofiber for NGF-β on neurite outgrowth was then analyzed *in vitro* by using PC-12 cells by quantifying neurite

length and percentages of neurite-bearing cells. NGFB-PA nanofiber induced PC-12 cells to extend much longer neurites than the scrNGFB-PA nanofiber group, and that the number of neurite-bearing cells was also increased in the NGFB-PA nanofiber group. These results were then confirmed by analyzing the expression of a general neural marker (βIII-tubulin) by immunostaining and Western blot analyses, which confirmed the prior observation that NGFB-PA nanofiber induces differentiation of PC-12 cells into neuron-like cells. The gene expression level of βIII-tubulin was also analyzed by quantitative real time PCR (qRT-PCR) and together with western blot analysis it was shown that βIII-tubulin expression was upregulated in PC-12 cells cultured on NGFB-PA nanofibers and PLL and expression of βIII-tubulin was regulated at protein level.

The most challenging step of developing a growth factor-binding material is to enhance the binding of growth factor to its cell surface receptor, which initiates the downstream signaling pathways for differentiation of cells. [100, 112] Ras pathway and MAPK pathway are two distinct signaling cascades in PC-12 cells which are induced by NGF for survival and differentiation of PC-12 cells. [113] It was previously shown that MAPK pathway is necessary and sufficient for PC-12 differentiation when stimulated by NGF. [114] ERK1/2 belongs to the MAPK family and is phosphorylated in response to NGF stimulation by MEK, which causes the induction of the genes responsible for cell proliferation and differentiation. [101, 115] In order to check whether PC-12 cells cultured on NGFB-PA nanofibers are induced to differentiate into neuron-like cells by NGF stimulation, phosphorylation levels of MEK-ERK1/2 proteins were analyzed with Western blotting. According to the results, the expression of MEK1/2 and ERK1/2 levels were decreased while the levels of pMEK1/2 and pERK1/2 proteins were significantly increased in PC-12 cells cultured on NGFB-PA nanofiber when compared to PLL. The scrNGFB-PA nanofiber scaffold was found not to activate the MAPK pathway, which also shows that NGFB-PA nanofiber scaffold is a selective biomaterial for neural differentiation purposes.

Finally, the biocompatibility of NGFB-PA nanofiber was analyzed for primary rat SCs because the further aim of developing NGF-binding PA nanofiber is to enhance functional recovery from PNS and CNS injuries. Since SCs are the glia

cells of PNS, the biocompatibility of developed material for SCs is also important. According to viability assay of SCs cultured on NGFB-PA nanofibers, it was shown that NGFB-PA nanofiber was compatible for SCs. Therefore, it can be concluded that NGFB-PA nanofiber is a good candidate for studying PNS injury regeneration.

Chapter 3

Materials and Methods

3.1 Materials

The Ph.D.^{TM}-7 Phage Display Peptide Library was purchased from New England Biolabs. *Echerichia coli* strain XL1Blue (recA1 endA1 gyrA96 thi-1 hsdR17 supE44 relA1 lac [F′ proAB lacIq ZM15 Tn10 (Tetr)]) was courtesy of Professor Alper Arslanoğlu from Izmir Institute of Technology, Molecular Biology Department (Izmir, Turkey). Nerve growth factor-β (NGF-β) was purchased from Thermo Fisher Scientific. HRP/Anti-M13 monoclonal conjugate was purchased from GE Healthcare Life Sciences. LB broth, agar, NaCl, polyethylene glycol 8000 (PEG), Tris-HCl, sodium azide, sodium bicarbonate ($NaHCO_3$), ethylene diamine tetra-acetic acid (EDTA), bovine serum albumin (BSA) and other chemicals were purchased from Sigma-Aldrich. Glycine-HCl was purchased from Alfa Aesar. Isopropyl β-D-1-thiogalactopyranoside (IPTG) was purchased from Amresco. 5-Bromo-4-Chloro-3-Indolyl-Beta-G (XGAL) was purchased from Biotium. 9-Fluorenylmethoxycarbonyl (Fmoc) and tert-butoxycarbonyl (Boc) protected amino acids, [4-[a-(20, 40-dimethoxyphenyl)Fmocaminomethyl] enoxy]acetamidonorleucyl-MBHA resin (Rink amide MBHA resin) and 2-(1H-benzotriazol-1-yl)-1,1,3,3-tetramethyluronium hexafluorophosphate (HBTU)

were purchased from NovaBiochem and ABCR. Poly-L-lysine (PLL) was purchased from Trevigen. Live/Dead Assay and other cell culture materials were purchased from Invitrogen. ELISA reagents were purchased from Invitrogen. Paired antibodies for NGF were purchased from R&D systems. Antibodies for immunocytochemistry and western blot analyses were purchased from Abcam and Millipore. Other chemicals mentioned in this thesis were purchased from Fisher, Merck, Alfa Aesar or Aldrich. All chemicals were used as provided.

3.2 Media and solution preparation for phage library screening

LB Medium: LB medium containing 10 g bacto-tryptone, 5 g yeast extract, 5 g NaCl was dissolved in ddH_2O and autoclave sterilized, and stored at 4 ^oC for further use.

IPTG/Xgal Stock: 1.25 g IPTG (isopropyl--D-thiogalactoside) and 1 g Xgal (5-Bromo-4-chloro-3-indolyl--D-galactoside) were dissolved in 25 mL DMF (dimethyl formamide). The solution was stored at -20 ^oC under dark conditions.

LB/IPTG/Xgal Plates: LB agar was dissolved in ddH_2O and autoclave sterilized. The solution was cooled to 55 ^oC, and 1 mL IPTG/Xgal stock per liter was added to the medium solution. Then the solution was poured into plastic petri dishes and plates were stored at 4 ^oC in the dark.

LB/Tetracycline Plates: 50 mg/mL tetracycline stock was prepared in 95% ethanol and filter sterilized. Then, the solution was stored at -20 ^oC in the dark. LB agar was dissolved in ddH_2O and autoclave sterilized. The solution was cooled to 55 ^oC, and 1 mL tetracycline stock stock per liter was added to the medium solution. Then the solution was poured into plastic petri dishes and plates were stored at 4 ^oC in the dark.

Top Agar: LB and 7g bacto-agar were dissolved in ddH_2O and autoclave

sterilized. Then, the solution was dispensed into 50 mL aliquots and stored at room temperature. When necessary, the solution was melted in microwave.

Blocking Buffer: Blocking buffer was prepared as dissolving 0.1 M $NaHCO_3$ (pH 8.6), 5 mg/mL BSA and 0.02% NaN_3 in ddH_2O. The solution was filter sterilized and stored at 4 ^oC.

PEG/NaCl: PEG/NaCl solution was prepared by dissolving 20% (w/v) polyethylene glycol-8000 and 2.5 M NaCl in ddH_2O. The solution was then autoclaved, and mixed well to combine separated layers while still warm.

Iodide Buffer: Iodide Buffer was prepared by dissolving 1 mM EDTA, 4 M sodium iodide (NaI) and 10 mM Tris-HCl (pH 8.0) in ddH_2O. The solution was stored at room temperature in the dark.

3.3 Phage library screening against NGF

Library screening was performed against NGF according to the manufacturers instructions (New England Biolabs). NGF (10 μg/mL for each well) was dissolved in 100 μL of 0.1 M $NaHCO_3$ (pH 8.6), coated on the wells of a 96-well tissue culture plate by swirling and incubated overnight at 4 ^oC with agitation in a sealed box with a damp paper. Then, the plate was blocked with blocking buffer (0.5% (w/v) bovine serum albumin (BSA) in 0.1 M $NaHCO_3$ (pH 8.6) for at least 1 h at 4 ^oC. Blocking buffer was washed 6 times with Tris-buffered saline pH 7.5 + 0.1% (v/v) Tween 20 (TBS-T). Then, Ph.D.-7 Phage Display Library with a complexity of 1.9 x 10^9 plaque forming units (pfu) was added at approximately 1 x 10^{11} pfu in 0.1% TBS-T into each well and incubated at room temperature for 1 h. Unbound phages were washed 10 times with 0.1% TBS-T, while bound phages were eluted with 0.2 M glycine-HCl (pH 2.2) containing 1 mg/mL BSA for no more than 10-20 min at room temperature, and this reaction was neutralized by adding 1 M Tris-HCl (pH 9.1). Eluates from the first two rounds were amplified and titered with XL1Blue and, for the second and third rounds, the percentage

of Tween-20 was increased to 5% (v/v) for washing steps. After the third round of screening, the eluates were not amplified but titered; and 24 random plaques from the third round of titering was selected for sequence identification.

3.4 Phage titering

5-10 mL of LB medium was inoculated with XL1Blue from LB/tetracycline /XL1Blue plates overnight at 37 ^{o}C in shaking incubator at 200 rpm. The next day, the grown XL1Blue cells were diluted at 1:10 ratio in 5 mL LB medium and grown at 37 ^{o}C for around 4 h until the cells reached at mid-log phase (OD $\sim$ 0.5). While cells were growing, top agar was melted in microvawe and dispensed as 3 mL into sterile culture tubes, one per expected phage dilution. The tubes were maintained at 45 ^{o}C. The LB/IPTG/Xgal plates were pre-warmed for at least 1 h at 37 ^{o}C. For unamplified phages, 10^1 to 10^4 and for amplified phages, 10^8 to 10^{11} serial dilutions were prepared in LB. After cells reached to mid-log phase, 200 μL for each dilution was dispensed into microfuge tubes. 10 μL of each phage dilution was added to each tube, vortexed for 10 s and incubated at room temperature for 1-5 min. The infected cells were transferred as one infection at a time to top agar containing culture tubes. After mixed quickly, the solution was poured onto pre-warmed LB/IPTG/Xgal plates. The plate was tilted and rotated to spread top agar evenly. After plates were cooled for 5 min at room temperature, they were incubated at 37 ^{o}C overnight. The next day, blue plaques were counted from the dilution group which had approximately 100 plaques. Each number was multiplied by dilution factor for that plate in order to get the phage titer in plaque forming units (pfu) per 10 μL.

3.5 Amplification of phage eluates

For amplification of phage eluates, XL1Blue cells were cultured overnight in 5-10 mL LB at 37 ^{o}C in shaking incubator. The next day, the culture was diluted at

1:100 ratio in 20 mL LB per each group. Phage eluate was added into diluted culture and incubated for 4.5 h at 37 ^{o}C at 250 rpm. Then, the culture was transferred to ultracentrifuge tube and spinned for 10 min at 12,000 g at 4 ^{o}C. The supernatant was transferred to fresh ultracentrifuge tube and re-spinned. Then, upper 80% of the supernatant was transferred to a fresh tube and 1/6 volume of 20% PEG/2.5 M NaCl was added. The phage was precipitated overnight at 4 ^{o}C and spinned at 12,000 g for 15 min at 4 ^{o}C. The supernatant was discarded and the tube was re-spinned and the residual supernatant was discarded by pipette. The pellet was dissolved in TBS and transferred to microcentrifuge tube. The suspension was then spinned at 14,000 rpm for 5 min at 4 ^{o}C to pellet residual cells. The supernatant was transferred into fresh microfuge tube and reprecipitated by adding 1/6 volume of 20% PEG/2.5 M NaCl and incubated on ice for around 60 min. Then, PEG precipitate was microcentrifuged at 14,000 rpm for 10 min at 4 ^{o}C. The supernatant was removed and re-spinned and the residual supernatant was removed with micropipet. The pellet was dissolved in 200 μL TBS and microcentrifuged for 1 min to pellet any remaining insoluble material. The supernatant, which is the amplified eluate, was transferred to a fresh tube and stored at either for 1 week at 4 ^{o}C or mixed with sterile glycerol in 1:1 ratio and stored at -20 ^{o}C for long term.

3.6 DNA sequence analysis

For the identification of peptide sequences from selected phage plaques, DNA was isolated from each individual plaque as described in the manufacturers instructions (New England Biolabs). Each individual clone was amplified and precipitated in 20% (w/v) PEG/2.5 M NaCl. After centrifugation at 14,000 rpm for 10 min at 4 ^{o}C, the pellet was dissolved in an iodide buffer containing 10 mM Tris-HCl (pH 8.0), 1 mM ethylene diamine tetra-acetic acid (EDTA), and 4 M NaI. Phage DNA was subsequently precipitated with absolute ethyl alcohol and dissolved in DNase/RNase free ultrapure water. DNA sequences were analyzed by using an automated DNA sequencer (Refgen Biotechnology, Ankara, Turkey) with the primer sequence 5′-CCCTCATAGTTAGCGTAACG-3′ (synthesized by

Sentegen Biotechnology, Ankara, Turkey).

3.7 Phage ELISA for the identification of binding selectivity of candidate phage clones

After sequence analysis, 3 of the peptide sequences were observed to be displayed by more than 2 phage clones (Figure 2.2). These sequences were selected for further analysis, and the affinity of one clone for each candidate peptide sequence was analyzed with phage ELISA by following manufacturers instructions. 10 μg/mL NGF (120 μL/well) was dissolved in 0.1 M $NaHCO_3$, immobilized on a Maxisorb (NUNC, Thermo Scientific) ELISA plate and incubated overnight at 4 ^{o}C in a sealed box with a damp paper. Wells were washed with 0.5% TBS-T and then blocked with blocking buffer for at least 1 h at 4 ^{o}C. The same number of wells in a separate ELISA plate were coated with blocking buffer as a negative control. Additionally, the same number of wells in a 96 well tissue culture plate were also coated with blocking buffer for phage dilution. After blocking and washing steps, the phage diluents (serially diluted at 1:8 ratios) in 0.1% TBS-T (100 μL/well) were incubated for 2 h at room temperature with agitation. The wells were washed 10 times with 0.5% TBS-T and incubated with 1:5000 horseradish peroxidase-conjugated anti-M13 monoclonal antibody (200 μL/well; GE Healthcare) in blocking buffer. After washing steps with 0.5% TBS-T, HRP substrate (3,3',5,5 -tetramethylbenzidine (TMB); 50 μL/well) was added. After 30 min of incubation, the reaction was stopped with sulfuric acid. The change in absorbance resulting from color formation was measured by a Spectramax M5 microplate reader (Molecular Devices) at 450 nm wavelength. Then, this value was subtracted from the reference value measured at 650 nm.

3.8 Synthesis and purification of PA molecules

NERALTL-GEEGAVVK(Lauryl)-Am, (NGFB-PA) and RNTLLAE-GEEGAVVK (Lauryl)-Am, (scrNGFB-PA) peptide amphiphile molecules were synthesized via Fmoc-based reverse solid phase peptide synthesis. Lauryl-VVAGKK-Am peptide amphiphile (KK-PA) molecule was synthesized via Fmoc-based solid phase peptide synthesis. Amino acid couplings were performed by using 2 equivalents of fluorenylmethyloxycarbonyl (Fmoc) protected amino acids, 1.95 equivalents of O-benzotriazole-N,N,N,N-tetramethyl-uronium-hexafluoro-phosphate (HBTU) and 3 equivalents of N,N-diisopropylethylamine (DIEA) for 3 h. After each coupling, remaining free amine groups were blocked by treating the resin with 10% acetic anhydride/DMF solution for 30 min. Fmoc protecting groups were removed by shaking the PA with 20% piperidine/DMF solution for 20 min. Between each step, resin was washed thoroughly with DMF, DCM and DMF, respectively. Mtt groups on lysine residues were removed by shaking the resin with 5% TFA cleavage cocktail containing TFA: TIS: H_2O: DCM at the ratio of 5: 2.5: 2.5: 90, 6 times in 5 min periods. Cleavage of the NGFB-PA and scrNGFB-PA from the resin and deprotection of side groups were carried out by shaking the peptide with a mixture of TFA: TIS: phenol: H2O in the ratio of 88: 5: 5: 2 for 2 h. Cleavage of the KK-PA from the resin and deprotection of side groups were carried out by shaking the peptide with a mixture of TFA: TIS: H_2O at the ratio of 95: 2.5: 2.5 for 3 h. The resin was washed with DCM after two h to collect the PA. DCM and TFA were removed by vacuum distillation. The remaining PA solution was triturated with ice-cold ether. The resulting white product was freeze-dried under vacuum. The PA was then characterized by LC-MS (LC-MS). Since the NGFB-PA and scrNGFB-PAs contain long aminoacid residues, large amounts of impurities were observed on LC-MS; therefore, the resulting peptides were purified further by preparative HPLC technique by using 0.1% NH_4OH-water and 0.1% NH_4OH-acetonitrile solutions as eluents. After removing acetonitrile, the peptide was freeze-dried and collected as a white powder. An Agilent Technologies 6530 Accurate-Mass Q-TOF LC-MS with ESI source and Zorbax Extend-C18 2.1 x 50 mm column for basic conditions and Zorbax SB-C8 4.6 mm x 100 mm column for acidic conditions was used to perform liquid chromatography-mass

spectrometry to characterize PA molecules. The concentration of the sample was adjusted as 1 mg/mL. A gradient of (a) water (0.1% NH_4OH-water) and (b) acetonitrile (0.1% NH_4OH-acetonitrile) solutions were used as eluents.

3.9 SEM imaging of PA nanofibers

Nanofiber networks formed by peptide amphiphiles were imaged by scanning electron miscroscopy (SEM). Oppositely charged PA solutions (1 wt% for NGFB-PA and scrNBP/PA, 0.44 wt% KK-PA) were mixed on a silicon wafer at a 1:1 volume ratio (final volume being 40 μL) to produce gels as used for cell culture experiments. Then, the gels were dehydrated by transferring to 20%, 40%, 60%, 80% and 100% v/v ethanol sequentially. After one more dehydration step in 100% alcohol, the gels were critical point dried by using Autosamdri-815B equipment from Tousimis. For imaging, dried gels were coated with 6 nm Au/Pd and SEM (FEI Quanta 200 FEG) images were taken at high vacuum mode with 15 keV beam energy by using an Everhart-Thornley Detector (ETD).

3.10 TEM imaging of PA nanofibers

A FEI Tecnai G2 F30 transmission electron microscope (TEM) was used for TEM imaging. 1.5 mM PA solutions were prepared in ddH_2O and aged overnight. PA solutions were mixed and incubated at room temperature for 1.5 h. PA gels were then diluted with water to a concentration of 2.0 x 10^{-4} M. 10 μL of solutions were dropped on carbon-covered copper grids and incubated for 10 min. Then, 2% (w/v) uranyl acetate solution was used for staining and the grids were washed with water after staining. Finally, carbon grids were dried in air overnight.

3.11 Circular Dichroism (CD) spectroscopy

Secondary structures of PA solutions were analyzed with JASCO J-815 CD spectrometer under inert nitrogen atmosphere. PA solutions were prepared at 2 x 10^4 M in 300 μL final volumes to produce nanofibers with neutral charge. The samples were measured from 350 nm to 190 nm with 0.1 data pitch, 100 nm/min scanning speed, 1 nm band width and 4 seconds Digital Integration Time (DIT). The average of three measurements were adjusted and sensitivity was selected as standard.

3.12 Zeta potential measurements

A Nano-ZS Zetasizer (Malvern) was used for measuring zeta potentials of PA solutions. Measurements were done at 25 ^{o}C and pH 7.0. PA solutions with 1.5 mM concentrations were prepared, mixed at 1:1 ratio as necessary, and diluted with ddH_2O to a final concentration of 5.0 x 10^{-5} M prior to the measurements. A dip cell was used for the measurements. Zeta potential converts measured mobility to zeta potential by using Smoluchowski equation.

3.13 Formation of PA nanofiber scaffolds

Formation of nanofiber scaffolds for *in vitro* experiments was performed by mixing oppositely charged PAs, which enables their self-assembly to higher-order nanofibers through the neutralization of the charges in the backbones of PA molecules. In this study, 2 different types of nanofibers were used. NGFB-PA (net charge is -2) as well as scrNGFB-PA (net charge is -2) were separately mixed with KK-PA (+2 charge) at a 1:1 molar ratio. scrNGFB-PA was used in order to determine the effect of sequence order on affinity of the epitope for NGF. All PAs were used at pH 7.4 for nanofiber formation.

3.14 Affinity analysis of PA nanofibers for NGF-β

ELISA method was used in order to analyze and compare the binding affinity of NGFB-PA, and scrNGFB-PA. Maxisorb ELISA plates (NUNC, Thermo Scientific) were coated overnight at 4 ^{o}C with blocking buffer or PA nanofibers prepared by mixing negatively and positively charged PAs. For each PA group, 0.1 M, 0.25 M and 0.5 M negatively charged PAs were mixed with 0.1 M, 0.25 M and 0.5 M positively charged PAs in equal volumes (50 μL for each PA molecule/well). In order to prevent false positive results, separate wells were coated with human NGF-β antibody and serially diluted NGF-β concentrations (from 500 ng/mL to 0 ng/mL). On the next day, the solutions were removed and the wells were washed with washing buffer (Tween 20 in 0.9% (w/v) NaCl solution, pH 7.4) and dried by tapping to towels to remove excess solution. It was previously shown that these plates have a high affinity for binding to a broad range of molecules with hydrophilic or hydrophobic properties, and therefore the plates were assumed to bind to PA molecules with high affinity even after extensive washing steps. The wells were then blocked with blocking buffer for 2 h and dried by tapping again. 3 empty plates were also blocked with blocking solution in order to preclude the possibility of nonspecific binding by anti-NGF-β. Then, 10 ng/mL and 50 ng/mL NGF-β in blocking solution were added to separate wells and incubated overnight at 4 ^{o}C. Next day, the solution was removed and the wells were washed with washing buffer, dried and incubated for 30 min following the addition of biotinylated antibody against human NGF-β (R&D systems), streptavidin-conjugated horseradish peroxidase (HRP) and HRP substrate (3,3,5,5-tetramethylbenzidine (TMB). After 30 min of incubation, sulfuric acid was added to stop the reaction. The change in color was measured as absorbance change by a Spectramax M5 Microplate Reader (Molecular Devices) at 450 nm wavelength and subtracted from the reference value, which was measured at 650 nm wavelength. All treatments were performed with 3 replicates and shown as mean standard deviation. Experiments were repeated at least two times independently.

3.15 Viability assay of PC-12 cells

96-well plates were coated with PA scaffolds and 0.01% PLL solution as described in the neurite outgrowth assay protocol above. 1.5 x 10^4 PC-12 cells were seeded for each well in growth medium and cultured for 24 h and 72 h. The medium was discarded on the day of analysis (24 h or 72 h) and fresh medium containing 10% Alamar Blue reagent (Invitrogen; 100 μL/well) was added to the wells. As a control, in a separate 96 well plate, wells were coated with same groups and the mixture was added on these wells in the absence of cells. The plates were incubated until the pinkish color was observed in experimental groups. Then, the medium in the wells was transferred into empty wells and absorbance was measured at 570 nm wavelength by using a Spectramax M5 microplate reader. As a reference, the wells were read at 600 nm and this value was subtracted from the first measurement. For imaging of the viability of PC-12 cells, the cells were co-stained with 2 μM calcein-AM (Invitrogen) for imaging of live cells and 4 μM ethidium homodimer (Invitrogen) for imaging of dead cells in 1X PBS for 30 min. Then, the representative images of the cells were taken with Zeiss Inverted Fluorescent Microscope at 100X magnification.

3.16 PC-12 neurite extension assay

Equal volumes of (40 μL) 1.5 mM NGFB-PA and KK-PA and 1.5 mM scrNGFB-PA and KK-PA were mixed to form gels at pH 7.4 in 96-well plate. After mixing the PAs, the plates were incubated at 37 ^{o}C for 45 min and then dried overnight in a laminar flow hood at room temperature for solvent evaporation. Because PC-12 cells are suspension cells and don't attach to tissue culture plate, 0.01% poly-L-lysine (PLL; Invitrogen) coating on surfaces (50 μL/well) were performed and used as positive control for all cell culture experiments.Then, PA-coated plates were UV sterilized for 1 h in a laminar flow hood. 5 x 10^3 PC-12 cells/well were seeded on coated surfaces in Roswell Park Memorial Institute medium (RPMI) with 10% horse serum (HS), 5% fetal bovine serum (FBS), 2 mM L-glutamine

and 1% penicillin/streptomycin (P/S). On the day after seeding PC-12 cells, culture medium was changed with neural induction medium consisting of minimal essential medium (MEM) with 2% HS, 1% FBS, 2 mM L-glutamine and 1% P/S along with 20 ng/mL NGF-β. At day three, half of the medium was discarded and neural induction medium containing 40 ng/mL NGF-β (final concentration was 20 ng/mL) was added to the wells. At day six after neural induction with NGF, optical images of the cells were taken at 5 random points of each well at 200x magnification. Total neurite length in each image was quantified by using ImageJ and normalized to cell numbers per image. Average neurite length was obtained from three replicate wells for each coating material. Neurite-extending cells were also counted in the same images by ImageJ and the percentage of cells with neurites was calculated. Cellular extensions spanning at least one cell body length were considered as neurites for quantifications.

3.17 Immunofluorescent staining of PC-12 cells against βIII-tubulin

13 mm glass coverslips placed in 24-well plates were coated with equimolar concentrations of PA solutions (60 μL/PA, 120 μL total volume) as described above. 3 x 10^4 PC-12 cells were seeded per well in culture medium and cells were induced for neural differentiation a day after with neural induction medium containing 20 ng/mL NGF. Six days after neural induction, cells were fixed with 4% paraformaldehyde, permeabilized with 0.3% TritonX-100 in 1X PBS, blocked with 10% goat serum and incubated with antibodies against βIII-tubulin (Abcam) at 1:500 dilution overnight at 4 ^{o}C. After washing with PBS several times, cells were incubated with goat-anti mouse IgG (H+L) Alexa Fluor 488 (Millipore) at 1:500 dilution for 1 h at room temperature. After washing steps, cells were incubated with 1 μM TO-PRO-3 (Invitrogen) in PBS at 1:2000 dilution for 15 min at room temperature in order to counter-stain nuclei, after which they were washed with PBS several times. Coverslips were then mounted with Prolong Gold Antifade Reagent (Invitrogen) and sealed with nail polish. Images were

taken with confocal microscopy (Zeiss LSM510) at 200x magnification.

3.18 Gene expression analysis of PC-12 cells

Gene expression profiles of PC-12 cells differentiated on PA scaffolds and PLL were assessed by quantitative real time PCR (qRT-PCR). PA coatings were performed by mixing equimolar concentration (1.5 mM from each PA) of positively and negatively charged PA solutions (400 μM from each PA) in 6 well plates. PA coating was followed as described in PA concentration optimization section. Then, 1 x 10^5 PC-12 cells/well were seeded on wells in growth medium. Induction was also performed as described in PA concentration optimization section. At day six after neural induction, RNA samples were isolated from each group by using TRIzol reagent (Invitrogen) according to manufacturers instructions. Briefly, cells were homogenized with TRIzol reagent and 1/5 v/v chloroform was added into the samples. Then, samples were kept at room temperature for 2-3 min and then centrifuged for 17 min at 15000 rpm at 4 ^{o}C. The resulting aqueous upper phase (clear) containing the RNA was transfered into a fresh microfuge tube. 1/2 (v/v) isopropanol was added to the RNA containing phase and mixed 15 times (up and down) and then centrifuged for 12 min at 15000 rpm at 4 ^{o}C. Supernatant was discarded and the pellets were washed one time with 75% and one time with 100% ethanol by centrifuging at 8000 rpm for 8 min at 4 ^{o}C. Ethanol was totally removed from samples and pellet was dissolved in 20 μL of RNAse free water. Yield and purity of extracted RNAs were assessed by Nanodrop 2000 (Thermo Scientific). cDNA synthesis from RNA and qRT-PCR were performed using SuperScript III Platinum SYBR Green One-Step qRT-PCR Kit (Invitrogen) according to the manufacturers instructions. Reaction conditions were briefly as follows: 55 ^{o}C for 5 min, 95 ^{o}C for 5 min, 40 cycles of 95 ^{o}C for 15 s, 58 ^{o}C for 30 s for βIII-tubulin or 57 ^{o}C for 30 s for GAPDH, and 40 ^{o}C for 1 min, followed by a melting curve to confirm product specificity. The reaction efficiencies for each primer set were evaluated with a standard curve using 5-fold serial dilutions of total RNA. Each run was internally normalized to GAPDH, and each group was normalized to the expression levels of differentiating PC-12

cells cultured on scrNGFB-PA nanofiber group. A comparative Ct method with efficiency correction was used to analyze the results. Expression ratios greater than 1 indicate the up regulation of the gene of interest, while ratios less than 1 correspond to its down regulation.

3.19 Protein analysis

3.19.1 Protein isolation

Analysis of βIII-tubulin expression in PC-12 cells differentiated on PA scaffolds and PLL was performed with western blot analysis. PA coatings, cell seeding and induction was performed as described in gene expression analysis section. Cells were washed twice with ice-cold PBS and lysed in RIPA buffer (1 M Tris; pH 8, 5 M NaCl, 0.5 mM EDTA; pH 8, NP-40, 10% sodium deoxycholate, 10% SDS and ddH2O) including freshly added protease inhibitor cocktail (Thermo Scientific) for 15 min on ice. The lysates were sonicated (Branson Digital Sonifier set at 50% amplitude) three times for two seconds. Then lysates were incubated for 15 more min on ice and then clarified by centrifugation at 13,000 g for 5 min at 4 ^{o}C and supernatants were collected in new microfuge tubes.

Also for analysis of expression levels of MAPK pathway protein complexes which are MEK1/2, phosphorylated MEK1/2 (pMEK1/2), ERK1/2 and phosphorylated ERK1/2 (pERK1/2) western blot was performed. Because these protein complexes are expressed in the beginning of differentiation process, at day 1 after induction with 20 ng/mL NGF-β, the proteins were isolated by using the same protocol for βIII-tubulin. For lysis process, phosphatase inhibitor cocktail (Sigma Aldrich) was added in RIPA buffer together with protease inhibitor coctail (Thermo Scientific). The following steps were performed as described above.

The protein samples were quantified using BCA assay which is based on bicinchoninic acid for colorimetric detection. In order to obtain standard curve to determine the concentrations of protein samples, BCA assay standards, which

are the series of dilutions of known concentration starting from 2000 μg/mL to 0 μg/mL), were prepared by using bovine serum albumin (BSA). In order to prepare BCA developing solution, 200 μL from reagent A from BCA assay kit was mixed with 4 μL from reagent B from BCA assay kit (50:1 ratio) and 200 μL from the mix and 25 μL of each sample were pipetted on 96 well microplate. After adding the developing solution to each probe, plate was incubated at 37 ^{o}C for 30 min and cooled to room temperature for 5-10 min. Then, absorbance was measured at 560 nm by Spectramax M5 microplate reader and concentration of the proteins was calculated from BSA standard curve.

3.19.2 Western Blot analysis

In order to separate the proteins according to their molecular weight, SDS PAGE (Sodium Dodecyl Sulfate Polyacrylamide Gel Electrophoresis) technique was performed. For this purpose, resolving gel (12%) and stacking gel were prepared by mixing the components provided in Table 3.1. TEMED and 10% APS was added at the last step and very quickly in order to prevent polymerization of the gel before pouring.

Components	12% resolving gel
1.5 M Tris HCl pH 8.8	2500 µL
ddH2O	4290 µL
40% acryl:bis 37.5 :1	3000 µL
10 % SDS	100 µL
10% APS	100 µL
TEMED	10 µL

Components	Stacking gel (10 mL)
0.5 M Tris HCl pH 6.8	2500 µL
ddH2O	6290 µL
40% acryl:bis 37.5 :1	1000 µL
10 % SDS	100 µL
10% APS	100 µL
TEMED	10 µL

Table 3.1: Components of resolving and stacking gels used for SDS PAGE.

First, the resolving gel was poured which seperates the proteins according to their molecular weights by leaving approximately 2 cm space for stacking gel. In order to remove bubbles from the gel and prevent drying of the gel, ice-cold isopropanol was poured at the top of the resolving gel. After the gel solidified, stacking gel was poured which stack the protein samples into a narrow zone before resolving. A comb was inserted into stacking gel and incubated for 20 min at room temperature to solidify before use.

For loading protein samples into the wells of the gel for electrophoresis, protein samples were mixed with loading dye (6X stock, 1X final concentration). Loading dye was prepared by mixing 6X laemmli buffer, which is composed of 50.4% Glycerol, 12% SDS, 0.375 M Tris-HCl (pH 6.8) and bromophenol blue, with DTT (in 1:5 ratio to total volume). Protein samples were diluted (50 μg/mL for βIII-tubulin and 40 μg/mL for MEK1/2, pMEK1/2, ERK1/2 and pERK1/2 analyses) with ddH_2O and loading dye was added. After vortexing and spinning down, the samples were incubated at 95 ^{o}C for 5 min in order for denaturing of structure of proteins. Running chamber was loaded with electrode buffer and 30 μL of protein samples were loaded into the wells. 3 μL of pre-stained protein ladder (Abcam) was also loaded into a seperate well. Proteins were run at 70 V for 30 min until all the samples exit from the stacking gel and then at 100 V for 2 h for seperation. After electrophoresis was completed, the gels were transferred (or blotted) onto polyvinylidene difluoride (PVDF) membrane by using "Semi-Dry Electrophoretic Transfer Cell" transfer system. For this method, Whatman papers were equilibrated in anode and cathode buffers as seen in Figure 2.1.

Then, anode buffer treated Whatman paper was placed on transfer platform and PVDF membrane was activated with 100% methanol and placed on the paper. Then, they were rolled with a clean cylindrical tube in order to prevent bubble formation. The gel was placed on the membrane and the other Whatman paper treated with cathode buffer was placed on the gel. Then, they were again rolled with a clean cylindrical tube in order to prevent bubble formation. The system was closed and transfer was carried out for 45 min at 12 V.

After the transfer was completed, the membrane was transferred into a box

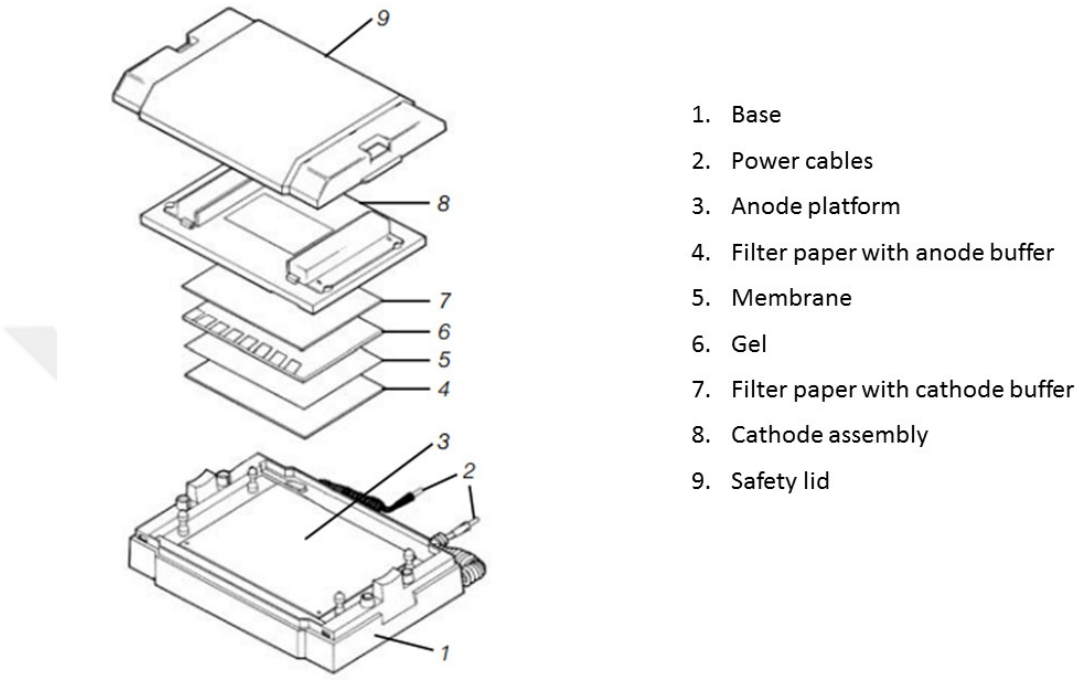

Figure 3.1: Semi-dry blotting system used for transfer of proteins from gel to PVDF membrane. [116]

filled with blocking buffer (5% non-fat dry milk dissolved in TBS-Tween 20 (0.1 %)) and blocked for 2 h on nutator shaker.

The antibodies as provided in Table 3.2 were diluted in blocking buffer and incubated overnight at 4 ^{o}C. The next day, the membrane was taken out from 4 ^{o}C and incubated at room temperature for 30 min. Then, primary antibody solutions were collected and stored at -20 ^{o}C for further use. The membranes were washed with TBS-T 3 times for 5 min and then incubated with secondary antibody solution (provided in Table 3.2) which was also diluted in blocking buffer for 1 h at room temperature. Then, membrane was washed with TBS-T 2 times for 5 min. The BIO-RAD Clarity Western ECL Substrate (1:1 volume ratio) was prepared and added on membrane in dark inside the punched pocket. The reactio was developed for 8-10 min and the membrane was visualized with BIO-RAD ChemiDoc MP imaging system.

	Name	Company	Concentration
Primary Antibody	β III tubulin	Abcam ab78078	1:1000
Primary Antibody	MEK1+MEK2	Abcam ab178876	1:2500
Primary Antibody	MEK1(Ser218/222)/ MEK2 (Ser222/226)	Millipore 05-747	1:1000
Primary Antibody	ERK1+ERK2 [IL-13]	Abcam ab130004	1:2000
Primary Antibody	ERK1 (pT202/pY204) + ERK2 (pT185/pY187)[MAPK -YT]	Abcam ab50011	1:2000
Secondary Antibody	Anti-mouse IgG-HRP	Millipore 12-349	1:1000
Secondary Antibody	Anti-rabbit IgG-HRP	Millipore Ab6721	1:2000

Table 3.2: List of primary and secondary antibodies and dilution rates used in Western blot analysis

Analysis of the expression level of a housekeeping gene is required as loading control for western blot. For this purpose, glyceraldehyde 3-phosphate dehydrogenase (GAPDH) expression level was analyzed. The membrane was washed with TBS-T for 5 min and incubated in mild stripping buffer for 2 times for 10 min (mild stripping buffer was prepared by dissolving 15 glycine, 1 g SDS, 10 mL Tween-20 in ddH_2O, the pH was adjusted to 2.2 and the volume was completed to 1 L ddH_2O.). Then, the membrane was washed 2 times in PBS for 10 min and 1 time in TBS-T for 5 min. Then, blocking, primary and secondary antibody incubations by using GAPDH antibody (Millipore, MAB374 used after 1:500 diluted in blocking buffer) as primary antibody and Goat anti mouse IgG, HRP conjugated antibody as secondary antibody (Merck Millipore, 2488791, 1:2000 diluted in blocking buffer) and imaging was performed as described above.

3.19.3 Coomassie staining of gels after blotting

In order to confirm that the proteins were not degraded during electrophoresis and could be properly transferred to membrane, gels were stained with Coomassie blue stain (content is described in Table 3.3 after transfer was completed. Gels were incubated in Coomassie blue stain solution for 45 min on shaker at room temperature. Then, the gels were destained with destaining solution for 10 min to remove the excess dye and incubated in water to remove the remaining dye at room temperature.

Commassie Staining Components	Volume
Isopropanol	250 mL
Acetic acid	100 mL
Coomassie brilliant blue	2.5 mL
dH_2O	Up to 1 L

Table 3.3: Components of Coomassie blue stain solution used for staining of proteins on gel.

3.20 Schwann cell isolation and culturing

Isolation of Schwann cells from sciatic nerves of male Sprague-Dawley rats was performed according to a previously published protocol [117]. A day before isolation, 6 well plates were coated with 0.01% PLL solution and dried for 2 h in cell culture hood. On the day of isolation, wells were washed with ddH_2O and then coated with 1 mL of laminin solution (0.1% (vol/vol) prepared in PBS, Sigma Aldrich) by incubating the plate for 30 min at 37 ^oC. After coating, wells were

washed 3 times with PBS and left in PBS until the isolated cells were seeded. For isolation, ten weeks old male Sprague-Dawley rats were used under the approval of Animal Ethics Committee of Gulhane Military Medical Academy. 1.5 cm sciatic nerve segments were excised, teased and cut into 2-3 mm fragments after removing epineurium. Then, the tissue was incubated in 0.05% collagenase at 37 ^{o}C for 60 min and tissue debris was removed by transferring the suspension through a 40 μm cell strainer. Cells were cultured on previously coated surfaces described above in medium prepared with DMEM-D-valine (4.5 mg/mL glucose) with 2 mM glutamine, 10% (v/v) fetal calf serum, 1% (v/v) N2 supplement, 20 μg/mL bovine pituitary extract, 5 μM forskolin, 1% penicillin/streptomycin, 0.25 μg/mL amphotericin B (Schwann cell medium). Half of the medium on the cells was changed after 7 days and then replaced completely with fresh medium at day 10. The cells were continued to be cultured and medium change was performed at day 13 and every 2-3 days thereafter until day 19-20 when cultures were confluent and ready for analysis of cell purity and density. The cells were continued to be passaged until passage number 7 and then frozen in FBS / 10% DMSO solution and stored in liquid nitrogen tank for further usage.

3.21 Viability assay for Schwann cells

For viability assay for Schwann cells, PA and PLL coatings on 96 well plate was performed as described in PC-12 cell culture experiments. Then, 1 x 10^4 Schwann cells at passage 8 were seeded on the wells in Schwann cell medium. After culturing for 72 h, the medium was discarded and cells were co-stained with 2 μM calcein-AM and 4 μM ethidium homodimer mixed in 1X PBS (100 μL/well) and incubated for 30 min at room temperature. Then, five random images of Schwann cells were taken by using Zeiss fluorescence microscope with multiple acquisition at 100X magnification from each well for both quantitative and qualitative analysis. Both live and dead cells were counted from images by using Image J software.

3.22 Statistical analysis

Statistical analyses were performed by using GraphPad Prism 6. One-way ANOVA was used to compare the differences between the groups and Bonferronis multiple comparisons test was used for post-hoc analyses. Error bars indicate SEM (standard error of mean). At least three independent repeats were performed for experiments and with a minimum of n=3 for each repeat and p values less than 0.05 were considered to be statistically significant, except where noted.

Chapter 4

Conclusions and Future Perspectives

In this dissertation, we developed a synthetic NGF-affine nanofibrous scaffold which can promote axonal outgrowth in PC-12 cells by enhancing the availability of NGF for TrkA receptor. The first time with this study a 7 amino-acid phage display peptide library was utilized or identification of NGF-β binding epitope. Also, this is the first time that NGF-β binding sequence was incorporated into the structure of PAs by mimicking the natural display of epitope in M13 phage. Because the biocompatibility and bioactivity of PA nanofibers were already shown by several studies, PA nanofibers are widely used synthetic materials for regenerative purposes which enabled us to develop biocompatible and bioactive NGF-β binding synthetic material. With *in vitro* studies, it was shown that developed NGF-binding synthetic material is able to differentiate PC-12 cells into neuron-like cells by altering the expression of proteins responsible from axon elongation. Also, developed material was shown to alter the expression of the MAPK pathway elements, and also was shown to phosphorylate these elements for neuronal differentiation of PC-12 cells. The first time with this study the effect of NGF-β binding material on the differentiation pathway of NGF was examined.

Since NGF plays an important role in the nervous system development and

regeneration, the developed NGF-affine synthetic scaffold can be used as a therapeutic agent for the regeneration of the peripheral nerve injuries (such as sciatic nerve injury) by binding to NGF secreted by Schwann cells and inflammatory cells and enhancing the neuroregeneration of broken nerve ends. In addition, NGFB-PA nanofiber scaffold can also be used for central nervous system regeneration, especially for spinal cord injuries where NGF also plays important roles in circuit formation [32]. In addition, the developed synthetic material is a good candidate for the study of neural stem cell differentiation for inducing the stem cells to differentiate into sensory and sympathetic neurons in the PNS or to the CNS neurons. Overall, NGF binding nanofiber is promising material for development of novel therapeutic approaches and can be applied in further pre-clinical studies for neuroregeneration purposes.

Bibliography

[1] E. R. Kandel, J. H. Schwartz, T. M. Jessell, S. A. Siegelbaum, and A. Hudspeth, *Principles of neural science*, vol. 4. McGraw-hill New York, 2000.

[2] "Human nervous system function." `http://healthfavo.com/`.

[3] G. H. Orians, W. K. Purves, D. E. Sadava, and D. M. Hillis, *Life: The Science of Biology*. Sinauer Associates, Inc, 2011.

[4] G. W. Kreutzberg, "Microglia: a sensor for pathological events in the cns," *Trends in neurosciences*, vol. 19, no. 8, pp. 312–318, 1996.

[5] N. Baumann and D. Pham-Dinh, "Biology of oligodendrocyte and myelin in the mammalian central nervous system," *Physiological reviews*, vol. 81, no. 2, pp. 871–927, 2001.

[6] A. Sierra, M.-E. Tremblay, and H. Wake, *Never-resting microglia: physiological roles in the healthy brain and pathological implications*. Frontiers E-books, 2015.

[7] K. R. Jessen and R. Mirsky, "The origin and development of glial cells in peripheral nerves," *Nature Reviews Neuroscience*, vol. 6, no. 9, pp. 671–682, 2005.

[8] P. T. Ohara, J.-P. Vit, A. Bhargava, and L. Jasmin, "Evidence for a role of connexin 43 in trigeminal pain using rna interference in vivo," *Journal of neurophysiology*, vol. 100, no. 6, pp. 3064–3073, 2008.

[9] M. E. Schwab and D. Bartholdi, "Degeneration and regeneration of axons in the lesioned spinal cord," *Physiological reviews*, vol. 76, no. 2, pp. 319–370, 1996.

[10] J. Silver and J. H. Miller, "Regeneration beyond the glial scar," *Nature Reviews Neuroscience*, vol. 5, no. 2, pp. 146–156, 2004.

[11] J. W. Fawcett and R. A. Asher, "The glial scar and central nervous system repair," *Brain research bulletin*, vol. 49, no. 6, pp. 377–391, 1999.

[12] P. Richardson, U. McGuinness, and A. Aguayo, "Axons from cns neurones regenerate into pns grafts," 1980.

[13] P. G. Popovich and W. F. Hickey, "Bone marrow chimeric rats reveal the unique distribution of resident and recruited macrophages in the contused rat spinal cord," *Journal of Neuropathology & Experimental Neurology*, vol. 60, no. 7, pp. 676–685, 2001.

[14] A. M. Avellino, A. T. Dailey, J. M. Harlan, S. R. Sharar, R. K. Winn, L. D. McNutt, and M. Kliot, "Blocking of up-regulated icam-1 does not prevent macrophage infiltration during wallerian degeneration of peripheral nerve," *Experimental neurology*, vol. 187, no. 2, pp. 430–444, 2004.

[15] G. Yiu and Z. He, "Glial inhibition of cns axon regeneration," *Nature Reviews Neuroscience*, vol. 7, no. 8, pp. 617–627, 2006.

[16] S. L. Shuman, J. C. Bresnahan, and M. S. Beattie, "Apoptosis of microglia and oligodendrocytes after spinal cord contusion in rats," *Journal of neuroscience research*, vol. 50, no. 5, pp. 798–808, 1997.

[17] M. E. Vargas and B. A. Barres, "Why is wallerian degeneration in the cns so slow?," *Annu. Rev. Neurosci.*, vol. 30, pp. 153–179, 2007.

[18] "Difference between peripheral and central nervous system regeneration." http://www.wingsforlife.com/en/latest/the-difference-between-centre-and-periphery-411/.

[19] S. P. Frostick, Q. Yin, and G. J. Kemp, "Schwann cells, neurotrophic factors, and peripheral nerve regeneration," *Microsurgery*, vol. 18, no. 7, pp. 397–405, 1998.

[20] D. Lindholm, R. Heumann, M. Meyer, and H. Thoenen, "Interleukin-l regulates synthesis of nerve growth factor in non-neuronal cells of rat sciatic nerve," *Nature*, pp. 658–659, 1987.

[21] M. F. Pazyra-Murphy, A. Hans, S. L. Courchesne, C. Karch, K. E. Cosker, H. M. Heerssen, F. L. Watson, T. Kim, M. E. Greenberg, and R. A. Segal, "A retrograde neuronal survival response: target-derived neurotrophins regulate mef2d and bcl-w," *The Journal of Neuroscience*, vol. 29, no. 20, pp. 6700–6709, 2009.

[22] L. d. McKerracher, S. David, D. Jackson, V. Kottis, R. Dunn, and P. Braun, "Identification of myelin-associated glycoprotein as a major myelin-derived inhibitor of neurite growth," *Neuron*, vol. 13, no. 4, pp. 805–811, 1994.

[23] V. Kottis, P. Thibault, D. Mikol, Z.-C. Xiao, R. Zhang, P. Dergham, and P. E. Braun, "Oligodendrocyte-myelin glycoprotein (omgp) is an inhibitor of neurite outgrowth," *Journal of neurochemistry*, vol. 82, no. 6, pp. 1566–1569, 2002.

[24] A. Faroni, S. A. Mobasseri, P. J. Kingham, and A. J. Reid, "Peripheral nerve regeneration: experimental strategies and future perspectives," *Advanced drug delivery reviews*, vol. 82, pp. 160–167, 2015.

[25] H. J. Weinberg and P. S. Spencer, "The fate of schwann cells isolated from axonal contact," *Journal of neurocytology*, vol. 7, no. 5, pp. 555–569, 1978.

[26] J. Sketelj, M. Bresjanac, and M. Popović, "Rapid growth of regenerating axons across the segments of sciatic nerve devoid of schwann cells," *Journal of neuroscience research*, vol. 24, no. 2, pp. 153–162, 1989.

[27] D. M. Skovronsky, V. M.-Y. Lee, and J. Q. Trojanowski, "Neurodegenerative diseases: new concepts of pathogenesis and their therapeutic implications," *Annu. Rev. Pathol. Mech. Dis.*, vol. 1, pp. 151–170, 2006.

[28] R. L. Ernst, J. W. Hay, C. Fenn, J. Tinklenberg, and J. A. Yesavage, "Cognitive function and the costs of alzheimer disease: an exploratory study," *Archives of neurology*, vol. 54, no. 6, pp. 687–693, 1997.

[29] A. Association *et al.*, "2012 alzheimers disease facts and figures," *Alzheimer's & Dementia*, vol. 8, no. 2, pp. 131–168, 2012.

[30] D. Acosta and M. Wortmann, "Alzheimers disease international world alzheimer report 2009," *Prince, M*, pp. 1–92, 2009.

[31] "Cns injury." http://mbi.ufl.edu/research/research-areas/cns-injury/.

[32] J. M. Shulman and P. L. De Jager, "Evidence for a common pathway linking neurodegenerative diseases," *Nature genetics*, vol. 41, no. 12, pp. 1261–1262, 2009.

[33] J. J. Duby, R. K. Campbell, S. M. Setter, K. Rasmussen, *et al.*, "Diabetic neuropathy: an intensive review," *American Journal of Health-System Pharmacy*, vol. 61, no. 2, pp. 160–173, 2004.

[34] W. W. Campbell, "Evaluation and management of peripheral nerve injury," *Clinical neurophysiology*, vol. 119, no. 9, pp. 1951–1965, 2008.

[35] H. Seddon, "Three types of nerve injury," *Brain*, vol. 66, no. 4, pp. 237–288, 1943.

[36] "Grades of injury described in seddon's classification.." http://www.gms-books.de/book/living-textbook-hand-surgery/chapter/nerve-injury-classification-clinical-assessment.

[37] D. Grinsell and C. Keating, "Peripheral nerve reconstruction after injury: a review of clinical and experimental therapies," *BioMed research international*, vol. 2014, 2014.

[38] L. Aloe, "Rita levi-montalcini: the discovery of nerve growth factor and modern neurobiology," *Trends in cell biology*, vol. 14, no. 7, pp. 395–399, 2004.

[39] R. Levi-Montalcini and B. Booker, "Excessive growth of the sympathetic ganglia evoked by a protein isolated from mouse salivary glands," *Proceedings of the National Academy of Sciences*, vol. 46, no. 3, pp. 373–384, 1960.

[40] R. Levi-Montalcini, "Growth control of nerve cells by a protein factor and its antiserum," *Science*, vol. 143, no. 3602, pp. 105–110, 1964.

[41] S. Cohen, "Purification of a nerve-growth promoting protein from the mouse salivary gland and its neuro-cytotoxic antiserum," *Proceedings of the National Academy of Sciences*, vol. 46, no. 3, pp. 302–311, 1960.

[42] R. H. Angeletti and R. A. Bradshaw, "Nerve growth factor from mouse submaxillary gland: amino acid sequence," *Proceedings of the National Academy of Sciences*, vol. 68, no. 10, pp. 2417–2420, 1971.

[43] J. Scott, M. Selby, M. Urdea, M. Quiroga, G. I. Bell, and W. J. Rutter, "Isolation and nucleotide sequence of a cdna encoding the precursor of mouse nerve growth factor," *Nature*, vol. 302, no. 5908, pp. 538–540, 1983.

[44] A. Lambiase, P. Rama, S. Bonini, G. Caprioglio, and L. Aloe, "Topical treatment with nerve growth factor for corneal neurotrophic ulcers," *New England Journal of Medicine*, vol. 338, no. 17, pp. 1174–1180, 1998.

[45] F. Landi, L. Aloe, A. Russo, M. Cesari, G. Onder, S. Bonini, P. U. Carbonin, and R. Bernabei, "Topical treatment of pressure ulcers with nerve growth factor: a randomized clinical trial," *Annals of internal medicine*, vol. 139, no. 8, pp. 635–641, 2003.

[46] L. Aloe and L. Calzà, *NGF and related molecules in health and disease*, vol. 146. Elsevier, 2003.

[47] "Structure of 7s ngf.." http://www-cryst.bioc.cam.ac.uk/.

[48] Wikipedia, "Nerve growth factor wikipedia, the free encyclopedia," 2016. [Online; accessed 10-October-2016].

[49] M. V. Sofroniew, C. L. Howe, and W. C. Mobley, "Nerve growth factor signaling, neuroprotection, and neural repair," *Annual review of neuroscience*, vol. 24, no. 1, pp. 1217–1281, 2001.

[50] D. M. Loeb, J. Maragos, D. Martin-Zanca, M. V. Chao, L. F. Parada, and L. A. Greene, "The trk proto-oncogene rescues ngf responsiveness in mutant ngf-nonresponsive pc12 cell lines," *Cell*, vol. 66, no. 5, pp. 961–966, 1991.

[51] C. Wiesmann, M. H. Ultsch, S. H. Bass, and A. M. de Vos, "Crystal structure of nerve growth factor in complex with the ligand-binding domain of the trka receptor," *Nature*, vol. 401, no. 6749, pp. 184–188, 1999.

[52] X.-l. He and K. C. Garcia, "Structure of nerve growth factor complexed with the shared neurotrophin receptor p75," *Science*, vol. 304, no. 5672, pp. 870–875, 2004.

[53] T. Basu, P. H. Warne, and J. Downward, "Role of shc in the activation of ras in response to epidermal growth factor and nerve growth factor.," *Oncogene*, vol. 9, no. 12, pp. 3483–3491, 1994.

[54] M. Rozakis-Adcock, J. McGlade, G. Mbamalu, G. Pelicci, R. Daly, W. Li, A. Batzer, S. Thomas, J. Brugge, P. Pelicci, *et al.*, "Association of the shc and grb2/sem5 sh2-containing proteins is implicated in activation of the ras pathway by tyrosine kinases," *Nature*, vol. 360, no. 6405, pp. 689–692, 1992.

[55] C. J. Marshall, "Map kinase kinase kinase, map kinase kinase and map kinase," *Current opinion in genetics & development*, vol. 4, no. 1, pp. 82–89, 1994.

[56] C. A. Lange-Carter and G. L. Johnson, "Ras-dependent growth factor regulation of mek kinase in pc12 cells," *Science*, vol. 265, no. 5177, pp. 1458–1461, 1994.

[57] R. Chen, C. Sarnecki, and J. Blenis, "Nuclear localization and regulation of erk-and rsk-encoded protein kinases.," *Molecular and cellular biology*, vol. 12, no. 3, pp. 915–927, 1992.

[58] L. Pang, C.-F. Zheng, K. Guan, and A. Saltiel, "Nerve growth factor stimulates a novel protein kinase in pc-12 cells that phosphorylates and activates mitogen-activated protein kinase kinase (mek)," *Biochemical Journal*, vol. 307, no. 2, pp. 513–519, 1995.

[59] V. Kumar and B. Mahal, "Ngf–the trka to successful pain treatment," 2012.

[60] K. G. Ruit, P. A. Osborne, R. E. Schmidt, E. M. Johnson, and W. D. Snider, "Nerve growth factor regulates sympathetic ganglion cell morphology and survival in the adult mouse," *The Journal of Neuroscience*, vol. 10, no. 7, pp. 2412–2419, 1990.

[61] S. Wood, J. Pritchard, and M. Sofroniew, "Re-expression of nerve growth factor receptor after axonal injury recapitulates a developmental event in motor neurons: differential regulation when regeneration is allowed or prevented," *European Journal of Neuroscience*, vol. 2, no. 7, pp. 650–657, 1990.

[62] R. Heumann, D. Lindholm, C. Bandtlow, M. Meyer, M. J. Radeke, T. P. Misko, E. Shooter, and H. Thoenen, "Differential regulation of mrna encoding nerve growth factor and its receptor in rat sciatic nerve during development, degeneration, and regeneration: role of macrophages," *Proceedings of the National Academy of Sciences*, vol. 84, no. 23, pp. 8735–8739, 1987.

[63] R. Mirsky and K. R. Jessen, "The neurobiology of schwann cells," *Brain pathology*, vol. 9, no. 2, pp. 293–311, 1999.

[64] S. P. Frostick, Q. Yin, and G. J. Kemp, "Schwann cells, neurotrophic factors, and peripheral nerve regeneration," *Microsurgery*, vol. 18, no. 7, pp. 397–405, 1998.

[65] A. Derby, V. W. Engleman, G. E. Frierdich, G. Neises, S. R. Rapp, and D. G. Roufa, "Nerve growth factor facilitates regeneration across nerve gaps: morphological and behavioral studies in rat sciatic nerve," *Experimental neurology*, vol. 119, no. 2, pp. 176–191, 1993.

[66] K. M. Rich, T. D. Alexander, J. C. Pryor, and J. P. Hollowell, "Nerve growth factor enhances regeneration through silicone chambers," *Experimental neurology*, vol. 105, no. 2, pp. 162–170, 1989.

[67] E. S. Anton, G. Weskamp, L. F. Reichardt, and W. D. Matthew, "Nerve growth factor and its low-affinity receptor promote schwann cell migration," *Proceedings of the National Academy of Sciences*, vol. 91, no. 7, pp. 2795–2799, 1994.

[68] R. D. Madison and S. J. Archibald, "Point sources of schwann cells result in growth into a nerve entubulation repair site in the absence of axons: effects of freeze-thawing," *Experimental neurology*, vol. 128, no. 2, pp. 266–275, 1994.

[69] V. Verge, K. Gratto, L. Karchewski, and P. Richardson, "Neurotrophins and nerve injury in the adult," *Philosophical Transactions of the Royal Society B: Biological Sciences*, vol. 351, no. 1338, pp. 423–430, 1996.

[70] M. D. Kawaja and F. H. Gage, "Reactive astrocytes are substrates for the growth of adult cns axons in the presence of elevated levels of nerve growth factor," *Neuron*, vol. 7, no. 6, pp. 1019–1030, 1991.

[71] H.-C. von Büdingen, F. Mei, A. Greenfield, S. Jahn, Y.-A. A. Shen, H. H. Reid, D. D. McKemy, and J. R. Chan, "The myelin oligodendrocyte glycoprotein directly binds nerve growth factor to modulate central axon circuitry," *The Journal of cell biology*, vol. 210, no. 6, pp. 891–898, 2015.

[72] Y. Murakami, S. Furukawa, A. Nitta, and Y. Furukawa, "Accumulation of nerve growth factor protein at both rostral and caudal stumps in the transected rat spinal cord," *Journal of the neurological sciences*, vol. 198, no. 1, pp. 63–69, 2002.

[73] J. P. Hollowell, A. Villadiego, and K. M. Rich, "Sciatic nerve regeneration across gaps within silicone chambers: long-term effects of ngf and consideration of axonal branching," *Experimental neurology*, vol. 110, no. 1, pp. 45–51, 1990.

[74] M. S. Ramer, J. V. Priestley, and S. B. McMahon, "Functional regeneration of sensory axons into the adult spinal cord," *Nature*, vol. 403, no. 6767, pp. 312–316, 2000.

[75] M. I. Romero, N. Rangappa, M. G. Garry, and G. M. Smith, "Functional regeneration of chronically injured sensory afferents into adult spinal cord after neurotrophin gene therapy," *The Journal of Neuroscience*, vol. 21, no. 21, pp. 8408–8416, 2001.

[76] M. D. CHRISTENSEN and C. E. HULSEBOSCH, "Chronic central pain after spinal cord injury," *Journal of neurotrauma*, vol. 14, no. 8, pp. 517–537, 1997.

[77] N. R. Krenz, S. O. Meakin, A. V. Krassioukov, and L. C. Weaver, "Neutralizing intraspinal nerve growth factor blocks autonomic dysreflexia caused by spinal cord injury," *The Journal of neuroscience*, vol. 19, no. 17, pp. 7405–7414, 1999.

[78] E. G. Fine, I. Decosterd, M. Papaloïzos, A. D. Zurn, and P. Aebischer, "Gdnf and ngf released by synthetic guidance channels support sciatic nerve regeneration across a long gap," *European Journal of Neuroscience*, vol. 15, no. 4, pp. 589–601, 2002.

[79] J. Bloch, E. G. Fine, N. Bouche, A. D. Zurn, and P. Aebischer, "Nerve growth factor-and neurotrophin-3-releasing guidance channels promote regeneration of the transected rat dorsal root," *Experimental neurology*, vol. 172, no. 2, pp. 425–432, 2001.

[80] W. Sun, C. Sun, H. Lin, H. Zhao, J. Wang, H. Ma, B. Chen, Z. Xiao, and J. Dai, "The effect of collagen-binding ngf-β on the promotion of sciatic nerve regeneration in a rat sciatic nerve crush injury model," *Biomaterials*, vol. 30, no. 27, pp. 4649–4656, 2009.

[81] W. Sun, H. Lin, B. Chen, W. Zhao, Y. Zhao, and J. Dai, "Promotion of peripheral nerve growth by collagen scaffolds loaded with collagen-targeting human nerve growth factor-β," *Journal of biomedical materials research Part A*, vol. 83, no. 4, pp. 1054–1061, 2007.

[82] G. P. Smith, "Filamentous fusion phage: novel expression vectors that display cloned antigens on the virion surface," *Science*, vol. 228, no. 4705, pp. 1315–1317, 1985.

[83] "Commercially available phage display peptide libraries.." https://www.neb.com/.

[84] E. J. Kim, C. S. Jeon, I. Hwang, and T. D. Chung, "Translocation pathway-dependent assembly of streptavidin-and antibody-binding filamentous virus-like particles," *Small*, 2016.

[85] K. E. Langley, M. R. Villarejo, A. V. Fowler, P. J. Zamenhof, and I. Zabin, "Molecular basis of beta-galactosidase alpha-complementation," *Proceedings of the National Academy of Sciences*, vol. 72, no. 4, pp. 1254–1257, 1975.

[86] J. Messing, B. Gronenborn, B. Müller-Hill, and P. H. Hopschneider, "Filamentous coliphage m13 as a cloning vehicle: insertion of a hindii fragment of the lac regulatory region in m13 replicative form in vitro," *Proceedings of the National Academy of Sciences*, vol. 74, no. 9, pp. 3642–3646, 1977.

[87] S. M. Willerth, P. J. Johnson, D. J. Maxwell, S. R. Parsons, M. E. Doukas, and S. E. Sakiyama-Elbert, "Rationally designed peptides for controlled release of nerve growth factor from fibrin matrices," *Journal of Biomedical Materials Research Part A*, vol. 80, no. 1, pp. 13–23, 2007.

[88] K. Lee, E. A. Silva, and D. J. Mooney, "Growth factor delivery-based tissue engineering: general approaches and a review of recent developments," *Journal of the Royal Society Interface*, vol. 8, no. 55, pp. 153–170, 2011.

[89] H. Cui, M. J. Webber, and S. I. Stupp, "Self-assembly of peptide amphiphiles: From molecules to nanostructures to biomaterials," *Peptide Science*, vol. 94, no. 1, pp. 1–18, 2010.

[90] G. A. Silva, C. Czeisler, K. L. Niece, E. Beniash, D. A. Harrington, J. A. Kessler, and S. I. Stupp, "Selective differentiation of neural progenitor cells by high-epitope density nanofibers," *Science*, vol. 303, no. 5662, pp. 1352–1355, 2004.

[91] R. Mammadov, B. Mammadov, M. O. Guler, and A. B. Tekinay, "Growth factor binding on heparin mimetic peptide nanofibers," *Biomacromolecules*, vol. 13, no. 10, pp. 3311–3319, 2012.

[92] B. Mammadov, R. Mammadov, M. O. Guler, and A. B. Tekinay, "Cooperative effect of heparan sulfate and laminin mimetic peptide nanofibers on the promotion of neurite outgrowth," *Acta biomaterialia*, vol. 8, no. 6, pp. 2077–2086, 2012.

[93] M. J. Webber, E. J. Berns, and S. I. Stupp, "Supramolecular nanofibers of peptide amphiphiles for medicine," *Israel journal of chemistry*, vol. 53, no. 8, pp. 530–554, 2013.

[94] M. Sever, M. Turkyilmaz, C. Sevinc, A. Cakir, B. Ocalan, M. Cansev, M. O. Guler, and A. B. Tekinay, "Regenerative effects of peptide nanofibers in an experimental model of parkinsons disease," *Acta Biomaterialia*, 2016.

[95] B. Mammadov, M. Sever, M. Gecer, F. Zor, S. Ozturk, H. Akgun, U. H. Ulas, Z. Orhan, M. O. Guler, and A. B. Tekinay, "Sciatic nerve regeneration induced by glycosaminoglycan and laminin mimetic peptide nanofiber gels," *RSC Adv*, 2016.

[96] S. Toksoz, R. Mammadov, A. B. Tekinay, and M. O. Guler, "Electrostatic effects on nanofiber formation of self-assembling peptide amphiphiles," *Journal of colloid and interface science*, vol. 356, no. 1, pp. 131–137, 2011.

[97] C. K. Smith, J. M. Withka, and L. Regan, "A thermodynamic scale for the. beta.-sheet forming tendencies of the amino acids," *Biochemistry*, vol. 33, no. 18, pp. 5510–5517, 1994.

[98] T. Nishida, K. Yasumoto, T. Otori, and J. Desaki, "The network structure of corneal fibroblasts in the rat as revealed by scanning electron microscopy.," *Investigative ophthalmology & visual science*, vol. 29, no. 12, pp. 1887–1890, 1988.

[99] L. A. Greene and A. S. Tischler, "Establishment of a noradrenergic clonal line of rat adrenal pheochromocytoma cells which respond to nerve growth factor," *Proceedings of the National Academy of Sciences*, vol. 73, no. 7, pp. 2424–2428, 1976.

[100] S. O. Yoon, P. Casaccia-Bonnefil, B. Carter, and M. V. Chao, "Competitive signaling between trka and p75 nerve growth factor receptors determines cell survival," *The Journal of neuroscience*, vol. 18, no. 9, pp. 3273–3281, 1998.

[101] D. Vaudry, P. Stork, P. Lazarovici, and L. Eiden, "Signaling pathways for pc12 cell differentiation: making the right connections," *Science*, vol. 296, no. 5573, pp. 1648–1649, 2002.

[102] C. D. Katsetos, M. M. Herman, and S. J. Mörk, "Class iii β-tubulin in human development and cancer," *Cell motility and the cytoskeleton*, vol. 55, no. 2, pp. 77–96, 2003.

[103] M. Frödin, P. Peraldi, and E. Van Obberghen, "Cyclic amp activates the mitogen-activated protein kinase cascade in pc12 cells.," *Journal of Biological Chemistry*, vol. 269, no. 8, pp. 6207–6214, 1994.

[104] S. C. Apfel, "Neurotrophic factor therapy–prospects and problems," *Clinical chemistry and laboratory medicine*, vol. 39, no. 4, pp. 351–355, 2001.

[105] S. J. Jhaveri, M. R. Hynd, N. Dowell-Mesfin, J. N. Turner, W. Shain, and C. K. Ober, "Release of nerve growth factor from hema hydrogel-coated substrates and its effect on the differentiation of neural cells," *Biomacromolecules*, vol. 10, no. 1, pp. 174–183, 2008.

[106] P.-R. Chen, M.-H. Chen, J.-S. Sun, M.-H. Chen, C.-C. Tsai, and F.-H. Lin, "Biocompatibility of ngf-grafted gtg membranes for peripheral nerve repair using cultured schwann cells," *Biomaterials*, vol. 25, no. 25, pp. 5667–5673, 2004.

[107] C. M. Valmikinathan, S. Defroda, and X. Yu, "Polycaprolactone and bovine serum albumin based nanofibers for controlled release of nerve growth factor," *Biomacromolecules*, vol. 10, no. 5, pp. 1084–1089, 2009.

[108] A. Dehsorkhi, V. Castelletto, and I. W. Hamley, "Self-assembling amphiphilic peptides," *Journal of Peptide Science*, vol. 20, no. 7, pp. 453–467, 2014.

[109] R. N. Shah, N. A. Shah, M. M. D. R. Lim, C. Hsieh, G. Nuber, and S. I. Stupp, "Supramolecular design of self-assembling nanofibers for cartilage regeneration," *Proceedings of the National Academy of Sciences*, vol. 107, no. 8, pp. 3293–3298, 2010.

[110] C. J. Newcomb, S. Sur, J. H. Ortony, O.-S. Lee, J. B. Matson, J. Boekhoven, J. M. Yu, G. C. Schatz, and S. I. Stupp, "Cell death versus cell survival instructed by supramolecular cohesion of nanostructures," *Nature communications*, vol. 5, 2014.

[111] K. Saar, M. Lindgren, M. Hansen, E. Eiríksdóttir, Y. Jiang, K. Rosenthal-Aizman, M. Sassian, and Ü. Langel, "Cell-penetrating peptides: a comparative membrane toxicity study," *Analytical biochemistry*, vol. 345, no. 1, pp. 55–65, 2005.

[112] M. V. Chao *et al.*, "Neurotrophin receptors: a window into neuronal differentiation," *Neuron*, vol. 9, no. 4, pp. 583–593, 1992.

[113] L. Klesse, K. Meyers, C. Marshall, and L. Parada, "Nerve growth factor induces survival and differentiation through two distinct signaling cascades in pc12 cells.," *Oncogene*, vol. 18, no. 12, 1999.

[114] S. Cowley, H. Paterson, P. Kemp, and C. J. Marshall, "Activation of map kinase kinase is necessary and sufficient for pc12 differentiation and for transformation of nih 3t3 cells," *Cell*, vol. 77, no. 6, pp. 841–852, 1994.

[115] D. R. Kaplan and R. M. Stephens, "Neurotrophin signal transduction by the trk receptor," *Journal of neurobiology*, vol. 25, no. 11, pp. 1404–1417, 1994.

[116] "Semi-dry blotting system.." http://www.bio-rad.com/.

[117] R. Kaewkhaw, A. M. Scutt, and J. W. Haycock, "Integrated culture and purification of rat schwann cells from freshly isolated adult tissue," *Nature protocols*, vol. 7, no. 11, pp. 1996–2004, 2012.

Appendix A

Data

Appendix B

Code